Republic of Iraq
Ministry of Higher Education and Scientific Research
University of Babylon
College of Engineering
Civil Engineering Department

# Modelling the Hydrological Impact of Land Use/Land Cover Alteration on the Lower Zab River Basin, Iraq

A Thesis

Submitted to the Department of Civil Engineering, College of Engineering, University of Babylon in Partial Fulfilment of the Requirements for the Master Degree in Engineering /Civil Engineering /Water Resources

*By:*

***Zahraa Ali Mahdi Abood***

(B.Sc. in Civil Engineering 2010)

*Supervised by:*

***Asst. Prof. Dr. Ruqayah Kadhim Mohammed***

**2023 A.D** **1444 A.H**

بِسْمِ اللَّهِ الرَّحْمَنِ الرَّحِيمِ

وَلَوْلَا فَضْلُ ٱللَّهِ عَلَيْكَ وَرَحْمَتُهُ لَهَمَّت طَّآئِفَةٌ مِّنْهُمْ أَن يُضِلُّوكَ وَمَا يُضِلُّونَ إِلَّآ أَنفُسَهُمْ ۖ وَمَا يَضُرُّونَكَ مِن شَيْءٍ وَأَنزَلَ ٱللَّهُ عَلَيْكَ ٱلْكِتَٰبَ وَٱلْحِكْمَةَ وَعَلَّمَكَ مَا لَمْ تَكُن تَعْلَمُ ۚ وَكَانَ فَضْلُ ٱللَّهِ عَلَيْكَ عَظِيمًا"

صدق اللَّهُ العظيم

سورة النساء {الأية:113}

# *Supervisor Certification*

I certify that this thesis which is entitled ***(Modelling the Hydrological Impact of Land Use/Land Cover Alteration on the Lower Zab River Basin, Iraq)*** has been prepared by ***(Zahraa Ali Mahdi)*** under my supervision at College of Engineering, Babylon University, in partial fulfilment of the requirements for the degree of Master of Science in Water Resources Engineering.

Signature:

Name: ***Asst. Prof. Dr. Ruqayah Kadhim Mohammed***

Date: / / 2023

**EXAMINATION COMMITTEE CERTIFICATE**

We certify that we have read this thesis entitled ***"Modelling the hydrological impact of land use/land cover alteration on the Lower Zab River Basin, Iraq"*** presented by **"Zahraa Ali Mahdi Al_Quraishi"** and as an examining committee, we examined the student in its content and in what is connected with it, and that in our opinion it meets standard of a thesis for the degree of Master of Science in Civil Engineering / Water Resources Engineering.

Signature:

Name: ***Asst. Prof. Dr. Ruqayah Kadhim Mohammed***

(Supervisor and Member)

Date: / / 2023

Signature:

Name**: *Asst. Prof. Dr.* Imad Habeeb Obead**

(Member)

Date: / / 2023

Signature:

Name: ***Asst. Prof. Dr.*** **Najah kadhim Abbas**

(Member)

Date: / / 2023

Signature:

Name: ***Prof. Dr.*** **Waqed Hameed Hassan**

(Chairman)

Date: / / 2023

**Approved by the Head of the Civil Engineering Department**

Signature:

Name: ***Prof. Dr. Thair J.Mizhir Alfatlawi***

Date: / / 2023

**Approved by the Dean of college of Engineering**

Signature:

Name: ***Prof. Dr.*** **Hatem Hadi Obeid**

Date: / /2023

# *Deduction*

*I would like to dedicate*

*"To My GOD Almight who is always there when I am in need, and for giving me this apportainity to do my master degree which would not have been possible other wish"*

*"To the messenger of GOD and prophet of mercy, the prophet Mohammed "my GOD's prapers and peace be upon him"*

*"To the spirits of the martyrs of Iraq"*

*"To my beloved parents, who have been source of inspiration and gave me strength when I thought of giving up, and containually provide their moral, spiritual, emotion, and financial support"*

*"To everyone who helped me tomove the ro cks on my way, to everyone who believed on me."*

*With love and respect*

*Zahraa Ali*

## *Acknowledgements*

*In the name of Allah, the Most Gracious, the Most Merciful. Praise be to Allah for the blessing he has bestowed upon me, and prayers and peace be upon the one who was sent with mercy, and upon his family, and upon his honourable companions and after.*

*"Who does not thank people does not thank God". And when I am putting the final touches on my humble effort, which would not have seen the light without the strenuous efforts and meticulous follow-up of those loyal and in the forefront of them* ***Asst. prof. Dr Ruqayah Kadhim Mohammed****" my supervisor and my support, thanks to her, after God, I completed my thesis, those who spared no effort in helping me, may Allah reward them with the best reward and I have all the appreciation and respect. Also, I cannot forget the efforts made by "****prof. Dr Thair Jabbar Mizhir Alfatlawi****" Head of civil engineering department and all of my teachers since I took my first steps in my primary school until today, especially my teachers my department, and all the people of the hidden effort in there.*

*To,* ***Asst. prof Dr. Ayser Jamil Abdel-Kadhim****, who did not skimp on any information or advice that I asked him to complete my work*

*To my wonderful friend,* ***Rasha Khairallah Obyes****, who was the first reason to encourage me to complete my master's studies*

*To all* ***my family members, and my close friends*** *who supported me with prayers or information*

*Finally, many thanks to everyone who helped me in the departments and everyone who contributed to showing this effort for existence.*

***Zahraa Ali Mahdi***

## Abstract

The current study aims to investigate the LU/LC pattern and measure the correlation change in the Lesser Zab river basin. Data Landsat imagery from 1989, 1999, 2010 and 2021 were used. In general, six, classes have been identified, utilizing supervised image classification process maximum likelihood in ARC GIS10.7. Urban lands, increased from 0.46% in 1989, to 5.59% in 2021 of total land area. In comparison with 1989, Agricultural lands have been reduced by 11.1% at 2021. And this study aims to predict the prospect LU/LC alterations by applying the synergy Cellular Automata-Markov. With the categorized (1999–2010) and (2010–2021) LU/LC maps in the hybrid model, the LU/LC maps for 2021 and 2041 were modeled correspondingly. The agreements accuracy between the categorized and the modeled images were Kno = 0.8635, Klocation = 0.8541, Kstandard = 0.7851 and $R^2$=0.951. Prospect likelihoods validate between 2021 classified and 2041 predicted, urban area would rise by 364.4%, water bodies 33%, however, bare lands/light, agricultural lands, bare lands/dark, forest lands would decrease by 3.5%, 11.96%, 42.85 %, and 76.27%, correspondingly. And investigate the impact of LU/LC change on the hydrological process of the study area for 21 years. The Soil Water Assessment Tool (SWAT) model used for the simulation of the streamflow. The model results showed that the streamflow characteristics changed due to the LU/LC change such as change of flood frequency and climate change. The SWAT model evaluation revealed the annual surface runoff in the Dukan watershed increased due to the flood wave that occurred in 2019 according to hydrological data obtained from the Ministry of Water Resources / National Center for Water Resources Management. As a result, the Dukan Dam's capacity was depleted and reduce surface runoff in the Dibis watershed due to precipitation decreases. Curve number (CV), an available

water capacity of the soil layer, and soil evaporation composition factor were the most sensitive parameters identified for the streamflow and snow melt effective in Dukan watershed as the years progress, the thickness of the snow decreases and its contribution to the stream flow not effective to Dibis watershed. By utilizing SWAT CUP two LU/LC (2000, 2010) have been developed. Both the calibration and validation results showed a relationship between observed and simulated streamflow. For example ($R^2$) and (NSE) values for the model statistical test are 0.87 and 0.81 for the calibration period 2000-2007, and 0.79 and 0.63 for the validation period 2007-2010, respectively. The output of this study are helpful for effective management of river basin.

# List of Contents

## List of Figures.

## List of Tables

## List of Abbrivations

| Abbreviation | Desicription |
|---|---|
| 95PPU | 95% Prediction Uncertainty |
| AGRL | Agricultural land |
| CA | Cellular Automata |
| CC | Climate Change |
| CFSR | Climate Forecast System Reanalysis |
| CN | Curve Number |
| DEM | Digital Elevation Model |
| ETM | Enhanced Thematic Mapper |
| FAO | Food and Agriculture Organization |
| GIS | Geographic Information System |
| HEC-HMS | Hydrologic Modeling System |
| HRU | Hydrological Response Unit |
| KI | Kappa coefficient |
| LULC | Land Use Land Cover |
| LZRB | Lower Zab River Basin |
| m. a. s. l | Meters Above Sea Level |
| MoWR | Iraqi Ministry of Water Resources |
| NASA | National Aeronautics and Space Administration |
| NDVI | Normalized Difference vegetation Index |
| NIR | Near Infra-Red |
| NSE | Nash–Sutcliffe model efficiency |
| OA | Overall Accuracy |
| $R^2$ | Coefficient of determination |
| RMSE | Root Mean Squared Error |

| | |
|---|---|
| SRTM | Shuttle Radar Topography Mission |
| SUFI-2 | Sequential Uncertainty Fitting version |
| SWAT | Soil and Water Assessment Tool |
| SWAT-CUP | SWAT Calibration and Uncertainty Programs |
| TM | Thematic Mapper |
| WGS84 | World Geodetic System Reference 1984 |
| USDA | United States Department of Agriculture |
| USGS | United States Geological Survey |
| UTM | Universal Transverse Mercator |
| WGS84 | World Geodetic System Reference 1984 |

# Chapter one

# Introduction

## 1.1 General

Alterations of land use land cover have been displayed to have a direct effect on both the regional and universal atmosphere, land poverty, and environment that in turn diminishes ecology facilities and purposes (Oliver and Morecroft 2014; Padmaja and Giridhar 2022). Compared with the past, the land use and land cover (LULC) concentration, quickness, as well as the amount of alteration are currently quicker as a result of the public development and the quick growth in inhabitants caused disturbing a big quantity of lands on the Globe (Saleh and Ahmed 2021). Thus, simulating present and prospect alteration in LU/LC would be important to the policy making of ecological managing and future development. As a result of their capability to offer recurrent statistics at changed spatiotemporal coverage, there has been raising concern for applying remote sensing information for observing LU/LC variations. Accordingly, the remote sensing information is considered as vital data to the LU/LC classification and modification exposure simulation. Landsat image is freely available and access to four eras of world recording data and moderately great areal resolution and it has been extensively considered to investigate LU/LC variations (Sakthivel et al. 2021; Padmaja and Giridhar 2022). Markov model and cellular automata (CA) have probable profits in the investigation of land use variations. The CA-Markov simulation is capable to incorporate the data of geographic information system (GIS) and remote sensing well, therefore; is a strong and appropriate technique for simulating spatiotemporal change of LU/LC (Yi et al., 2022). Recently, the CA Markov model have effectively applied to simulate the spatiotemporal change patterns of LU/LC by numerous

studies (Gidado et al., 2019; Hishe et al. 2020; Munthali et al. 2020; Cui et al., 2021; Wang and Zheng 2022; Yi et al., 2022). Accordinaly and considering the ability of the model to expand understanding about the difficulty of spatial system components, the current study considered the CA-Markov simulation to examine prospect LU/LC variations within LZRC, north part of Iraq. Nevertheless, numerous studies have used classification methods that founded on remote sensing data to estimate LU/LC at local scale (Degife et al. 2019; Juliev et al. 2019; Yesuph and Dagnew 2019; Kan-In and Khunrattanasiri 2020; Maury and Sharma 2020; Sakthivel et al. 2021; Padmaja and Giridhar 2022). Nearly all the earlier research works in Iraq have concentrated either on present or on historical LU/LC variations, and there have been some research work on prediction of spatial future LU/LC variations in the country (Hadi et al. 2014; Omar et al. 2014).

The SWAT model is a widely used semi distributed, continuous, physically based, and efficient hydrological model that was originally developed to quantify the impact of land use and management practices on water, sediment, and agricultural chemical yields at the watershed level under varying soil, land use, and management conditions (Arnold et al., 2012). The model application (SWAT) is a common technique used to examine LU/LCC consequences on water resources, notably in watershed management. Many investigations (Abraham et al., 2006; Setegn et al., 2008; Getachew and Melesse, 2012) have demonstrated the appropriateness of such as model in LU/LCC water resource impact assessments.

This research contained (1) Explore the LU/LC pattern for the basin, and identify the LU/LC alteration during the past three decades (1989–2021) to detect the spatiotemporal changes in these years by using GIS software (2) Investigate and record NDVI changes during the past three decades (1989–

2021) by remote sensing approaches information (3) Use CA-Markov simulation to address the past, present, and future changes of LU/LC for the LZRC. (4) The SWAT model's applicability to the research field was evaluated in relation to the impact of the LU/LC shift on examining the hydrological response of the Lesser zab basin. This will let policymakers use more realistic techniques to sustain the water resources while also drawing significant attention to the basin ecosystem.

## 1.2 Aim and Objectives

The main target of the study is estimating the past and future LU/LC alteration in the Lower Zab River Basin hydrology as well as translating the outcomes into a management decision to overcome the negative consequences of such changes on the hydrological balance of the basin. However, this study aimed to achieve the following objectives at a basin scale:

1. Identify LU/LC and NDVI spatiotemporal alteration for the basin during the past three decades (1989–2021).
2. Address the past, present, and future changes of LU/LC for the basin by CA-Markov simulation.
3. Evaluate the effect of LU/LC changes on the hydrological processes from 2000 until 2021 by using ARC SWAT software.

## 1.3 Limitations and Assumptions

- Assuming that interactions between LU/LC and climate change were overlooked while isolating the effects of two elements is the main likelihood the methodology utilized in this investigation. However, the hydrology of the basin would be significantly influenced by LU/LC and climate change.

**Uncertainty:**

• The hydrological simulation is one of the main sources of uncertainty, along with uncertainties in the hydro-climatic time series and modelling parameters. The calibration process of SWAT's conceptual model results in a high level of parameterization, which introduces uncertainty.

## 1.4 The Thesis's Organization:

The research outline and findings are provided in five chapters, as mentioned below:

The first chapter provides an introduction to the research topic, the aim and objectives to be achieved, and the structure of the research

The second chapter presents a literature review of relevant topics of the research, which dealt with detecting changes in land use land cover over several decades by creating a LU/LC map and classifying them using a GIS program, as well as studying the impact of this change on hydrological behavior using the ARC SWAT program and predicting the future map using Markov Model.

The third chapter present the technique employed in the current study and provides a full description of the tools and source input data that used to prepare land use and land cover maps, classification and evaluation of classification accuracy using the Kappa coefficient, estimate their hydrological influence, and forcasting future maps for the study region.

The fourth chapter presents the results obtained based on the tools and input data that were explained in the third chapter

The fifth chapter summarizes the study's significant results and gives recommendations for further research

# Chapter Two

# Concept, Theory and Literature Review

## 2.1 Land use Land cover

Land cover refers to the physical and biophysical characteristics or state of the Earth's surface and immediate surroundings as represented by the distribution of vegetation, water, desert, ice, and other physical features of the land, including those created solely by human activities, such as settlements. The intended use or management of a land cover type by humans is referred to as land use. Thus, land use encompasses both the manner in which the biophysical attributes of land are manipulated and the intent behind that manipulation (the purpose for which the land is used, e.g., agriculture, grazing, etc.), which are more subtle changes that affect the character of the land cover without changing its overall classification. This definition of land use creates a direct link between land cover and human actions in their environment (FAO, 1998a).

A comprehensive analysis is necessary for proper land cover management. Knowledge of the land cover's physical properties from direct measurements and the use of physical models extends to disciplines like biology and soil sciences hydrology meteorology (Hagos et al., 2014). Human adjustments to the surface of the earth result in changes to the land cover. These modifications significantly affect how crucial components of the Earth system work (such as energy, water, and soil balance). Additionally, population growth increases the demand for scarce natural resources, changing the land's surface cover (Islam et al., 2018). The effect of land cover on runoff is an essential component in the production of runoff, as the vegetation that splits the water has an impact on how much is intercepted into infiltration and runoff (Winnaar et al., 2007). The impact of land cover on surface runoff generation might be shown by the results

of Water flow patterns are altered by urbanization due to an increase in impervious surfaces. (Barron et al.,2009)

## 2.2 Classification of remote sensing imagery

Remote sensing image classification is required to identify information about the earth's surface and environment. The classification technique determines the object information corresponding to the image and extracts the necessary information related to that object (Breiman,2001) Remote sensing image classification is roughly divided into two categories: supervised classification and unsupervised classification as shown details in table (2.1).

### 2.2.1 Supervision of classification

The supervised classification method is a popular method for classifying remote sensing data. To train the algorithm, training data and thus analyst intervention are required. Algorithm training necessitates that the analyst have a thorough understanding of the geographical area under consideration and its land cover (Richards,2013). The delineation of training areas representative of a cover type is most efficient when an image analyst is familiar with the topography of a region. These areas are known as training sites on the picture, which include the predictor variables assessed in each sample unit.

### 2.2.2 Unsupervised classification

Unsupervised image classification is entirely based on the automatic assignment of image pixels to spectral groupings. It only considers spectral distance measures and requires little user interaction. This method necessitates interpretation after classification. To understand the spectral characteristics of land cover classes, unsupervised classification techniques are commonly used. Unsupervised classification yields a clustered image, which is defined by groups of pixels called clusters that have similar properties (Jensen,1996).

commonly employed K-mean Clustering, ISODATA, Spectral Clustering, and other unsupervised methods are examples

Table (2.1) Techniques for Remote Sensing Classification (Jensen, 2005)

| Methods | Examples | Characteristics |
|---|---|---|
| Parametric | Unsupervised classification and maximum likelihood classification | Assumptions: Data area normally distributed prior Knowledge of class density functions |
| Non parametric Non- metric | Support Vector, fuzzy categorization, neural networks, and a system for determining the closest neighbor Decision tree categorization using rules | There are no presumptions made can be used with nominal and real-valued data statistical analysis of scaled data |
| Supervised | Maximum Likelihood, minimal distance, classification using a parallelepiped, etc. | Each pixel is categorised based on statistical analysis, and the analyst selects training sites to represent them in classes |
| Unsupervised | ISODATA and K-means etc | The analyst selects training locations to represent in each pixel is categorized into groups according to analytical statistics. utilizing discrete categories to classify. considers the diversity of the actual world |
| Hard (parametric) Soft (non- Parametric) Object-oriented for pre-pixels | Unsupervised and Supervised Classifications | Each pixel is given a share of the available land. sort of cover shown in the images |

| | | |
|---|---|---|
| Hybrid Approaches | Logic for Fuzzy Set Classification | Image classification, pixel by pixel.homogenous objects generated from an image.Each object and pixel underwent classification. |

## 2.3 Watershed

A watershed is a geographical region that is researched for the hydrological cycle and its components. This area of terrain gathers rain, snowmelt, and springs, which flow into reservoirs, bays, and the ocean via creeks, streams, and rivers. On different scales, the topography most relevant to a watersheds unique location determines the size of a watershed, also known as a drainage basin or catchment. These scales are known as "Hydrologic Unit Codes" (HUC). A watershed might be as little as a single county or as large as a small inland lake size, slope, form, drainage density, land use/land cover, geology and soils, and vegetation are all major elements influencing various aspects of runoff (Viessman, 2003)

## 2.4 Watershed Model Selection

### 2.4.1 Models of the Hydrologic System

The components of a watershed hydrology model are mathematically described cycle of the hydrologic system. The goal determines the model's architecture and organization. Which the model is constructed (Singh and Woolhiser, 2002). hydrology watershed models have many various shapes and have been created for many different causes However, they are typically created to achieve one of the two main goals. One the goal of watershed modeling is to better comprehend the hydrologic cycle a knowledge of the phenomena that occur in awatershed and how changes to the watershed may impact these

phenomena. The creation of synthetic sequences of data is another goal of watershed modeling. Every hydrological model needs two key elements, according to Beven,(2001): one to assess how much of the rainfall contributes to the runoff in the storm hydrograph the other to account for the distribution that runoff in time, to take into form the storm hydrograph's shape (the runoff routing component).

According to Singh and Woolhiser, (2002) Watershed models can be categorized using many standards, including explanation of the procedure, its duration, size, and method of resolution (Singh,1995) divided hydrologic models into many categories: (1) process description; (2) timescale (3) model type (4) space size, (5) methods of solution, (6) usage of the land, and (7) application of models. If a model has at least one component of random character which is not explicit in the model input, but only implicit or hidden it is called stochastic model. If the model components are described by a mix of deterministic and stochastic components, the model is called stochastic-deterministic or hybrid model. Deterministic model - A mathematical model which contains no. random components; consequently, each component and input is determined exactly. Stochastic model - A mathematical model that includes some sort of random forcing. A vast majority of the models are deterministic, and virtually no model is fully stochastic. On the basis of process description, the hydrological models can be classified into three main categories: lumped models, semi-distributed model and imperical as shown in fig(2.1), (Refsgaard, 1996)

The basin is divided into a number of smaller sub-basins in semi-distributed (simplified distributed) models, which partially permits parameters to fluctuate in space. The fundamental benefit of these models is that they have a structure

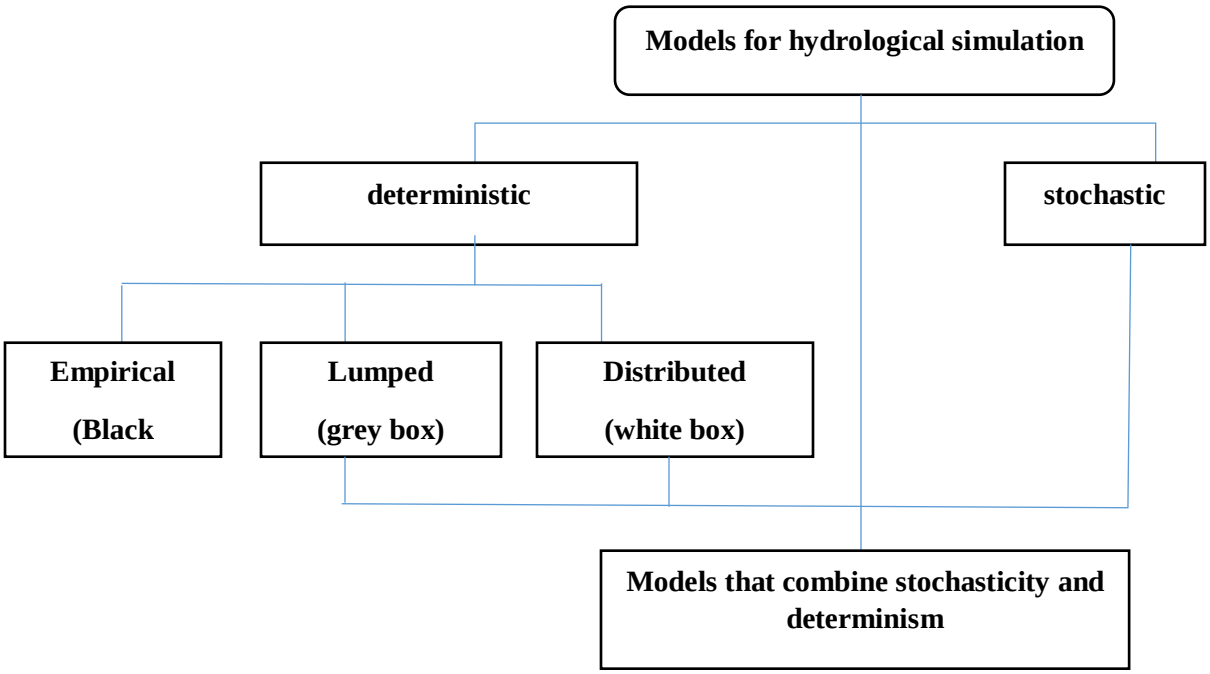


Fig (2.1) Model classification based on procedure (Refsgaard, 1996)

that is more physically based than lumped models and that they require less input data per model than fully distributed models.

## 2.5 The Soil Water Assessment Tool (SWAT) Model

The SWAT model, which was created by USDA-ARS (Arnold et al., 1998) throughout the course of almost 30 years of modeling experience. The prototype is semi- a physically based distributed simulation model that is able to foresee the effects of land use change and land use on hydrological regimes in watersheds with different soil types. largely as a tool for strategic planning over extended periods of time and managerial settings. It combines elements from a number of ARS models and is an immediate development of the SWRRB model. (Arnold and Williams, 1987). The SWAT 2005 effects of topographic, land-use, soil, and other spatial variables on watershed Subdivisions take hydrological aspects into account (Mengistu et al., 2019)

## 2.5.1 SCS Curve Number Method

The SCS curve number (Soil Conservation Service Engineering Division,1972 ) is a method for estimating surfacerunoff quantities from precipitations for a specific area.Despite the fact that the method is intended to calculate surface runoff from asingle rainstorm event, it can also be used to calculate annual surface runoff.

The basic requirements for the method equation are the rainfall amounts and the curve number (CN) of the area to which the surface runoff will be calculate d. The curve number is determined by land use land cover, hydrological soil group, treatment, and hydrological condition.

The SCS curve number method has the following general equation (USDA, 1972)

$$Qsurf=\frac{(P-I_a)^2}{(P-I_a)-S} \quad 2.1$$

Where Qsurf denotes daily surface runoff (mm), P precipitation (mm), S:the retention parameter (mm water.it varies spatially due to changes in soils, land use management, slope and temporally due to changes in soil water content, Ia Initial abstraction (Ia) refers to all water losses that occur prior to the start of runoff, such as water retained in surface depressions, water intercepted by vegetation, evaporation, and infiltration (USDA, 1986). $Ia$ is highly variable, but it is always associated with soil and land cover parameters. Many studies of various watersheds discovered that Ia is roughly given by the equation:

$$I_a = 0.2\ S \quad 2.2$$

By removing Ia from equation 2.1 and substituting it into equation 2.2, S and P are combined to produce a unique runoff equation.

$$Q = \frac{(P - 0.2S)^2}{(P + 0.8S)} \quad 2.3$$

The CN ranges from 0 to 100

$$S = \frac{25400}{CN} - 254 \quad 2.4$$

The SCS curve number is determined by soil permeability, LC, and previous soil water conditions. Runoff will occur only when Rday > Ia. Rday is the daily rainfall depth (mm of water), Figure 2.2 depicts a graphical representation of equation 2.1 for various CN values (Neitch et al., 2005)

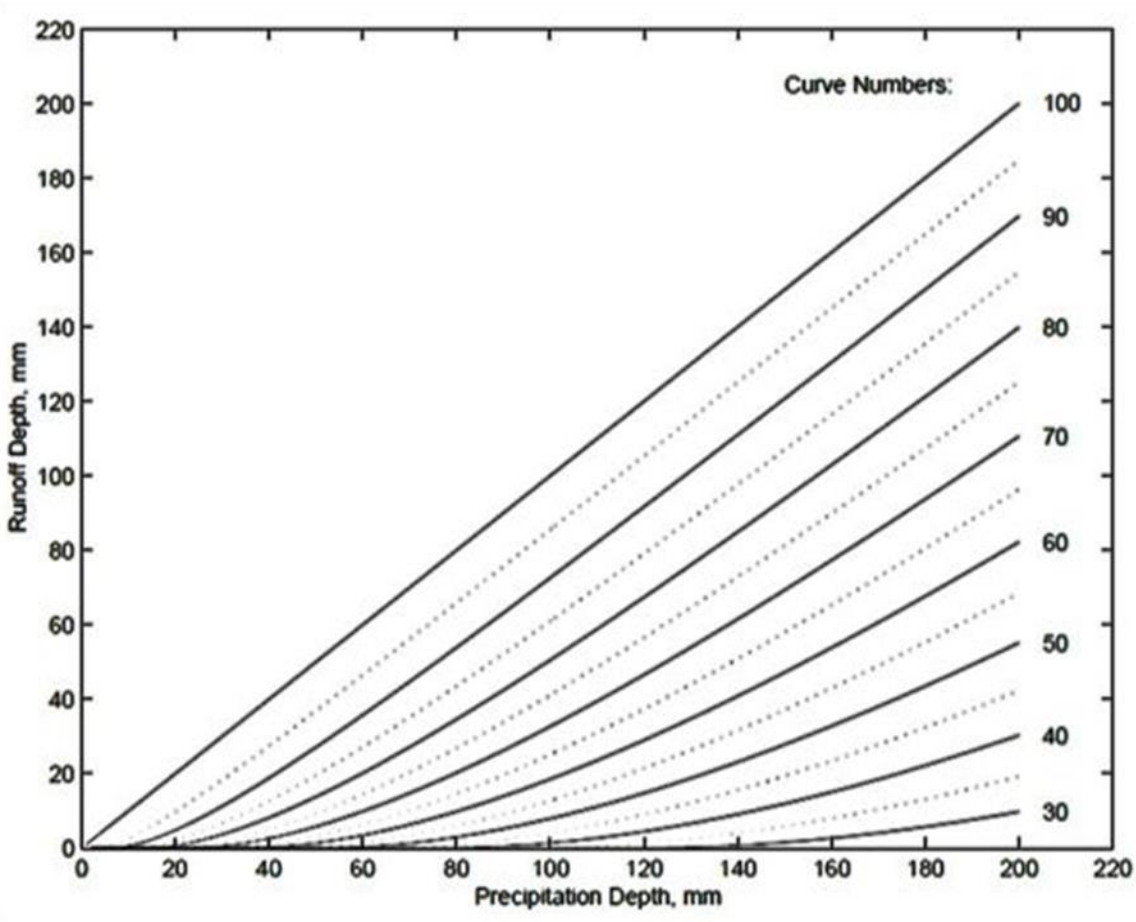


Figure (2.2): SCS CN equation ( Neitch et al., 2005)

## 2.5.2 Factors influencing curve number (CN)

The following factors will be clarified:

1. Groups of Hydrologic Soils.
2. Type Coverage.
3.Land Use/Land Cover Treatment.
4. Hydrologic State.
5.Antecedent Moisture Condition (AMC).

## 2.5.3 Hydrologic Soil Groups

The soil was divided into hydrological soil categories according to data on measuring moisture, runoff, and rainfall (Musgrave, 1955). As stated by the United States' National Resources Conservation Service (NRCS, 2007), a hydrological group is a collection of soils with similar properties. possible runoff under specific cover and storm conditions. NRCS separated the hydrological classes for soils based on characteristics of soil infiltration (Neitch et al., 2005), hence the SWAT Model made advantage of this classification.

a) Group A: Soils have strong infiltration rates, open water flow, and little possibility for runoff even when entirely saturated.

b) Group B :Soils, which have a modest rate of infiltration even when totally wet, and water may freely percolate through the soil.

c) Group C: Soils in this group have moderately high runoff potential when thoroughly wet. Water transmission through the soil is somewhat restricted.

d) Group D: Soils in this group have high runoff potential when thoroughly wet. Water movement through the soil is restricted or very restricted.

## 2.6 SWAT-CUP Calibration and Validation Program Overview

The SWAT Calibration and Uncertainty Program (SWAT-CUP) is an external software program designed specifically for calibration and uncertainty

analysis. (Abbaspour ,2007) developed five calibration programs (SUFI-PSO, GLUE, SUFI-2, ParaSol, and MCMC. SUFI-2 (Sequential Uncertainty Fitting) is an algorithm.steps to determine the majority of the observed data within the 95% confidence band uncertainty in estimation.The overall output uncertainty is measured by the 95% prediction uncertainty (95PPU), which is calculated at the 2.5% and 97.5% locations of the cumulative distribution of the simulated stream flow as an output element extracted from Latin hypercube sampling. The P-factor is the percentage of observed data that the 95PPU matches. It ranges from 0 to 1, with 1 being the ideal value, indicating that all of the observed data is within the model calculations. The R-factor is calculated by dividing the mean width of the band by the standard deviation of the observed variable. It ranges from 0 to ∞, with 0 indicating perfect match between simulation and observation. Based on the experience, an R-factor of around 1 is generally desirable (Abbaspour et al., 2015). The P-factor and R-factor indicators were used to assess the goodness of fit for calibration.). SUFI-2 supports the use of various optimization objective functions, such as Nash-Sutcliff efficiency (NS) (Nash and Sutcliffe, 1970) or coefficient of determination $R^2$. NS and $R^2$ values of 0.5 are considered poor, values greater than 0.5 are considered satisfactory, and values greater than 0.75 are considered excellent (Gassman et al., 2007).

## 2.7 Previous Research

Al Saady et al. (2015) assessed how the Lower Zab region's land use has evolved between 1976 and 2014 using aerial pictures from Landsat, classifying them by using GIS into several categories, determining the overall accuracy and Kappa coefficient 83.43 % ,0.811%, and determining the progression of urban areas.

Buyuksalih (2016) used aerial photographs from Landsat for period (1987-2007) and categorizing them into nine classes using the controlled classification

in arc GIS software method and calculating the 1987 Landsat image overall accuracy of 79 % and a kappa value of 0.76, the 2007 Landsat image overall accuracy of 83.50% and kappa value of 0.81. for Istanbul. As a consequence, a 20-year analysis of Istanbul's development was displayed. The categories have made it feasible to precisely and affordably quantify, map, and evaluate changes in land cover across time.

Azizi et al. (2016) retrieved and examined the land use maps of the Ardabil plained in Iran's northwest over a period of four years (1989, 1998, 2009, and 2013). Then, they predicted future land use changes for 2030 used an integrated CA-Markov model in IDRISI Selva 17.0 By 2030, the built environment and agricultural region accounted for the majority of the changes, which continuous increased.

Zhang et al. (2016) evaluated the separate and combined hydrological impacts of land use change and climate variability in the headwater region of a typical arid inland river basin, known as the Heihe River Basin, northwest China, in the recent past (1995-2014) and future (2015-2024) by combined two land use models (the Markov chain model and Dyna-CLUE) with a hydrological model (SWAT). Future climate change will very certainly have a far higher influence on hydrological regimes than on land use. The influence of altering land use, on the other hand, should not be overlooked, especially if future climates are dryer, since this may compound the hydrological consequences.

Omani et al. (2007) used (SWAT2000) model to study the water and sediment yields in the 5793 $km^2$ Gharasu watershed on Iran's extreme western frontier.The SWAT2000 software's digital elevation model (DEM), land cover, and soil map interfaced with Arc View GIS data layers.The model was calibrated between 1991 and 1996, and it was verified between 1997 and 2000. To estimate the load of suspended silt, the hydrological conditions calibration

model was utilized. The model was used to forecast the impact of various land use and conservation measures on the basin's sediment output. Two different management scenarios for soil conservation were considered in order to evaluate the effects on sediment yielding First scenario: With due attention to topographic conditions and possibility of "contouring" or "contouring and terracing" the critical sub-basin 16, 17, 19, 37 and 39 are suitable for land management practices. Reduction of erosion in the agricultural HRUs located in lower parts of these critical sub-basins.Second scenario: Because land management practices in hilly and mountainous areas are impracticable, land cover changing of these areas is recommended for soil conservation.

Regmi et al. (2017) compared the CA-Markov model with the GEOMOD model to predict future LULC changes in the Phewa Lake Watershed, Nepal, and found that the integration of the CA and Markov models was effective in projecting future LULC scenarios compared to GEOMOD. Considering the model's vast applications in the field of LULC change analysis and its ability to broaden understandings about complex spatial systems, the best them got, no study in Botswana has employed the CA-Markov model to simulate future LULCs, particularly in the country's important catchments. Therefore, this work was among the first to test the applicability of the CA-Markov model to simulate future LULC patterns for the Gaborone dam catchment, Botswana, and their implications on future water resource management in the catchment

Boran and Yadav (2017) created LULC maps for the years 1990 to 2000 in Jodhpur in western region of the Rajasthan by using remote sensing satellite data and GIS technologies, and they predicted the year 2020's LULC maps used a CA (Cellular Automata)-Markov process model. as aresult they anticipated built-up expansion

Welde and Gebremariam (2017) estimated the possible consequences of the land. the influence of land cover dynamics on hydrological responsiveness (stream flow and sediment yield). This was accomplished by combining GIS with the SWAT model. Simulation and sensitivity analysis were done for each land use by allocating HRUs based on multiple HRU definitions and subdividing the catchment into 47 sub-catchments. Changes in land cover had a favorable impact on the Tekeze dam Northern Ethiopia.The expected watershed response affected by the transition from grass and shrub land to agricultural land. Growing bare land and agricultural zones resulted in increased volume and seasonal as well as annual stream flow.

Hamad et al. (2018) used Landsat 5 images from years 1993, 1998, 2003, and 2008 as well as Landsat 8 images from the year 2017.they used GIS software to construct land use maps in The National Park's Halgurd-Sakran Core Zone (HSCZ) in Iraq's Kurdistan region. they proposed two scenarios and used A Cellular Automata (CA)-Markov chain model to simulate future land use changes to the year 2023 under two alternative scenarios (Iraq under siege and Iraq after siege). they finded indicate that in the next six years, areas became more stable and homogeneous.as depicted in the second scenario this circumstance had a beneficial effect on the park.

Alam et al. (2019) examined The Kashmir valley's changes in land use and land cover between 1992 and 2015 through this research. A maximum likelihood classifier used to classify Landsat satellite imageries and produce LULC using supervised approach. Three patterns of land use and land cover change were identified in the study area: (1) a consistent increase in the area covered by marshy, built-up, barren, plantation, and shrubs; (2) a continuous

decline in agriculture and water; and (3) a decrease (1992-2001) and increase (2001-2015) in the classes of forest and pasture.

Mengistu et al. (2019) conducted the investigation in South Africa's Soutloop River Catchment. The goal of theirs work was to construct, calibrate, and assess the SWAT model in catchments with limited data using the regionalization with physical similarity technique. This technique employed two calibration and validation processes, one in the donor catchment and the other on SWAT-CUP. The uncertainty analysis found that the P-factor (0.7) and R-factor (0.8) were at suitable levels. Furthermore, the model performance analysis identified acceptable value ranges, and the study contained recommendations for further inspection approaches to lower the study's model uncertainty.

Messele and Moti (2019) assessed how the hydrological response of the Weib watershed's basin of the upper Genale Dawa River located in the southeastern part of Ethiopia changed in the past and how it could change in the future. To compare the effects of stream land use change on the flow of the research region, the Model for Soil and Water Assessment was employed. The study served as a paradigm for replacing metered discharge with a ready supply of calibrated geographical and temporal data. When it comes to land usage, there has been an increase in habitation area and cultivated land. While amounts of woodland and grassland have decreased

Khwarahm et al. (2021) modelled LULC maps for 2017 and 2050 in Ca Marcov model by using the categorized (1988–2002, and (2002–2017) LULC maps in Erbil governorate in the Kurdistan region of Iraq (KRI). they expected Built-up land, agricultural land, plantation, dense vegetation, and water bodies rised. Sparse vegetation and barren terrain, on the other hand, dropped.

Abdulrahman and Ameen (2020) utilized GIS and remote sensing to categorize LULC classes in Duhok in the Kurdistan region of Iraq (KRI).

district from 1999 to 2018, and calculated the results using an integrated cellular automaton and ca-markov chain model to simulate LULC map in 2033. they concluded outcomes demonstrate that Duhok district has experienced a total of 184.91 km changes during the period and soil and grass constituted the majority of changes among LULC classes and increased continuously

Belihu et al. (2020) saw how land use and land cover changes (LULCC) affected stream flow in Ethiopia's upper Gidabo Watershed between 1985 and 2005. The Arc Swat algorithm was used to complete the synthesis of the swat and SWAT-CUP algorithms. According to LULCC, both agricultural and urban land have expanded. The effects of grassland dynamics on hydrological response. Evapotranspiration and surface runoff increased throughout the rainy season, and the dry season stretched as the flow lengthened. Variation in surface flow.

Hussain et al. (2021) identified the pattern of LULC, NDBI, and NDVI change in Lodhran district, Pakistan, from Landsat pictures collected over a 40-year period, by using supervised classification maximum likelihood in ERDAS software LULC classified into four class: water bodies, constructed space, bare dirt, and vegetation. Building areas grew in 2017 compared to 1977. The Lodhran district's NDVI values were highest in 1977 (up to + 0.86) and lowest in 1997 (up to- 0.33).

Liang et al. (2021) chosed The Minjiang River Basin as a study area. The analysis of land use, land cover, and division of the area using GIS using the Maximum method of Eclihud, dividing the area into six areas, and found that forests increase and constitute 62% of the total area and the majority of the building properties are located along the water body.

Shen et al. (2021) created land use categorization map used RS and GIS technologies by the greatest probability technique for the two phases of Nanjing

in China from 2015 to 2020. There were "two dips (arable land and bare land) and four gains lost in Nanjing overall land use shift" between 2015 and 2020. (urban development land, woodland, grassland, and water area). The quantity of area conversion varies depending on the type of land use as well.

Matlhod et al. (2021) simulated LULC variations in the Gaborone dam Location in Botswana. Country, Botswana. District by using cellular automata and Markov chain (CA-Markov) model combinations. they classified Landsat pictures for 1984, 1995, 2005, and 2015 and the simulation showed that between 2015 and 2035, the categories of cropland, built-up land, and bare land rised and shrubland, tree savanna, and water body, reduced in areal coverage.

Leta et al. (2021) examined the effects of LULC on the hydrological parameters of the Blue Nile River Basin's Nashe watershed East Africa .They fed historical and predicted LULC change scenarios for the Nashe watershed into a calibrated SWAT model . they concluded Between 2035 and 2050, grass will become more plentiful. Land might reduce the undesired proclivity. They expected the land's extent decline in urban and agricultural land will arise from an increased in surface runoff and a decreased in groundwater.

Engida et al. (2021) determined how LU/LC change has affected the Upper Baro Basin's hydrological.they used (SWAT) model to simulate streamflow. Changes in LU/LC between 1987 and 2017 include a change in flood frequency, greater peak flows, base flow, and soil erosion. The curve number, soil layer accessible water capacity, and soil evaporation composition factor were discovered to be the most sensitive streamflow features. Both the calibration and validation results demonstrated that observed and simulated streamflow agreed well for the calibration periods of 1990-2002 and 2003-2009, respectively.processes in the years 1987, 2002, and 2017

Tembo and Volk (2022) looked at the effects of changing land use and land cover on river flow in the Chalimbana river catchment, hongwe District, Zambia. This study analyzed, spatially, the impact of land use changes from the year 1980 to 2020. Remote sensing and GIS related soft wares were used to analyze the Landsat images; riverflow and rainfall data for the period 1980 to 2020 was analyzed using linear regression and trend analysis with the help of Xlstat (in excel) and Minitab soft waresForests and vegetables were in low supply, while grass, farmland, and buildings were on the rise. so did the number of people agriculture activities have made a substantial contribution to this a rise in the river's flow

Yeneneh et al. (2022) analyzed spatiotemporal changes in land use and land cover and their effects on land surface temperature in the Suha watershed, in Ethiopia's northwest highlands. They used GIS to classify images from Landsat by using controlled classification and accuracy assessment for period (1989-2019) LST also extracted from these satellite images' thermal bands. They concluded a rise in agriculture and a fall in grazing and shurbing.

Ghalehteimouri et al. (2022) created LULC scenario for 2049 by using CA marcov, and examined LULC variations in Iran's Zarrinérd River Basin (ZRB)and they used numerous pictures and data gathered from satellite data between 1989 and 2019. The grassland and mountain LULC classes have continued to drop at a greater pace than the other classes, according to the ZRB's results. Additionally, the regional and temporal growth of the LULC class depended on the availability of water resources and the amount of precipitation in the past and future.

Attuley et al. (2022) Used the Soil Water Assessment Tool and assessed how the hydrological components of the Vea reservoir catchment, a sub-catchment of the White Volta Basin in West Africa. responded to past, current, and future

land-use change scenarios (1985, 1996, 2006, 2020, 2030, and 2040) using SWAT). The example functioned well, with calibration and validation.The models outcomes showed that Between 1986 and the predicted 2040 increase in CN, ET and base are decreased. Vegetation restoration is essential to decrease eroded sediment production from the watershed to ensure reservoir storage.

The change in land use and land cover and the prediction of their future change and the investigation of the effects of this change on the hydrological processes in the Lesser Zab River Basin as a whole were not included in previous studies Therefore, this research included

# Chapter Three

# Research Data, Methodology, and Applications

## 3.1 The Study area

Lesser Zab River Basin is located in the borders of northeastern Iraq and northwest Iran as shown in (Fig 3.1). It covers an area of 20,000 $km^2$, contains a wide range of landscapes, and extends between (35° 10.00 - 36° 55.00) latitude and (43° 25.00 - 46° 20.00) longitude. The main tributary of the Tigris River, the Lesser Zab River (LZR), also known as Lower Zab or Little Zab River, has around 76 percent of its basin in Iraq and 24 percent in Iran. A river of eighth order, the LZR travels from northeast to southwest. It flows into the Tigris River after feeding the Dukan Lake Reservoir. The river receives its inflow from precipitation, snowmelt, and many springs, which result in a high spring flow and a low summer discharge. The LZR's average annual discharge is 71700000000 $m^3$, although since the Dukan Dam was built, that amount has decreased annually by 50700000000 $m^3$ (Frenken, 2009).

The climate in the basin varies from semi-arid to arid. In the north and northeast, the climate is humid; in the south and southwest, it is arid. higher altitude regions in with a mean annual precipitation of more than a meter, the north and northeast of the basin receive a lot of rain. as high as 850 meters. Its significantly decreases until the Tigris River's confluence, falling to less than 315 mm/a in the lower elevation region area to the south and southwest of Dukan Lake. The top part of the basin region is covered by the Zagros Suture Zone (3000 m.a.s.l) and the severely folded zone (Jassim and Goff, 2006). The foothills zone, which is characterized by clastic unresisting rocks, is where the higher portion of the basin is located.

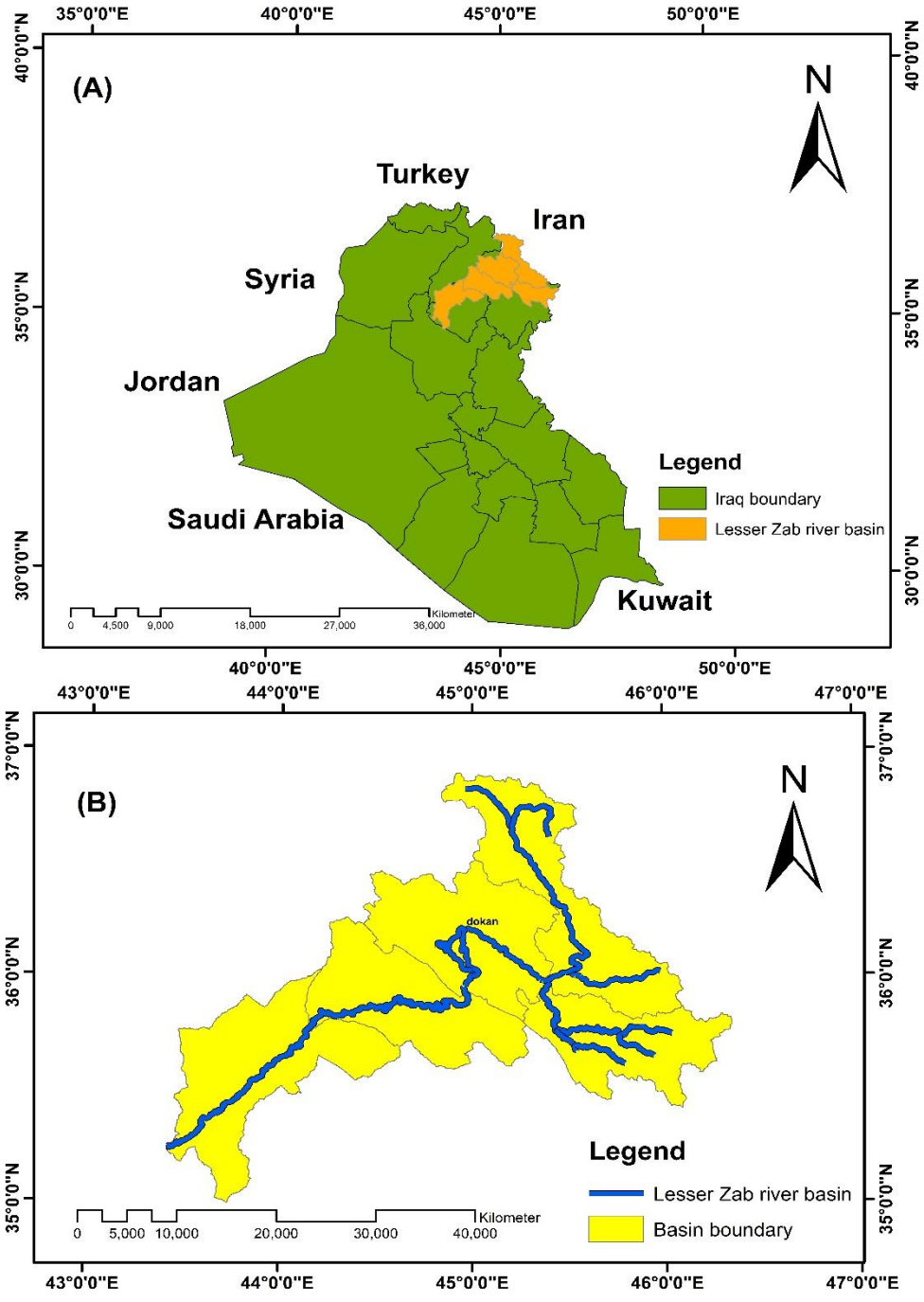


Fig (3.1) Lesser Zab River Basin

Two dams are constructed in the Iraqi, the Dukan dam and the Dibis dam in the Lesser Zab River Basin. The first was constructed as an arch dam in 1961 and is located upstream of Dukan City 6970 Million Cubic Meter is the maximum amount of storage. It provides water for hydropower production as well as irrigation and is used to control Tigris flow. It controls the water flow into the Kirkuk Project for agriculture. 130 kilometers upstream of where the Tigris and Lesser Zab meet is where it is situated. The Kirkuk Irrigation System was developed in the late 1960s and uses water.from the Lesser Zab and Lake Dukan to irrigate 3000000 hectares.

Iran continues to build the Sardasht in 2011 as part of its strategy to combat water scarcity.9 kilometers from the Iraqi border, a dam on the Little Zab river. Its use (starting in June 2017) led to in most areas in Sulaymaniyah Province, there is a lack of water for irrigation and drinking in Kurdistan.

## 3.2 Data Analysis

### 3.2.1. spatial data

The data used in this study is made up of four historical consecutive-years (1989, 1999, 2010, and 2021) Landsat satellite imagery with a spatial resolution of 30 m as shown in (Table 3.1), (Table 3.2). The pictures scenes with the least amount of cloud cover (less than 10%) were downloaded from the USGS Earth Explorer website (https://earthexplorer.usgs.gov) in December 2021.

Landsat satellite data was chosen for its open accessibility, appropriateness for the purpose of the study, lengthy observation time, and high spectral and spatial resolution for LULC studies. (Mancin et al., 2014)

Table (3.1) Earth observation imagery data collected for the Lesser Zab River Basin

| Path | Row | Date/time(sensor) | | | |
|---|---|---|---|---|---|
| | | 1989 | 1999 | 2010 | 2021 |
| 168 | 35 | 16.07.1989(TM) | 20.07.1999(TM) | 02.07.2010(TM) | 16.07.2021 (OLI) |
| 168 | 36 | 21.07.1989(TM) | 20.07.1999(TM) | 09.07.2010(TM) | 16.07.2021 (OLI) |
| 169 | 36 | | 27.07.1999(TM*) | 09.07.2010(TM) | 23.07.2021 (OLI) |
| 169 | 36 | 15.07.1989(TM) | | | 23.07.2021 (OLI) |
| 170 | 36 | | | | 30.07.2021(OLI)** |

* Thematic Mapper; ** Operational Land Image; Spatial resolution of 15 m is used for the panchromatic band 8 for Landsat 8

Table (3.2) desicription of land cover classes

| Class | Desicription |
|---|---|
| Forest | Very densely vegetated areas, mostly forest and dense shrub lands. |
| Agricultural land | Presently cropped area with noticeable greenness |
| Urban area | This class includes paved highways, businesses, industrial zones, residences, and other paved locations |
| Bare land/light | Lands with no apparent/or negligible plants, specially no evident covers of trees or shrubs, wasteland, rocky mounts and bare open lands |
| Bare land/dark | Lands with no evident/or negligible plants, particularly no noticeable covers of trees or plants. Rocky mounts, bare rocks, hills, and soil |
| Water | Open water bodies such as lakes, rivers, and permanent ponds are included in this category |

## 3.2.2. Metrological Data

The SWAT model requires the following data (climatic information, such as rainfall, solar radiation, and temperature ranges (maximum and minimum), relative humidity, and wind speed) on a daily basis for at least three station.

Due to the severe scarcity and fluctuation of the data obtained from the General Authority for Meteorology and Seismic Monitoring of the Iraqi Ministry of Transport, The Climate Forecast System Reanalysis (CFSR) dataset is made up of hourly weather forecasts from the National Centers for Environmental Prediction (NCEP), CFSR supplies weather criteria for SWAT runoff simulation (Fuka et al., 2013). SWAT has two input modes for weather data: simulated and gauged weather; in this investigation, the gauged mode was employed. The data for the watershed were acquired on May, 2022 for the period 1/1/1979 to 31/7/2014, from (http://globalweather.tamu.edu/),as shown in table (3.3).

As input weather data, all models used the CFSR dataset. SWAT recreated the weather data using the weather generator (wgen). Figures (3.2) depict the location of CFSR weather stations.

Table (3.3) The stations for study area

| Subbasin | Name | Latitude ($^0$) | Longitude ($^0$) | Elevation (m) |
|---|---|---|---|---|
| Up stream | 1 | 36.1 | 45.3 | 1203 |
| Up stream | 2 | 36.1 | 45.6 | 1473 |
| Up stream | 3 | 36.1 | 45.9 | 2420 |
| Down stream | 4 | 35.75 | 44.375 | 496 |
| Down stream | 5 | 35.75 | 44.688 | 833 |
| Down stream | 6 | 34.935 | 43.498 | 112 |

## 3.2.3 Prepiaring DEM's for the study area

Using data from LANDSAT Shuttle Radar Topography Mission Version 3.0 of the (SRTM) DEM has a spatial resolution of 1.0 arc. second (30mx30m). The US website provides free downloads of these imagery. Geological Survey (USGS) webpage via the internet from ESRI satellites using Tag Image File Format (https://earthexplorer.usgs.gov)) tiff with a World Geodetic System reference 1984 geographic projection (WGS84)

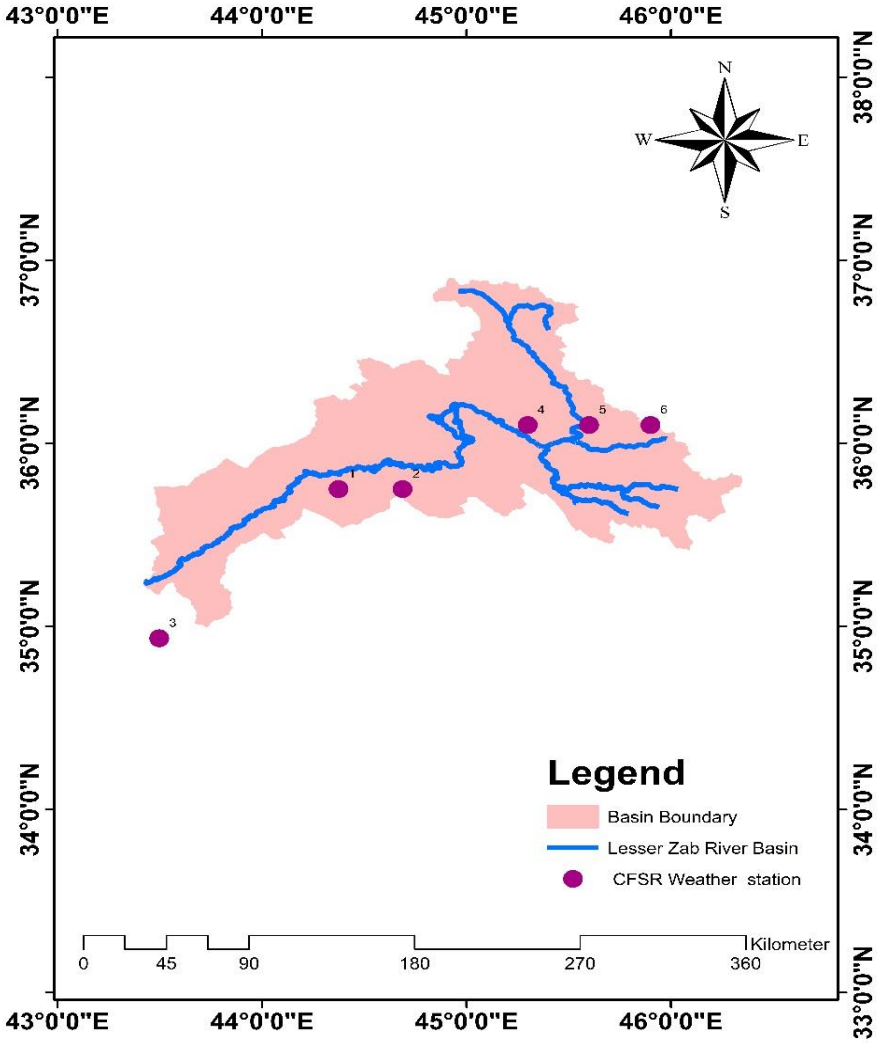


Fig (3.2) Weather Station Distribution over the Lower Zab river basin

Eight raster files from the DEM as shown in table (3.4) were downloaded in January 2022. Composed elements and mosic and extract on shape file study area (The shape files of the Iraqi borders and UZRB have been obtained from the Global Administrative Areas (GADM 2012) and the Global and Land Cover Facility (GLCF 2015) databases, respectively represented) on a UTM projection 38N as a single set of raster lines as shown in fig (3.3).

Table (3.4) The sensor, as well as the date and time of the scene, are captured from USGS for DEM

| Path/row | Date/Time |
|---|---|
| n35_e043 | 23-9-2014 |
| n35_e044 | 23-9-2014 |
| n35_e045 | 23-9-2014 |
| n35_e046 | 23-9-2014 |
| n36_e043 | 23-9-2014 |
| n36_e044 | 23-9-2014 |
| n36_e045 | 23-9-2014 |
| n36_e046 | 23-9-2014 |

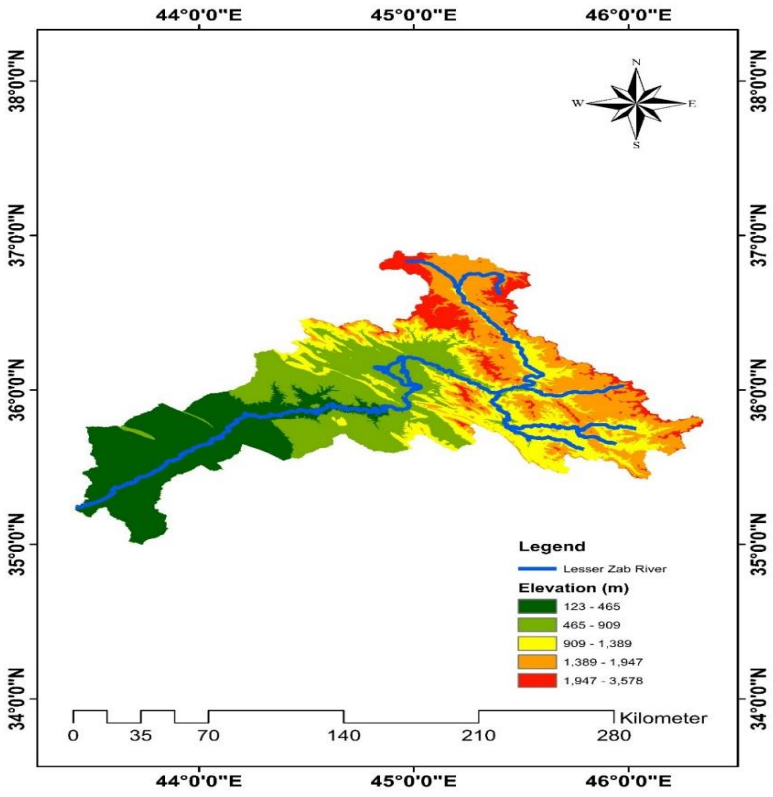


Fig (3.3) Digital Elevation Model for Lesser Zab River Basin with resolution of 30 m (USGS,2022)

### 3.2.4 Soil map

The Food and Agriculture Organization of the United Nations (FAO, 1995) provided data for 5000 varieties of soil in two levels (0-30 and 30-100 cm), from which soil data were gathered. depth) at a 1:5000000 spatial scale. The FAO soil database contains information on each soil, and this database was included. For soil categorization, a SWAT database and lookup tables were created (Fouad, 2016). The data were retrieved from http://www.fao.org/nr/land/soils/digital-soil-map-of-the-world/en/ datum and geographic projection WGS84 in June 2022.

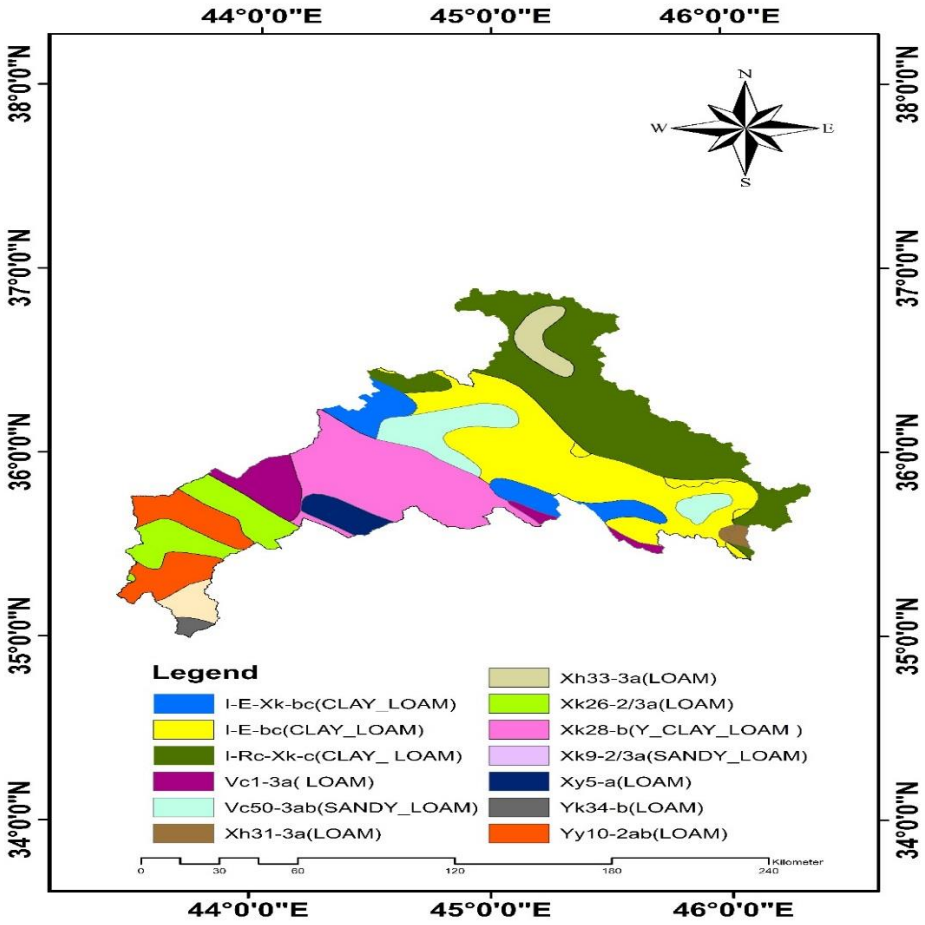


Fig (3.4) Soil map applied in ARC SWAT(FAO,2022) for the study area

### 3.2.5 Hydrological Data

The SWAT CUP program is used to calibrate and validate of the ARC SWAT results. This is accomplished by entering the actual data of the station that was obtained from Iraqi Ministry of Water Resources (MoWR), the National Center for Water Resources Management that includes average monthly inflow and absolute discharge of the Dukan dam for the period 1979 to 2021, The monthly average discharge of the Dibis dam, the average monthly discharge rate for the irrigation of Kirkuk for the period 2002 to 2021, as shown in Appendix B.

The table (3.5) shows the summary of data used in ARC SWAT program

Table (3.5): The data sources entered into the SWAT model

| Data Typ | Data Source | Organization | Format | Year |
|---|---|---|---|---|
| DEM | SRTM | United states geological survey (https://earthexplorer.usgs.gov/) | Raster | 2014 |
| Land use | Landsat 4,5,8 | United states geological survey https://earthexplorer.usgs.gov/)) | Raster | 2000,2010 |
| Soil | DSMW | FAO/UNESCO http://www.fao.org/nr/land/soils/digital-soil-map-of-the-world/en/ | Raster | 2022 |
| Weather Data | CFSR | CFSR | Vector | 979_20114 |
| Weather Data | General Authority for Meteorology and Seismic Monitoring | Iraqi Ministry of Transport | vector | Different, fluctuating years |
| Hydrogical data | National Center for Water Resources Management | Iraqi Ministry of Water Resources (MoWR), | vector | 2000-2022 |

## 3.3 Methodology of producing LU/LC maps

### 3.3.1: ARC GIS

Ageographic information system (GIS) is a system that creates, manages,analyzes, and maps all types of data. GIS connects data to a map, integrating location data with all types of descriptive information.In this study used ARC GIS version 10.7 to create LU/LC maps and image classification and accuracy assessment and calculate NDVI .and used version 10.5 to install ARC SWAT because 10.7 or earlier versions doesnot support downloading ARCSWAT as shown in fig (3.5)

### 3.3.2 SPSS software

The program SPSS stands for Statistical Package for Social Science. It is statistical software that makes data compilation and analysis easier. It used in this study to verify the reliability of the results obtained from the Markov program by finding the correlation between the map classified in the ArcGIS program and the predictive result from Markov for the same year.

### 3. 3. 3. IDRISI Selva 17.0

The software provides a platform for integrated modeling environments as well as utilities for importing and exporting GIS data.it contain many tools, In this study used MARCOV chain analysis to create transition area matrix and probability area matrix and used CA marcov to predict LU/LC Future maps. as shown in fig (3.6)

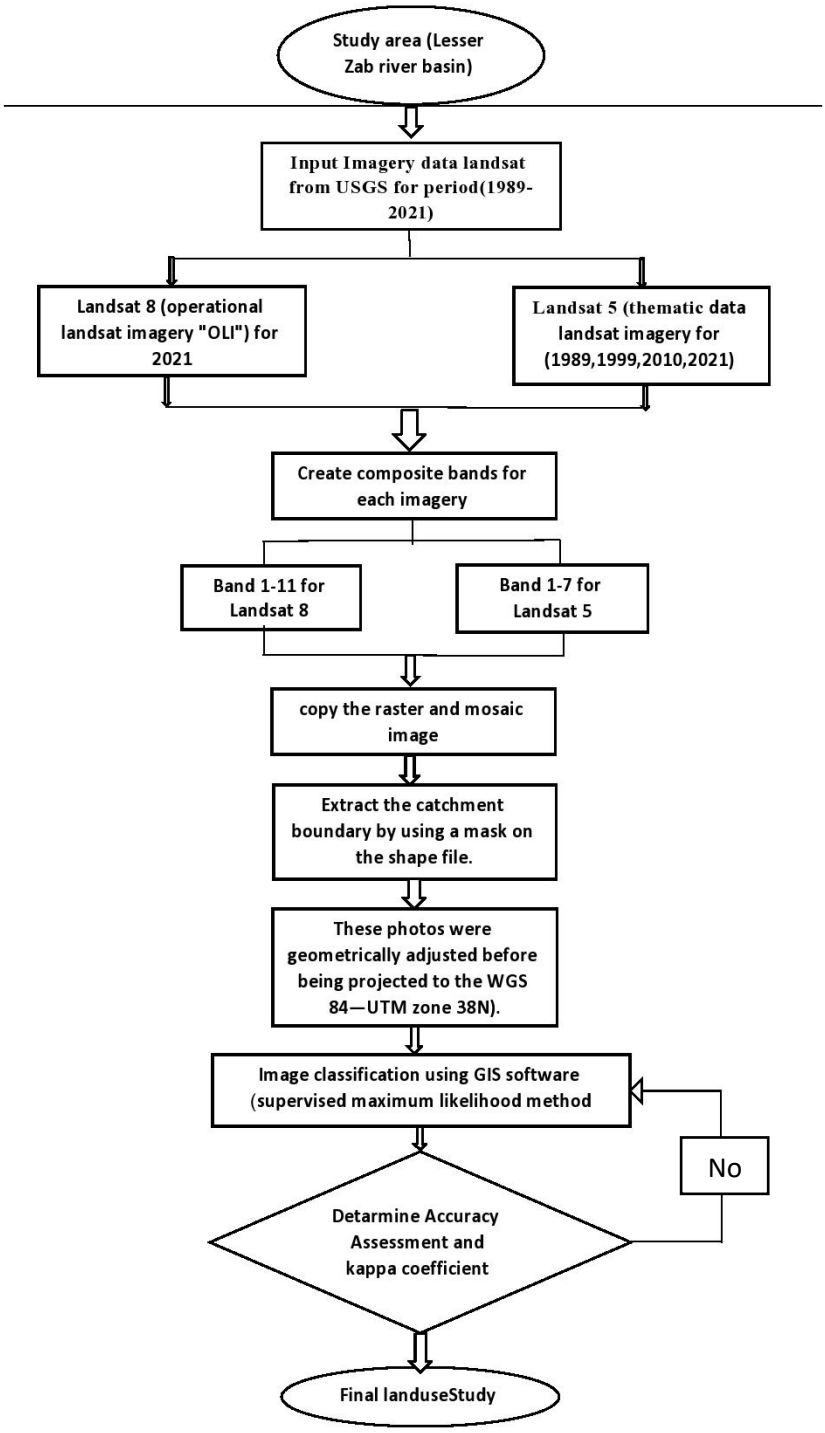


Fig (3.5) The applied methodology for assessing the implication of land use and land cover (LU/LC) alteration on the Lesser Zab River Basin, northeastern Iraq

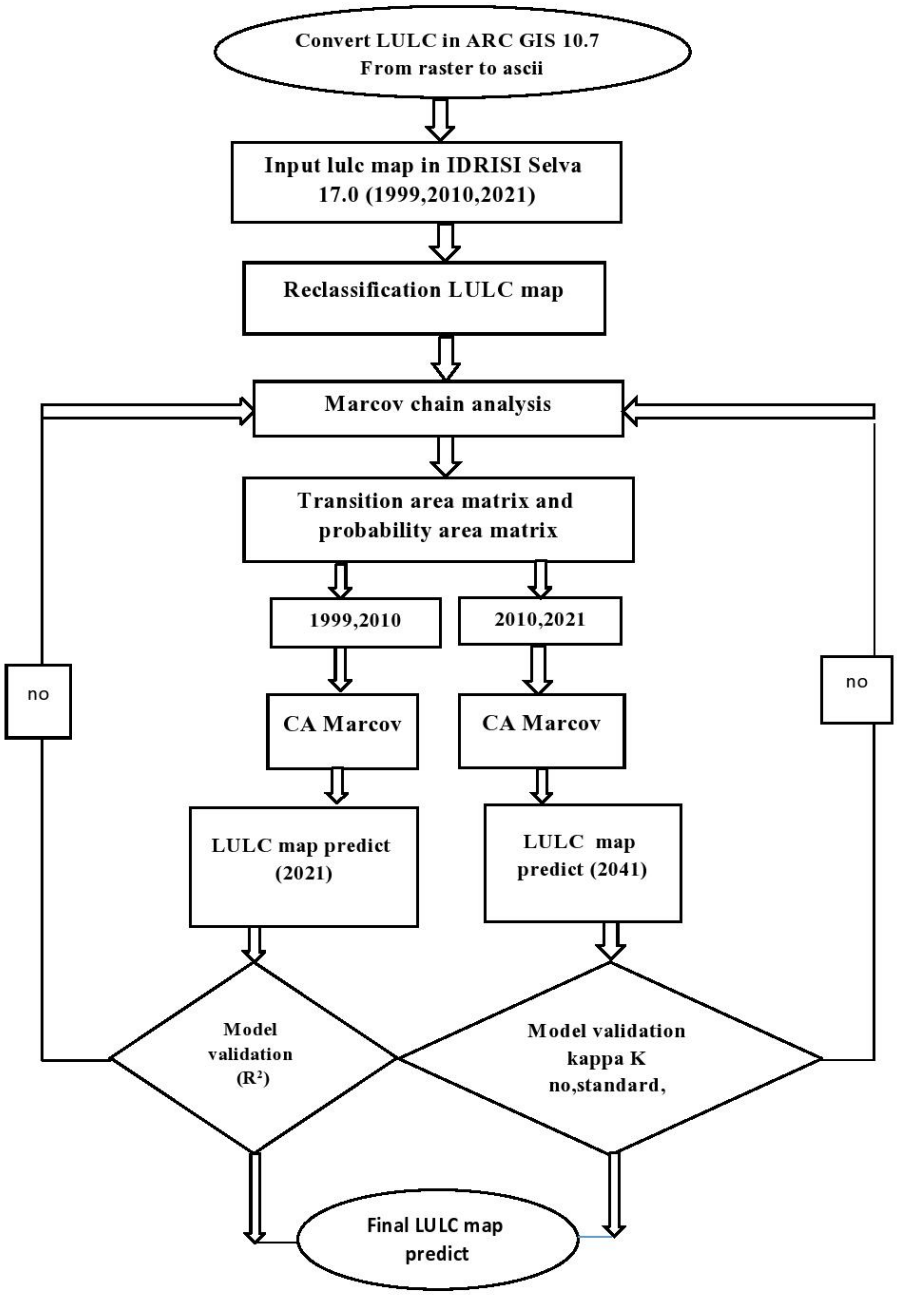


Fig (3.6) A simplified detailed explanation of the Markov model

### 3.3.4. ARC SWAT

This study used Arc SWAT version 2012, an extension of ArcMap 10.5 from the GIS software group, to determine the monthly runoff surface. All spatial data must be in the same projection for Arc SWAT. prior to any processing taking place. The WGS84 spatial datasets project (LANDSAT, DEM, LULC, and the FAO's soil map) was anticipated to WGS1984 UTM Zone38 N. Using ArcGIS 10.5, re-projections were carried out. The hydrological model SWAT includes a large number of parameters, and it has been successfully developed and used for more than 20 years. (Fouad ,2016). As shown in fig (3.7)

### 3.3.5 SWAT CUP

SWAT CUP was used to calibrate and validate the model. SWAT CUP has five calibration techniques, but the sequential uncertainty fiitting method is the most accurate was employed, according to (Wu and Chen, 2015) and (Molina et al., 2016), can describe observed data with modest errors. There are more uncertainties and more runs are required to attain a satisfying outcome.The calibration and validation of discharge occurred in two stage during period (2000-2021) respectively. The calibration and validation results are displaye P-BIAS (Nash and Sutcliffe, 1970) (Gupta and Sorooshian, 1999). The model performs better when the RMSE is low (Moriasi et al., 2007). Equations are used to express these matrixes

$$\mathbf{N}\text{SE}= 1 - \frac{\sum_{k=1}^{n}\left(Y_{obs,k}-Y_{sim,k}\right)^2}{\sum_{k=1}^{n}\left(Y_{obs,k}-\overline{Y_{obs}}\right)^2} \qquad 3.1$$

$$R^2=\left\{\frac{\sum_{k=1}^{n}\left(Y_{obs,k}-Y_{sim,k}\right)\left(\left(Y_{sim,k}-\overline{Y_{sim,k}}\right)\right)}{\sqrt{\sum_{k=1}^{n}\left(Y_{obs,k}-\overline{Y_{obs}}\right)^2}\sqrt{\sum_{k=1}^{n}\left(Y_{obs,k}-\overline{Y_{obs}}\right)^2}}\right\}^2 \qquad 3.2$$

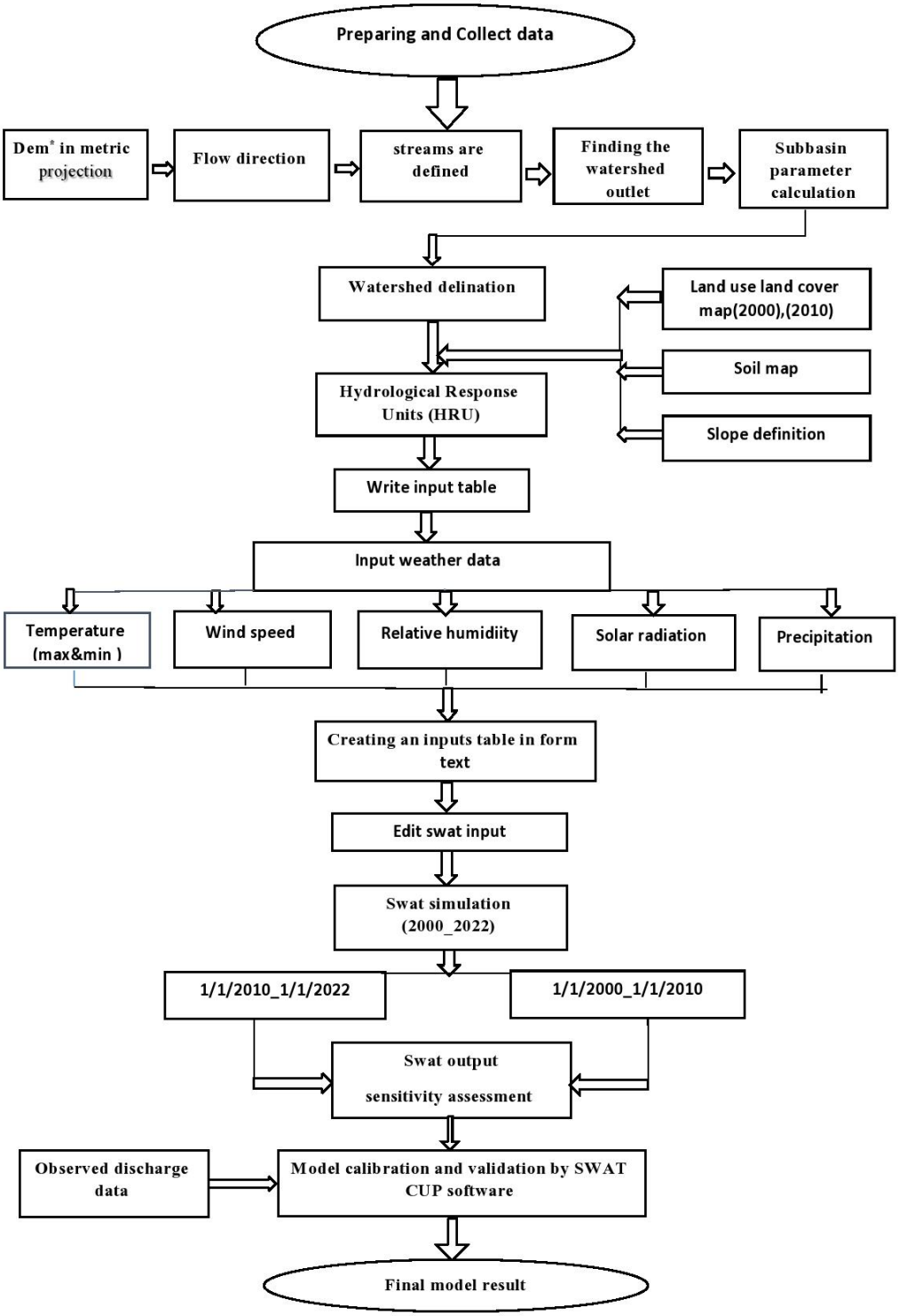


Fig (3.7) Explanation of the ARC SWAT** program's step

* Digital Elevation Model, **Soil water assessment tool

$$RSR = \frac{RMSE}{SD} \quad 3.3$$

$$P\text{-}BIAS = \frac{\sum_{k=1}^{n} \overline{(Y_{obs} - Y_{sim})}}{\sum_{k=1}^{n} Y_{obs}} \quad 3.4$$

Where: The Nash-Sutcliffe coefficient is NSE, the coefficient of determination is $R^2$, and the ratio of the root mean square error to the standard deviation of measured data is RSR, Performance Evaluation as shown in table (3.6). n is the number of observed data, $Y_{obs,k}$ is the observed stream flow on month k, $Y_{obs}$is the average observed stream flow, $Y_{sim,k}$ is the stream flow simulated on month k and $\bar{y}_{sim}$ is average simulated flow,$\overline{y_{obs}}$the mean of observed stream flow on month

Table (3.6) shows the performance evaluation metrics for stream flow simulation

| Performance Evaluation | NSE | PBIAS | $R^2$ |
|---|---|---|---|
| Unsatisfactory | NSE ≤ 0.5 | PBIAS ≥ ±25 | R2 < 0.50 |
| Satisfactory | 0.5 < NSE ≤ 0.65 | ±15 ≤ PBIAS < ±25 | 0.50 < $R^2$ < 0.70 |
| Good | 0.65 < NSE ≤ 0.75 | ±10 ≤ PBIAS < ±15 | 0.70 < $R^2$ < 0.80 |
| Very good | 0.75 < NSE ≤ 1 | PBIAS < ±10 | 0.80< |

# 3.4. APPLICATIONS

## 3.4.1 Image classification

Using identified ground truth, supervised classification was applied to categorize each pixel. It is advised to employ at least 20 trials when classifying an image using a map that has fewer than three classes (Mahdi and Muhammed 2022), hence thirty or more reference samples for each class were used in this study. The reference sites for 1989, 1999, 2010, and 2021, Google Earth was

taken into consideration. There are numerous steps in the overall process for classifying images. The initial step is to choose training locations.

Using the processed images as a guide, training locations were sampled using the polygon technique, which allowed for the sketching of polygons for a particular spectral class. Throughout the process, various band arrangements, picture enhancements, and color configurations were used to distinguish between and comprehend the surface structures of the photographs. As each band is a data set file for a specific ratio of the electromagnetic field in identifying the study features. The band groupings were chosen based on their applicability.

The same class signs were combined by selecting all the signs from each class. Additionally, the training data set is used to generate class signatures and the whole picture classification. A compound signature was used in the supervised image classification maximum likelihood to map the LULC.

### 3.4.2 Classification Accuracy Assessment

The accuracy evaluation process establishes the value of a map produced using remotely sensed data (Congalton and Green,2019). Using Google Earth serves as the standard reference. accuracy evaluation was performed. Ground control for fifty points at least for each LULC type (apart from aquatic bodies, which receive zero owing of its size) were plotted on the secret photographs.They were transformed into Keyhole Markup Language (KML) opened in Google Earth (as reference points) for the appropriate years.

For map, a total of 251 ground control points were sampled using stratified random sampling, where the number of points was stratified according to the different categories of land use and land cover. As a strong predictor of the accuracy estimate for the LULC map, the Kappa coefficient was also employed to evaluate the classification's correctness.

The defining metric, the Kappa statistic, is a superior measure of inter classifier agreement (Congedo, 2021). The total number of pixels divided by the total number of correctly categorized pixels yields the overall accuracy. The proportion reflects the degree of accuracy of the classification (Fitzgerald and Lees, 1994). The kappa statistic ranges from -1 to 1 as shown in table (3.7). A higher kappa statistic value indicates more accurate categorization results. Scholars discovered that the kappa statistic outperforms the total accuracy score statistically (Fitzgerald & Lees, 1994).

Table (3.7) Statistical measurements to evaluate the intelligent accuracy of a category (Viera and Garrett, 2005)

| s. no | kappa statistic | power of agreement |
|---|---|---|
| 1 | < 0 | Less than chance agreement |
| 2 | 0.01–0.20 | Slight agreement |
| 3 | 0.21– 0.40 | Fair agreement |
| 4 | 0.41–0.60 | Moderate agreement |
| 5 | 0.61–0.80 | Substantial agreement |
| 6 | 0.81–1 | Almost perfect agreement |

An error matrix and Kappa coefficient including user classification and a reference image was used to assess accuracy (Tembo and Volk ,2022). Because it gives a straight forward method of determining the individual accuracies of each class as well as both the errors of inclusion (commission errors) and errors of exclusion (omission errors), an error matrix is a very effective approach to express thematic map correctness. The overall accuracy,User's accuracy,Producer's accuracy, were calculated using the following equations

$$\text{Overall accuracy\%}=\frac{total\ number\ of\ classified\ pixels\ (\ daigonal)}{\text{total number of reference pixels}}\times 100 \qquad 3.5$$

$$\text{User's accuracy\%} =\frac{number\ of\ correct\ classified\ pixels\ for\ each\ classes}{\text{total number of pixels in the classif ied image}}\times 100 \qquad 3.6$$

The producer's accuracy was computed by the following equation:

Producer's Accuracy% =

$$\frac{total\ number\ of\ correct\ \ pixel\ in\ the\ classified\ map\ for\ every LU/\ LC\ class}{\text{total number of reference pixels(Google earth)}} \times 100 \quad 3.7$$

Then, the Kappa coefficient was estimated by the following formula (Al-Saady et al., 2015; Dibaba et al., 2020)

Kappa coefficient% =

$$\frac{\text{total no.of (diagonal} \times \text{reference pixels)} - (\sum(user\ pixel \times procdure\ pixel)}{(\text{reference pixel})2 - (\sum(user\ pixel \times procdure\ pixel)} \times 100 \quad 3.8$$

Producer and user accuracy; and the whole Kappa index of the agreement were calculated, depending on the error matrix. The transition error matrix of the LU/LC denotes the LU/LC change during three periods, 1999, 2010, and 2021 in this study. The following equation is used to estimate the transition matrix (Daba & You, 2022):

$$A_t = \begin{bmatrix} A_{t_{11}} & A_{t_{12}} \ldots\ldots\ldots & A_{t_{1j}} \\ A_{t_{21}} & A_{t_{22}} \ldots\ldots\ldots & A_{t_{2j}} \\ \ldots\ldots\ldots\ldots\ldots\ldots\ldots\ldots & & \\ A_{t_{i1}} & A_{t_{i2}} \ldots\ldots\ldots & A_{t_{ij}} \end{bmatrix}$$

where $A_{ij}$ = the area in transition from land i to j, and each element in the transition matrix is categorized assuming $A_{ij}$ is non-negative and $\sum_j^n A_{ij}=1$.

## 3.4.3 Analysis of Land Use Land Cover Changing

ARC GIS 10.7 (ESRI, 2011) was applied to make the LU/LC images of 1989, 1999, 2010 and 2021 firstly, the land cover classifications were completed, and the LU/LC categories were estimated, then LU/LC analysis and rates of alterations were calculated. Overall LU/LC between two time periods is computed as:

Total LU/LC alteration = Area of the (last year -first year)

Percentage of LU/LC alteration= $\frac{Total\ LU/LC\ alteration}{tatal\ basin\ area\ (\ km2\ )}$ 3.9

To examine the LU/LC inter-category alterations as well as testing the basin experience in LU/LC alterations, a LU/LC array was established for 1989, 1999, 2009, 2019, and 2021 via ARCGIS environment.The variation in area (expansion/shrinkage), stability, and changing between the LULC classes were computed via this matrix

## 3.4.4 The Normalized Difference Vegetation Index: NDVI

Landsat Surface Reflectance-derived Normalized Difference Vegetation Index (NDVI) is the most commonly used vegetation index as it is valuable for understanding vegetation density as well as evaluating plant health changes. NDVI can be derived from Landsat 4–5 Thematic Mapper (TM), and Landsat 8 Operational Land Imager (OLI)/Thermal Infrared Sensor (TIRS). The index is estimated as a ratio of the red (R) to the near-infrared (NIR) values, as equation 3.10 or 3.12 shows, (Hussain and Karuppannan, 2021)

$$\text{NDVI}=\frac{(NIR-R)}{(NIR+R)} \qquad 3.10$$

For Landsat (4,5)

$$\text{NDVI}=\frac{(Band\ 4-Band3)}{(Band\ 4+Band\ 3)} \qquad 3.11$$

For Landsat 8

$$\text{NDVI}=\frac{(Band\ 5-Band\ 4)}{(Band\ 5+Band\ 4)} \qquad 3.12$$

In Landsat 4-7, NIR (near-infrared: 0.76−0.90 mm) = Band 4; and R (red: 0.63−0.69 mm) = Band 3 However, in Landsat 8, NIR = Band 5; and R = Band 4. The NDVI has a popular measurement degree varying between -1 and 1 as shown in Table (3.8).

Table (3.8) Statstical descrioption of NDVI index (Hussain et al.,2021)

| No | NDVI index | Description |
|---|---|---|
| 1 | 0-1 | water bodies |

| | | |
|---|---|---|
| 2 | 0.4-1 | dense plant growth |
| 3 | 0.2-0.4 | Low plant density |
| 4 | 0.2 - 0 | to areas with no vegetation |
| 5 | -0.1 to 0.1 | barren rocks, sand, or snow |

### 3.4.5 Cellular automata and Markov chains simulation

Markov chain is one of the commonly known simulations to measure the degree of alteration during time through functioning the changing likelihood (transition probability) matrix, transition area matrix between $t_0$ and $t_1$ use/land cover time period maps (binary). Based on these matrices and their pixel-wise status, some restricted probability class classifications are expected (Khwarahm et al., 2021). Although the Markov model is verified capable of mimicking the LU/LC modification (Cui et al., 2021; Hyandye and Martz, 2017). Still, the model is inadequate in simulation the areal circulation of the class classifications in the LU/LC maps (Omar et al., 2014).

Alternatively, the Cellular Automata (CA) model (Khwarahm et al., 22021) fills the gap of the spatial dimension constraint. Based on pre-defined conversion situations over time, the CA model calculates the LU/LC class classification new status built on the previous LU/LC status and those of its adjacent class classifications (Omar et al., 2014; Li et al., 2018; Kan-In and Khunrattanasiri, 2020). Integrating Markov chain simulation with the CA model delivers a distinctive prospect to calculate and simulate the spatiotemporal alteration of LU/LC regularly. This interaction model is capable for predicting and simulating difficult LU/LC classes (Hyandye and Martz, 2017). In this study, the CA-Markov model in IDRISI software has been applied to predict LU/LC alteration in the LZRC, during 2021, 2041, based on the (1999–2010) and (2010–2021) and the maximum likelihood classification. The prediction of land-use changes as:

$$S\ (t + 1) \quad S_s\ (t, t+1) = TPM_{ij} \times S_s(t) \qquad 3.13$$

is the system status at the time of t + 1, $TPM_{ij}$ is the transition probability matrix, and $S_s\,(t)$ is the system status at the time of t

This was achieved by the following main steps. Firstly, the maps of built-up and non-built-up areas were arranged and loaded into the ArcGIS 10.7 software.The maps of land use for the years 1999, 2010, and 2021 were re-classified to suit the objective of predicting urban development in LZRC. The land use maps were converted from vector to raster and then to ASCII files using conversion tools within the ArcGIS environment. Then, the IDRISI_Selva environment was used to re-classified and convert the ASCII files to a raster format. Accordingly, they can be considered to predict prospect urban development. Markov chain model was applied to identify the transition probability matrix and transition rules for land use and land cover. Accordingly, the future LU/LC alteration was modeled, i.e., the transition probabilities for 1999 to 2010 were applied to predict the variations in 2021 and to calibrate and validate the model. Meanwhile, urban and non-urban maps of 2010 and 2021 were considered to predict future urban development in 2041. Markov simulation was firstly applied to produce transition probability matrices of zones and therefore conditional probability images for (1999–2010) and (2010–2021) LU/LC maps. Model settings allowable just 15% related error for input imageries is suggested (Sakthivel et al., 2021). Secondly, a map of LU/LC for 2021 was modeled by the probability of transition and conditional images as input to the CA-Markov simulation. Then, to calibrate the model, the resulted image was validated with the real

2021 image. Next, a 2041 LU/LC map was simulated from the present (2010–2021) maps.

### 3.4.6 Model Validation

It is essential to Validate the results of the model before simulating the LU/LC map for 2041. The validation was achieved by using an internal frame of the categorized data as reference data (categorized 2021 LU/LC image) compared to the modeled LULC map of 2021. IDRISI 17.0 has a fixed validate model that was used to compare the degree of the agreement between the classified and the modeled image. The agreement catalogues are founded on the typical KIA (Kappa Index of Agreement with particular areal relationship differences, which namely include; $K_{locationStrata}$ (Kappa for location Strata), $K_{location}$ (for location), $K_{no}$ (for no data), and $K_{standard}$ (standard) (Viera and Garrett, 2005; Khwarahm et al., 2021; Yi et al., 2022). Kappa locationStrata and location specify the aerial extents precision of the extent and positions of the grid-cells of a definite class classification of the LU/LC images. Kappa no, designates the overall agreement between the reference and simulated images parts, irrespective of having data on the amount and position of definite class categories. Kappa standard signifies the ratio of properly relating a class category compared to the ones that are linked properly through accidental. The following equations are used to estimate the typical KIA (Mondal et al., 2020)

$$K_{location} = \frac{M_{ag} \times N_{ag}}{P_{ag} - N_{ag}} \quad 3.14$$

$$K_{standard} = \frac{M_{ag} \times N_{ni}}{P_{pg} - N_{ag}} \quad 3.15$$

$$K_{no} = \frac{M_{ag} \times N_{ni}}{P_{pg} - N_{ni}} \quad 3.16$$

in which $M_{ag}$, $N_{ag}$, and $P_{ag}$ are average grid-cell level data; $N_{ni}$ is no data; and $P_{pg}$ is perfect grid-cell level data across the landscape. However, the Kappa statistics show the degree of agreement between the classification raster and its probability when contrasted with the real classification raster and the LULC prediction raster. The values of Kappa for these differences vary from 0 to 1; the nearer the number to 1, the well is the agreement precision (Khwarahm et al., 2021).

### 3.4.7 Delineation of the basin

Applying DEM data with a resolution of 30 m to the SWAT model allowed for the definition of the watershed and subbasins for all models. Make the SWAT project setup first. Five steps make up the watershed delineation process. key phases, metric unit DEM construction, and stream definition using DEM-based technique, defining exits and inlets, and identifying the watershed outlets, definitions, and hydrologic parameter calculation.

The outlets close to the end basin of the Lesser Zab River, and these outlets are matched with SWAT-defined streams. The flow directions and flow accumulations are calculated automatically by the model. Following that, topographic factors including altitude, slope, width, and depth of main and tributaries, as well as stream networks, watershed and subbasin boundaries, are also calculated.

By carefully choosing the threshold area (the smallest drainage region necessary to generate the streams' origin), the stream network definition and the size of the subbasins were established. The threshold subbasin area of 20000 $km^2$ was used on SWAT projections.

### 3.4.8 Hydrologic Response Unit Definition (HRU)

The smallest component of the Hydrological Response Unit (HRU) SWAT's hydrological modeling, specifically the subbasin's unique soil, slope, and LC/LU. HRU enables the model to take into account variations in for various land coverings, evapotranspiration and other hydrologic processing also soils. The classification of land use/land cover, soils, and short parts of subbasins known as Hydrologic Response Units (HRUs) have changed. slope (Winchell et al., 2017).

The initial stage in developing the HRUs was to insert the LU/LC map as a grid including classes for land uses in the basin, and these classes were matched with classes in the ArcSWAT database in order to re-classify the land use map using a lookup table containing these classes. It is, nevertheless, critical to evaluate land usage using high-resolution pictures and past study.

The next step was to import the soil map as a shape file. In order to match soil classes in the soil map attribute table with the databases provided, the FAO soil map was utilized in the model, The FAO soil datasets have been included into the standard SWAT databases in order to obtained all type of soils. A lookup table was built to correlate soil map classes with the FAO soil database.

The third step was to populate the model with slope classes based on the DEM elevations. The model provides the user two options: single slope or multiple slopes; for this study, multiple slopes were chosen.

The final step of the HRU Analysis was the overlay of the land use, soil, and slope layers. The land use, soil, and slope threshold areas were all zero percent. At this stage, the simulation took into consideration all land use, soil, and slope classifications.

### 3.4.9 Basin Simulation

It is advised that the simulation be divided into two sections. There are two time constraints: one for calibration and another for verification. The first SWAT operation run from January 1, 2000 to December 31, 2009, with the second beginning on January 1, 2010. to January 1,2022. output data was published in monthly time steps. After all of the input tables have been uploaded to the database, the form is now ready to use. Weather stations were utilized to estimate hydrological processes in waterways, according to all of the information in the original input database and the SWAT simulation.

### 3.4.10 Calibration and Validation

In this study. for calibration and validation, two sections of the Lower Zab River Basin were chosen: the first includes the Dukan basin, where the water supply is natural (precipitation), and the second includes the Dibis, where the water supply is absolute Dukan and precipitation, both natural and artificial. The calibration period for the Dukan dam and Dibis dam was from 1/1/2000 to 31/12/2006, and the validation period was from 1/1/2007 to 31/12/2009. Second LULC 2010 scenario: calibration for the Dukan and Dibis dams from January 1, 2010 to December 31, 2017, and validation from January 1, 2018 to December 31, 2021.

### 3.4.11 Prepare for SWAT-CUP

Established as the objective function of optimization processing (Moriasi et al. 2007). The first step in setting up SWAT-CUP is to insert a SWAT output file "TxtInOut" to the program interface, then starting SUFI-2 project for calibration. The second step is to select the most sensitive parameters for SWAT runoff modeling and the number of simulations to be iterated in SWAT-CUP execution processes. Twelve and eight sensitive parameters were selected in

Dukan and Dibis respectively based on the most common parameters (Arnold et al., 2012) These parameters were chosen because directly affect the surface runoff. The hydrologica response of the dukan was taken into consideration in the selection of the parameters, along with incorrect results for some parameters, which are defined within the SWAT. The other parameters were neglected because they have no effect on the surface runoff.The third step is to place the observed discharges for the outlet into SWAT-CUP input files and the forth step is to run SWAT-CUP to calibrate the observed with the measured discharges to make the best correction for the selected parameters

# Chapter Four

# Results and Discussion.

## 4.1 Analysis Land Use Land Cover

Landsat images from 1989, 1999, 2010, and 2021 were used to create LU/LC maps (Fig 4.1). Agricultural lands were the dominant LU/LC classification as shown in fig (4.1) in the LZRB during the most studied periods, accounting for 51.6, 49, 45, and 39.96% in 1989, 1999, 2010, and 2021, respectively as shown in table (4.1)

Bare lands decreased from it was obvious that approximately 39% in 1989, 37% in 1999, 35.3 in 2010, and 34.95% in 2021. However, urban land grew from 0.455% in 1989 to 1.2% in 1999 to 4.11% in 2010. Table (4.1) Land use and land cover (LU/LC) area coverage and percent of total basin area, for the Lower Zab River Basin for the water years 1989, 1999, 2010, and 2021, in the year 2021, the major LU/LC most common classifications were agricultural lands (39.96%), fol-bare lands (34.915%), and urban lands (5.59%). forest land experienced maximum growth from 2010 to 2021. Because the majority of the agricultural land in the regionis unirrigated, with low average annual precipitation caused acute dryness in the bodies of water and water supplies, as well as a significant decrease in soil and vegetation moisture content.

## 4.2 Land use and Land Cover Analysis Changing

The level of area increase and/or decrease of the zone occupied by the specific LU/LC class can be represented by the amount and ratio of the fluctuations identified. Positive numbers represent expansion,whereas negatives represent reduction of the spatial magnitude of the corresponded LU/LC class. The alteration value is estimated by subtracting the specific LU/LC class area for each latest Landsat image date from the corresponding earlier image date, or

subtraction between the recent and first satellite map, or between each consecutive year. The Forestlands experienced the greatest growth. while the main expansion in the upper basin portion urban areas were discovered in the basin's lower reaches as shown in table (4.2).

Table (4.1) Land use and land cover (LU/LC) area coverage and percent of total basin area, for the Lower Zab River Basin for the water years 1989, 1999, 2010, and 2021

| | **Area** | | | | | | | |
|---|---|---|---|---|---|---|---|---|
| LU/ LC Type | 1989 | % | 1999 | % | 2010 | % | 2021 | |
| | $km^2$ | | $km^2$ | | $km^2$ | | $km^2$ | % |
| WB[1] | 140 | 0.7 | 128 | 0.64 | 104 | 0.52 | 90 | 0.45 |
| FO[2] | 1724 | 8.62 | 2394 | 11.97 | 3021 | 15.105 | 3810 | 19.05 |
| AL[3] | 10.212 | 51.06 | 9800 | 49 | 9001 | 45 | 7992 | 39.96 |
| BLD[4] | 193 | 0.965 | 140 | 0.7 | 41 | 0.205 | 7 | 0.035 |
| BLL[5] | 7640 | 38.2 | 7298 | 36.49 | 7011 | 35.055 | 6983 | 34.915 |
| UL[6] | 91 | 0.455 | 240 | 1.2 | 822 | 4.11 | 1118 | 5.59 |
| Total | 20,000 | 100 | 20,000 | 100 | 20,000 | 100 | 20,00 | 100 |

Table (4.2) Land Use Land Cover analysis changing

| **Class** | % Land Use Land Cover area gain (+)/loss (-) | | |
|---|---|---|---|
| | 1989_1999 | 1999_2010 | 2010 _2021 |
| WB[1] | -0.06 | -0.105 | - 0.085 |
| FO[2] | 3.35 | 3.115 | 3.965 |
| AL[3] | -2.06 | -3.99 | -5.05 |
| BLD[4] | -0.00265 | -0.465 | -0.200 |
| BLL[5] | - 1.71 | -1.44 | -0.135 |
| UL[6] | 0.745 | 3.045 | 3.345 |

1Water Bodies; 2Forest; 3Agrucaltural Lands; 4Bare Lands Dark; 5Bare Lands Light; 6Urban Lands

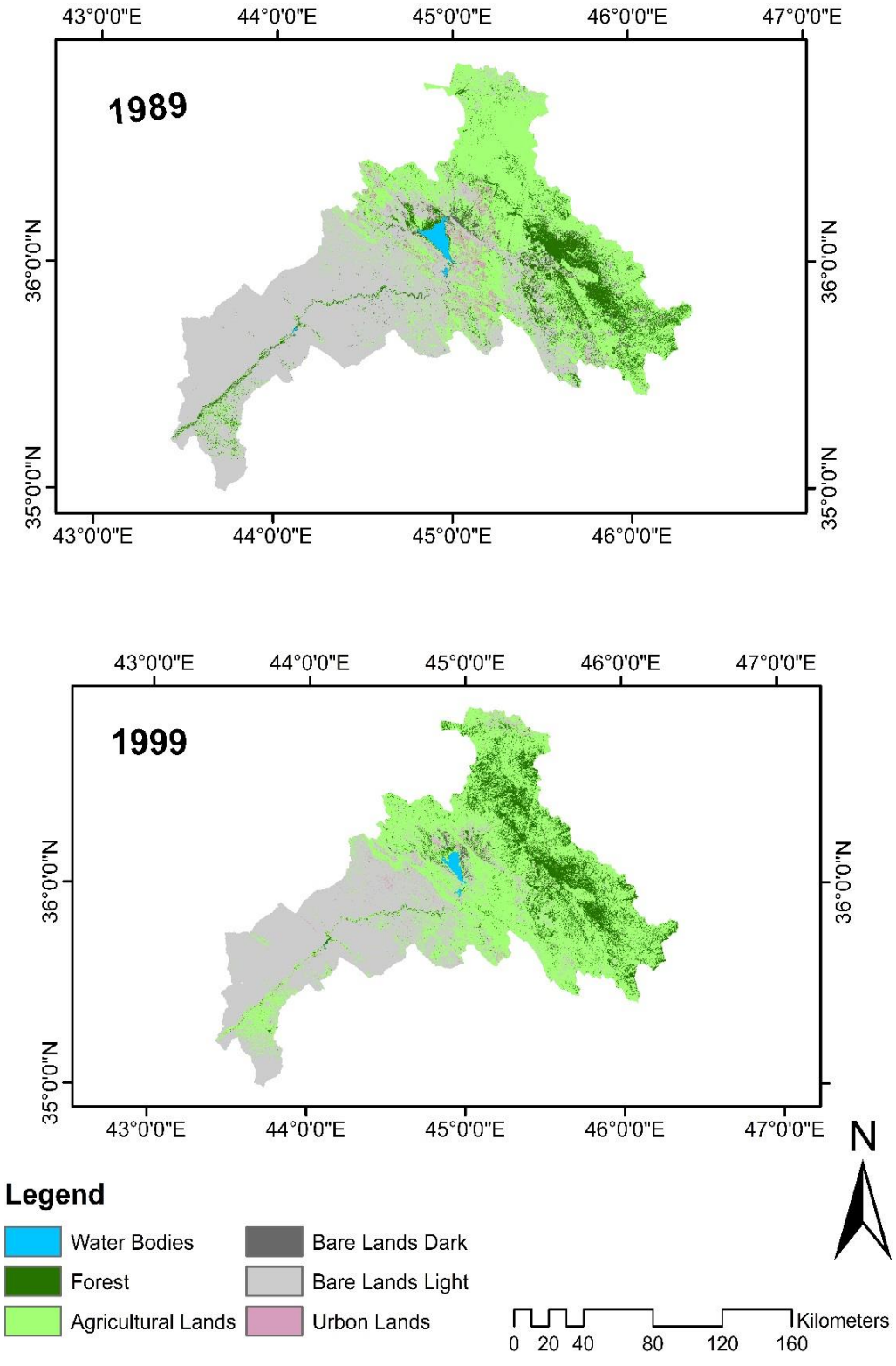


Fig (4.1) LULC maps for the year A)1989 B)1999

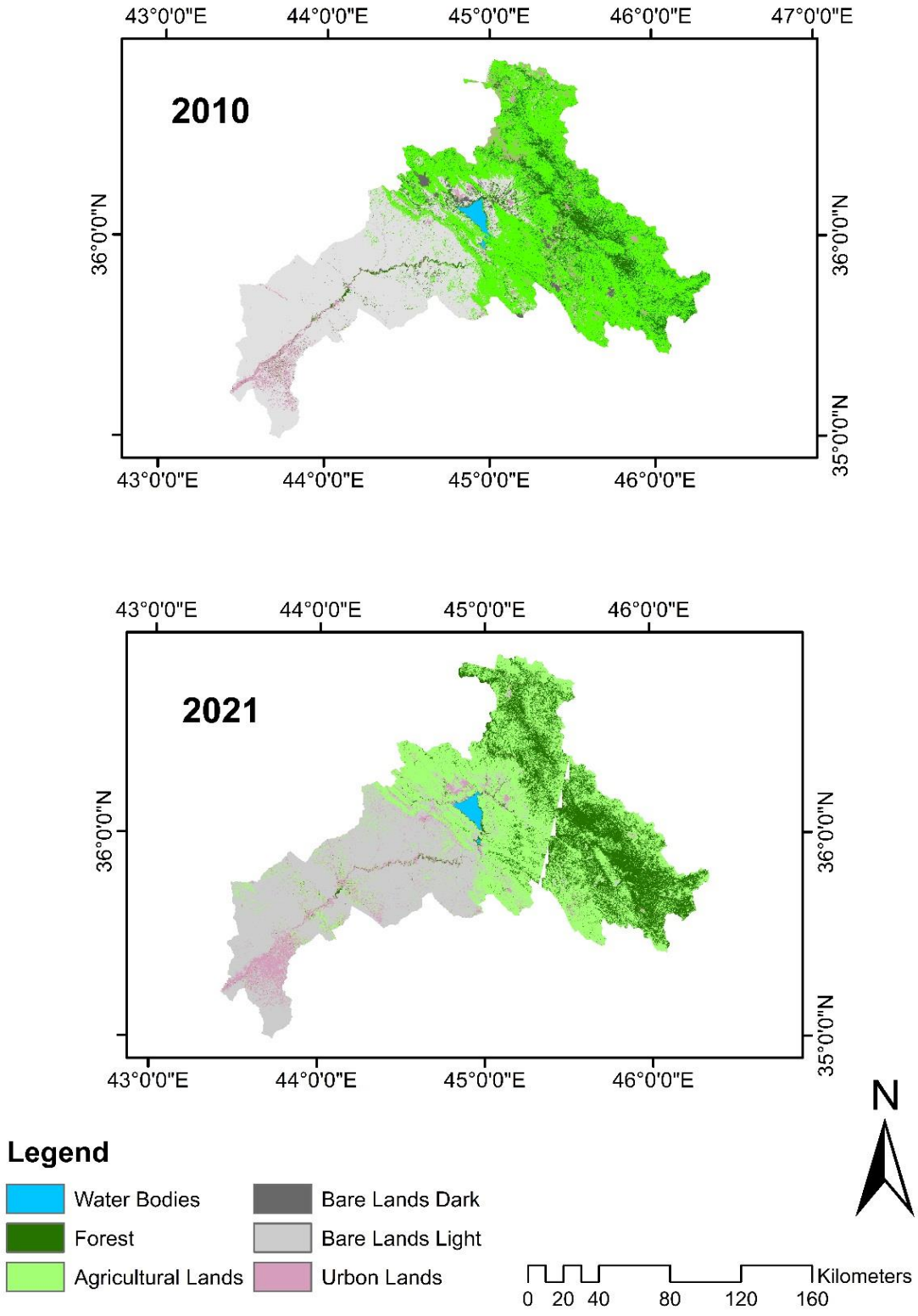


Fig (4.2) LULC maps for the year A) 2010 B) 2021

## 4.3 Classification Evaluation

Table (4.3) displays the overall accuracy assessment calculation results as well as the Kappa coefficient of the LU/LC images from 1989, 1999, 2010, and 2021respectively. 88.67%, 91.80%, and 95.9%.and 87.3%, as well as 0.8656, 0.9008, 0.9516, and 0.8476, respectively. The Kappa Index revealed almost perfect agreement for all years considered (Tadele et al., 2017).

Table (4.3) Calculations of overall accuracy (OA) and Kappa coefficient (KI) for the years 1989, 1999, 2010, and 2021

| Year | LU/LC | Ground control reference data | | | | | | | |
|---|---|---|---|---|---|---|---|---|---|
| | | WB[1] | FO[2] | AL[3] | $BL_D$[4] | $BL_L$[5] | UL[6] | GTH[*] | UA[**] |
| | WB[1] | 10 | 0 | 0 | 0 | 0 | 0 | 10 | 100 |
| | FO[2] | 0 | 9 | 0 | 0 | 0 | 0 | 9 | 100 |
| | AL[3] | 0 | 0 | 7 | 3 | 0 | 0 | 10 | 70 |
| **1989** | $BL_D$[4] | 1 | 0 | 0 | 6 | 0 | 0 | 7 | 85.7 |
| | $BL_L$[5] | 0 | 0 | 0 | 1 | 9 | 0 | 10 | 90 |
| | UL[6] | 1 | 0 | 0 | 0 | 0 | 6 | 7 | 85.7 |
| | Total | 12 | 9 | 7 | 10 | 9 | 6 | 53 | |
| | PA[***] | 83.3 | 100 | 100 | 60 | 100 | 100 | | |
| | | | OA = 88.67% | | | KI = 86.56% | | | |
| **Year** | LU/LC | WB[1] | FO[2] | AL[3] | $BL_D$[4] | BLL5 | UL[6] | GTH[*] | UA[**] |
| | WB[1] | 10 | 0 | 0 | 0 | 0 | 0 | 10 | 100 |
| | FO[2] | 0 | 9 | 0 | 0 | 1 | 0 | 10 | 100 |
| | AL[3] | 0 | 0 | 10 | 1 | 1 | 0 | 12 | 83.3 |
| **1999** | $BL_D$[4] | 0 | 0 | 0 | 9 | 1 | 0 | 10 | 90 |
| | $BL_L$[5] | 0 | 0 | 0 | 0 | 12 | 0 | 12 | 100 |
| | UL[6] | 0 | 0 | 0 | 0 | 1 | 6 | 7 | 85.7 |
| | Total | 10 | 9 | 10 | 10 | 16 | 6 | 61 | |
| | PA[***] | 100 | 100 | 100 | 90 | 75 | 100 | | |
| | | | OA = 91.8% | | | KI = 90.08% | | | |
| **Year** | LU/LC | WB[1] | FO[2] | AL[3] | $BL_D$[4] | $BL_L$[5] | UL[6] | GTH[*] | UA[**] |

| | | | | | | | | | |
|---|---|---|---|---|---|---|---|---|---|
| | WB[1] | 12 | 0 | 0 | 0 | 0 | 0 | 12 | 100 |
| | FO[2] | 0 | 12 | 0 | 0 | 0 | 0 | 12 | 100 |
| | AL[3] | 0 | 0 | 10 | 0 | 2 | 0 | 12 | 83.33 |
| **2010** | $BL_D$[4] | 0 | 0 | 0 | 12 | 0 | 1 | 13 | 92.2 |
| | $BL_L$[5] | 0 | 0 | 0 | 0 | 13 | 0 | 13 | 100 |
| | UL[6] | 0 | 0 | 0 | 0 | 0 | 12 | 12 | |
| | Total | 12 | 12 | 10 | 12 | 13 | 13 | 74 | |
| | PA*** | 100 | 100 | 100 | 100 | 100 | 92.3 | | |
| | | OA = 95.9% | | | | KI = 95.16% | | | |
| **Year** | LU/LC | WB[1] | FO[2] | AL[3] | $BL_D$[4] | $BL_L$[5] | UL[6] | GTH* | UA** |
| | WB[1] | 12 | 0 | 0 | 0 | 0 | 0 | 12 | 100 |
| | FO[2] | 0 | 8 | 0 | 1 | 0 | 0 | 9 | 88.88 |
| | AL[3] | 0 | 0 | 4 | 1 | 6 | 0 | 11 | 36.36 |
| | $BL_D$[4] | 0 | 0 | 0 | 10 | 0 | 0 | 10 | 100 |
| **2021** | $BL_L$[5] | 0 | 0 | 0 | 0 | 10 | 0 | 10 | 100 |
| | UL[6] | 0 | 0 | 0 | 0 | 0 | 11 | 11 | 100 |
| | Total | 12 | 8 | 4 | 12 | 16 | 11 | 63 | |
| | PA*** | 100 | 100 | 100 | 83.3 | 62.5 | 100 | | |
| | | OA = 87.30 % | | | KI = 84.76% | | | | |

[1]Water Bodies; [2]Forest; [3]Agricultural Lands; [4]Bare Lands Dark; [5]Bare Lands Light; [6]Urban Lands; *Ground Truth; **Use's accuracy (%); ***Producer accuracy (%)

## 4.4 kappa coefficient and Accuracy evaluation

In year 1989 details Kappa coefficient calculation the water bodies, 12 prediction points were used as a guide; 10 of the 12 pixels were correctly predicted, while 1 pixel was classified. as desolate dark lands, and 1 pixel as urban lands, implying that the precision of this LU class is high. was ("10"/ "12" × 100") 83.3%. Moreover, the overall forest accuracy, agricultural lands, bare. the LU/LC classes for light lands and urban lands were both 100% and (ground pixels were correctly identified) were the most precise classes in the research basin. Second, the overall classification accuracy was approximately

88.67%, indicating that the classification was more precise than random classification as shown in table (A.1, A.2 ,A.3, A.4 ) in Appendix A

## 4.5 The Normalized Difference Vegetation Index:

The vegetation land cover in 1989, 1999, 2010, and 2021 was identified. There were no notable exceptions. able changes in vegetation cover result-derived from NDVI estimation and as a result of the Landsat 5,7 TM, ETM Landsat 8 OLI supervised classification 1989, 1999, 2010, and 2021 images The Low-density plants were displayed decreasing trend with a ratio from 2010 to 2021of approximately 45% and 41% respectively. in contrast to the trend of vegetation-free area increased. with a ratio of approximately 3%, as shown inTable ( 4.4) and Fig (4.3).

Table (4.4) The Lower Zab River Basin Normalized Difference vegetation Index area coverage and proportion of total basin area for 1989, 1999, 2010, and 2021 water years

| Year | 1989 | | 1999 | | 2010 | | 2021 | |
|---|---|---|---|---|---|---|---|---|
| LU/LC | Area | | Area | | Area | | Area | |
| | $Km^2$ | % | $Km^2$ | % | $Km^2$ | % | $Km^2$ | % |
| WB[1] | 280 | 1.4 | 256 | 1.28 | 220 | 1.1 | 184 | 0.92 |
| VFA[2] | 8200 | 41 | 7800 | 39 | 8100 | 40.5 | 8400 | 42 |
| LDP[3] | 9920 | 49.6 | 9744 | 48.72 | 9000 | 45 | 8216 | 41.0 |
| HDP[4] | 1600 | 8 | 2200 | 11 | 2680 | 13.4 | 3200 | 16 |

[1]Water bodies; [2]Vegetation free area; [3]Low density plants; [4]High density plants;

The spatial distribution of NDVI was primarily caused by changes in meteorological variables such as the occurrence and intensity of rainfall (Fig 4.3). the impact of both climate and anthropogenic activities resulted in massive changes in vegetation cover between 2009 and 2021. Al-Saady et al. (2015) classified the LZRB vegetation cover as NDVI (cropland) or NDVI (natural vegetation).

According to their classification, (NDVI) showed an increasing trend from 1976 to 2014, whereas natural vegetation (NDVI) showed no clear trend

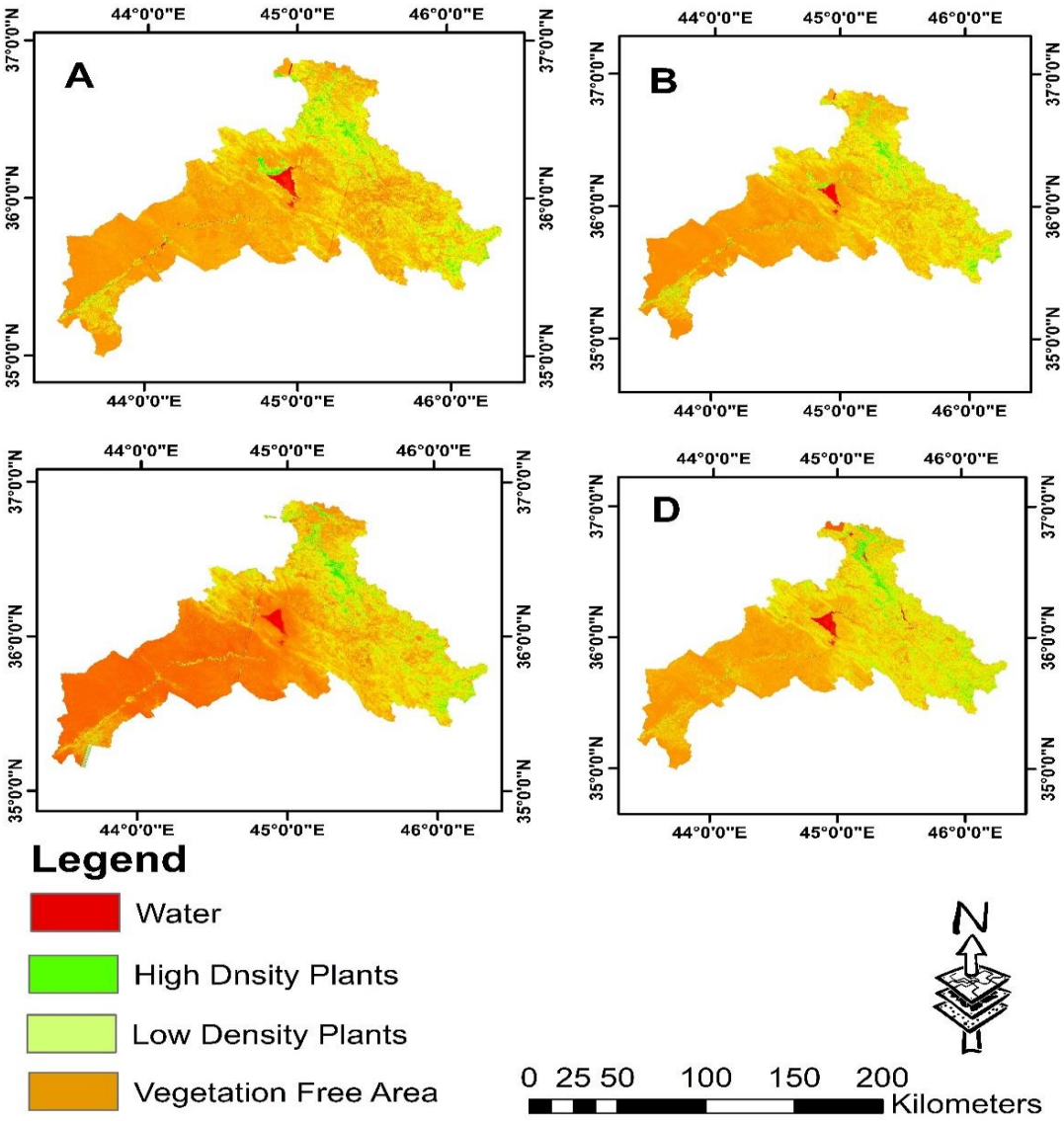


Fig (4.3) Maps of The Normalized Difference Vegetation Index for the year A)1989 B)1999 C)2010 D) 2021

## 4.6 Result the Modeling Prediction of Land Use/Land Cover

The classified LU/LC maps for the 1999–2010 and 2010–2021 were considered to model 2021 and 2041 LU/LC maps, in that order. The results of LU/LC maps prediction revealed that between 2021and 2041 urban area would increase by 364.79% (from 1117.1 to 5192.2 $km^2$). However, bare lands/light, agricultural lands, water bodies, bare lands/dark, forest lands would decrease by 3% (from 6921.34 to 6723.70 $km^2$), 12% (from 7972.85 to 7023.60 $km^2$), 15% (from 141.03 to 119.86 $km^2$), 30 (from 4.80 to 3.37 $km^2$), and 76 (from 3808.86 to 903.20 $km^2$), as shown in Table (4.5) and Fig. (4.4).

These alterations (increases/declines) are comparative variations in respect to LU/LC class classifications. For example, 365% increase in the urban area during 2041 would be at the cost of decreasing other class categories extent. Additionally, variations ration in each class category areas during the period from 2021 to 2041 designated that the maximum active class cover categories were urban lands, forest lands, and bare lands/dark. While, the least dynamic cover types were water bodies, agricultural lands, and bare lands/light. In 2041, the area of the bare lands/light would decline with only 3%, while the forest lands area with greater than 75% with respect to other land cover categories. The utmost substantial alteration that balance out the total active of the class classifications will be the agricultural lands and bare lands/light.

These classes covers a significant area in comparison to the other classes. This result shows that particular zones, which were enclosed by water bodies in 2021, will be changed by urban lands, sequentially, further water bodies will arise. Water bodies, agricultural fields, and bare lands/light were the least dynamic cover categories.

The agricultural lands and bare lands/light will be the most significant changes that balance out the overall activity of the class. In compared to the other classes, these classes cover a wide range of topics. This finding indicates that certain zones that were surrounded by water bodies in 2021 will be transformed by urban areas, and subsequent water bodies will emerge. The formation of water bodies will most likely be in the configuration of catchments and minor size lakes from fisheries events.

Table (4.5) Area and percentage of area of the land use land cover classes alteration predicting by CA Marcov

| | 2021 | Forcasting percentage | 2021 forcasted | Forcasting percentage | 2041 Forcasted | Forcasting percentage |
|---|---|---|---|---|---|---|
| | ($km^2$ | (%) | ($km^2$) | (%) | ($km^2$) | (%) |
| WB[1] | 90 | 0.45 | 134 | 0.67 | 120 | 0.60 |
| FL[2] | 3810 | 19.05 | 2408 | 12.04 | 904 | 4.52 |
| AL[3] | 7992 | 39.96 | 9648 | 48.24 | 7036 | 35.18 |
| BLD[4] | 7 | 0.035 | 238 | 1.19 | 4 | 0.02 |
| BLL[5] | 6983 | 34.915 | 7298 | 36.49 | 6736 | 33.68 |
| UL[6] | 1118 | 5.59 | 274 | 1.37 | 5200 | 26.00 |
| Total | 20000 | 100 | 20000 | 100 | 20000 | 100 |

[1]Water Bodies, [2]Forest, [3]Agrucaltural Lands, [4]Bare Lands Dark, [5]Bare Lands Light, Urban Lands

## 4.7 Validation of the Model Marcov

The genuine LU/LC map of 2021 acquired by satellite pictures was used to confirm the modelled LU/LC map of 2021 created by CA-Markov based on the historical situation of 1999-2021 as mention previously that there was a high degree of match between the simulated and real photos. Total Kappa numerical differences of Kno = 0.8635, Klocation = 0.8541, Klocation Strata = 0.8541, Kstandard = 0.7853 were achieved which are eligible for additional usage in terms of model justification consistency (Khwarahm et al. 2021).

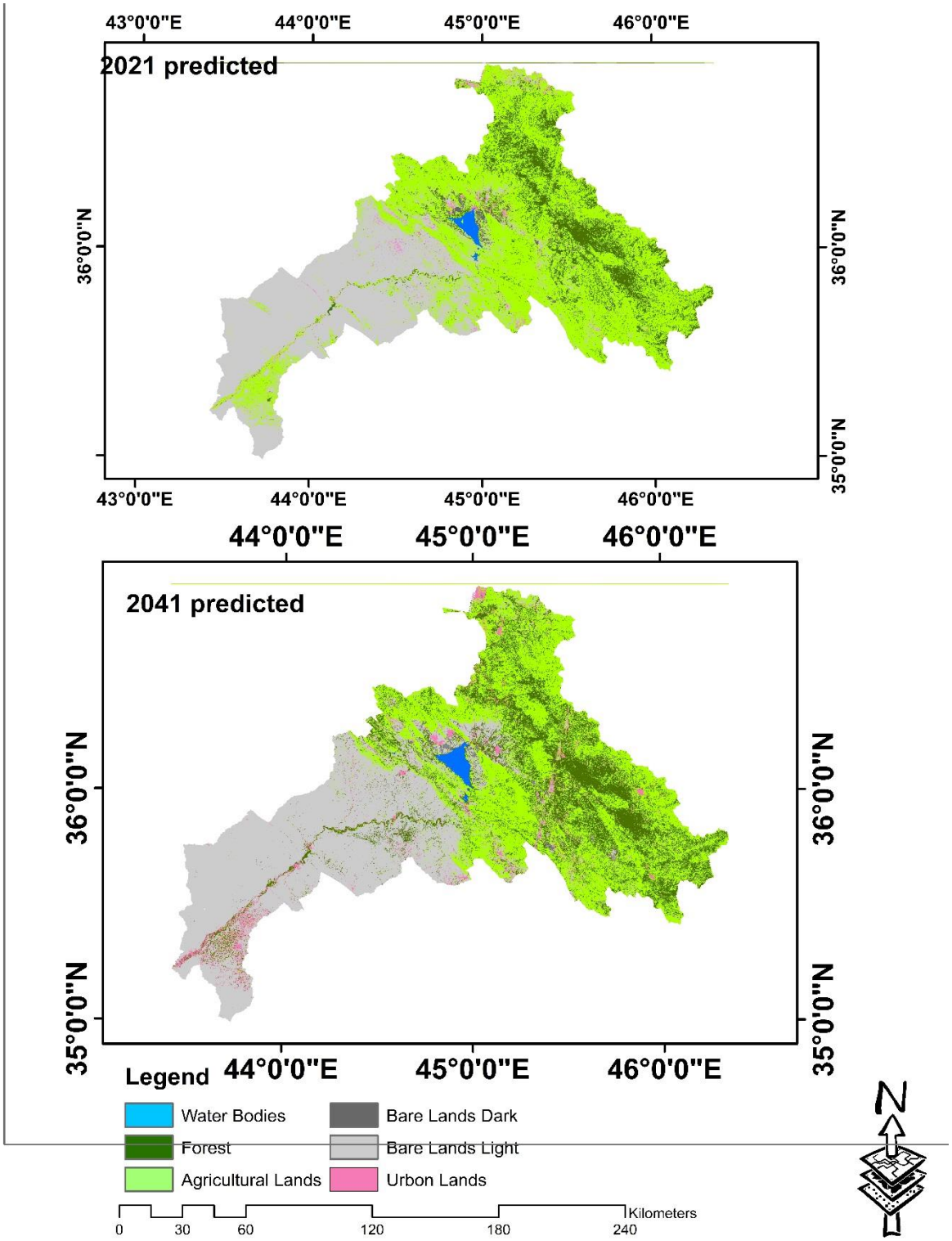


Fig (4.4) Marcov model prediction for Land Use Land Cover Map 2021,2041

However, the model underestimated agricultural and barren lands by 2.73% (6990 $km^2$) and 8.28% (7992 $km^2$), respectively, and aquatic bodies by 0.22% (90 $km^2$). In contrast, the model overestimated the forest and urban areas by 7.01% (3810 $km^2$) and 4.22 % (1118 $km^2$, respectively, of the true area.

Furthermore, the gap between the categorized and modelled LU/LC map of 2021 was expecteded to stem from underestimating certain class classifications, namely barren and urban area, there is an obvious interval variation from 2010 to 2021, the pace and number of LU/LC change dynamic were superficially adjusted related with the period from 1999 to 2010.

Table (4.6) shows that the whole model performance in predicting a potential scenario based on the transition probability matrix from 1999 to 2010 established excellent precision. Table (4.7) shows an agreement coefficients between the real and modeled land use and land cover 2021 maps and Kappa coefficient difference values for the CA-Markov approach. Figure (4.5) shows that there is good agreement between the predicted and categorized LULC maps, with a coefficient of determination value of $R^2$=0.951 the difference between real and anticipated LU/LC maps.

A reliability test was carried out to confirm the results of the Ca Markov using the SPSS program between the map of 2021 that was classified using (as an independent variable) the GIS program and the predictive map of 2021 resulting from the program Idrissi Selva (dependent variable), in order to accept the results of the 2041 prediction map and the following results were obtained.

Table (4. 6) Transition probability matrix resulting from land use maps for the period from 1999 to 2010 and 2010 to 2021

| | Matrix 2021 | | | | | |
|---|---|---|---|---|---|---|
| 1999 | 2010 | | | | | |
| | WB[1] | FL[2] | AL[3] | BLD[4] | BLL[5] | UL[6] |
| WB[1] | 0.8010 | 0.1989 | 0.0000 | 0.0000 | 0.0000 | 0.0001 |
| FL[2] | 0.0031 | 0.5669 | 0.3796 | 0.0040 | 0.0248 | 0.0215 |
| AL[3] | 0.0041 | 0.2721 | 0.5106 | 0.0068 | 0.1617 | 0.0446 |
| BLD[4] | 0.0085 | 0.2447 | 0.2358 | 0.0677 | 0.4078 | 0.0356 |
| BLL[5] | 0.0001 | 0.0618 | 0.1345 | 0.0040 | 0.7384 | 0.0612 |
| UL[6] | 0.0123 | 0.1408 | 0.2614 | 0.0056 | 0.3753 | 0.2047 |

| | Matrix 2041 | | | | | |
|---|---|---|---|---|---|---|
| 2010 | 2021 | | | | | |
| | WB[1] | FL[2] | AL[3] | BLD[4] | BLL[5] | UL[6] |
| WB[1] | 0.7659 | 0.1592 | 0.0330 | 0.0000 | 0.0087 | 0.0332 |
| FL[2] | 0.0056 | 0.3359 | 0.4866 | 0.0002 | 0.1105 | 0.0613 |
| AL[3] | 0.0009 | 0.3273 | 0.5445 | 0.0001 | 0.0934 | 0.0339 |
| BLD[4] | 0.0003 | 0.1854 | 0.5716 | 0.0002 | 0.1952 | 0.0473 |
| BLL[5] | 0.0001 | 0.0474 | 0.2778 | 0.0004 | 0.5636 | 0.1107 |
| UL[6] | 0.0014 | 0.1411 | 0.3465 | 0.0003 | 0.2984 | 0.2123 |

[1]Water Bodies, [2]Forest lands, [3]Agricultural land, [4]Bare land/dark, [5]Bare lands/light, [6]Urban land;

Table (4.7) Descriptive Statistics

| Pearson Correlation | 2021 forcasted | 2021 classified |
|---|---|---|
| 2021 simulated | 1.000 | 0.975 |
| 2021 classified | 0.975 | 1.000 |

a. Dependent Variable :2021 simulated

b. Independed Varible: (Constant): 2021 classified

Table (4.8) Agreement coefficients between the real and modeled land use and land cover 2021 maps.

| Classification agreement/disagreement | | | |
|---|---|---|---|
| According to the ability to specify accurately quantity and allocation | | | |
| Informationof Allocation | Information of Quantity | | |
| | No [n] | Medium [m] | Perfect [p] |
| P(x)[1] | 0.4996 | 0.9561 | 1.0000 |
| K(x)[2] | 0.4996 | 0.9561 | 0.9980 |
| M(x)[3] | 0.4163 | 0.8830 | 0.8851 |
| H(x)[4] | 0.1429 | 0.4549 | 0.4542 |
| N(x)[5] | 0.1429 | 0.4549 | 0.4542 |

[1]Perfect, [2]Perfect Stratum, [3]Medium Grid, [4]Medium Stratum, [5]No

The correlation analysis output between 2021 classified and 2021 simulated by CA Marcov. The correlation coefficient is 0.975 which is high degree of positive correlation between 2021 classified and 2021 simulated. Also the correlation coefficient is significant as its p-value is 0.001 and is less than significance level ($\alpha$ = 5 %). Table below shows coefficient of determination (R square) 0.951, which means 95.1% variation in dependent variable (2021 simulated) is explained by independent variable (2021 classified

The regression line will take the form $Y = b_0 + b_1X$

The theoretical expectations are b0 can take any value and $b_1 > 0$

$b_0$ is constant or y intercept and b1is regression coefficient of 2021 simulated (Y) on 2021 classified (X). Hence the regression equation using coefficient table is Y = 5.32E2 + 0.83 X The regression coefficient of 2021 simulated on 2021 classified is found to be 0.83.

a)

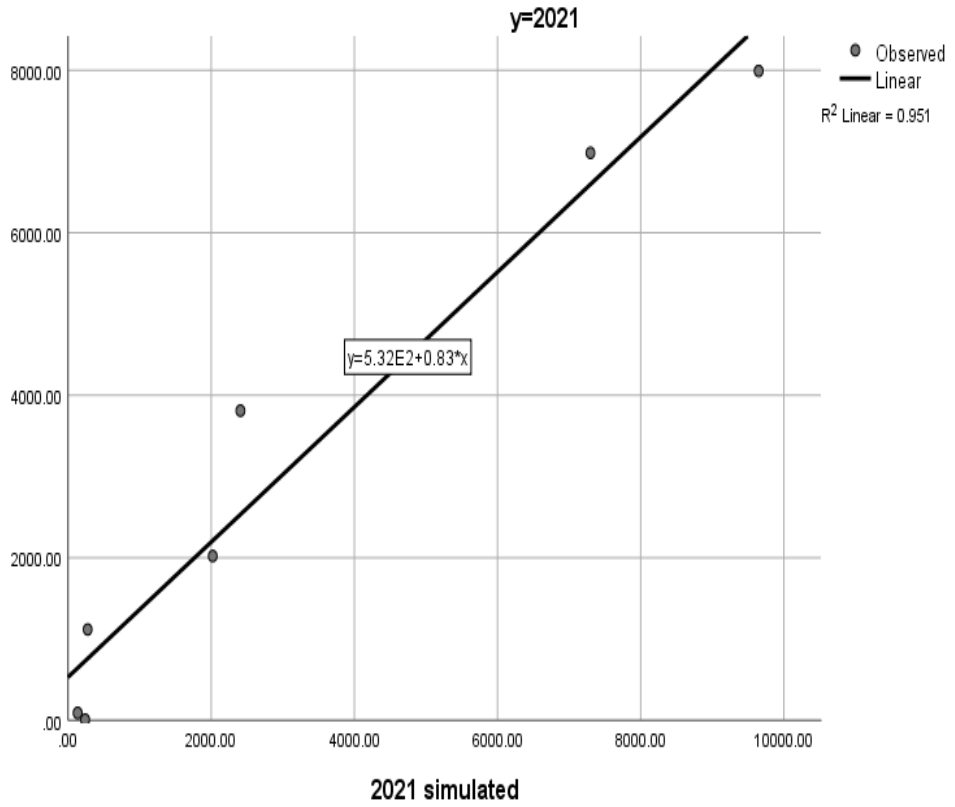


(b)

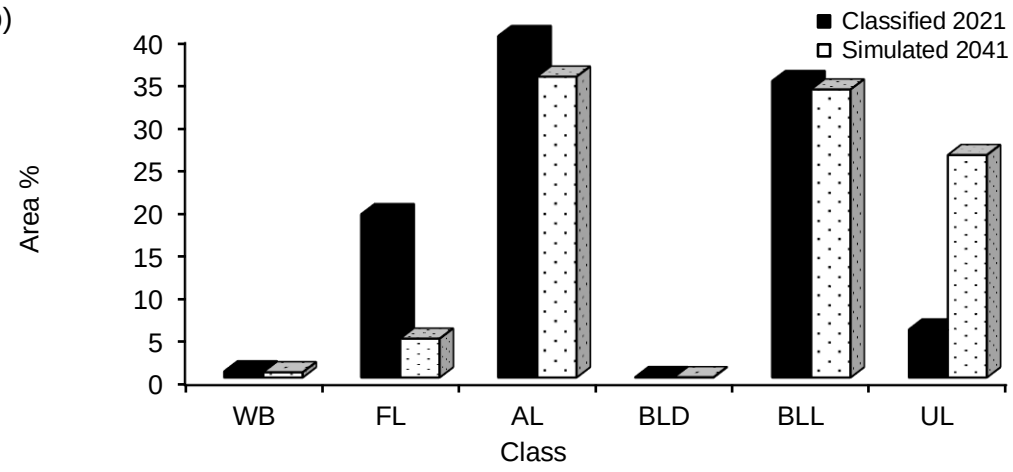


Fig (4.5) (a) The relationship between the actual and predicted land use and land cover maps of 2021; (b) Dynamics of land use/land cover for 2021 and 2041. Note: WB=Water Bodies, FL=Forest lands, AL=Agricultural lands, BLD=Bare lands/dark, BLL=Bare lands/light, UL=Urban lands

# 4.8 Watershed simulation

## 4.8.1 Boundaries and Stream Networks of the Watershed

Figure 4.6 show the results of the watersheds delineation by using the DEM based method that applied in ArcSWAT bacause of large difference in elevations between Upstream and Downstream in the catchment

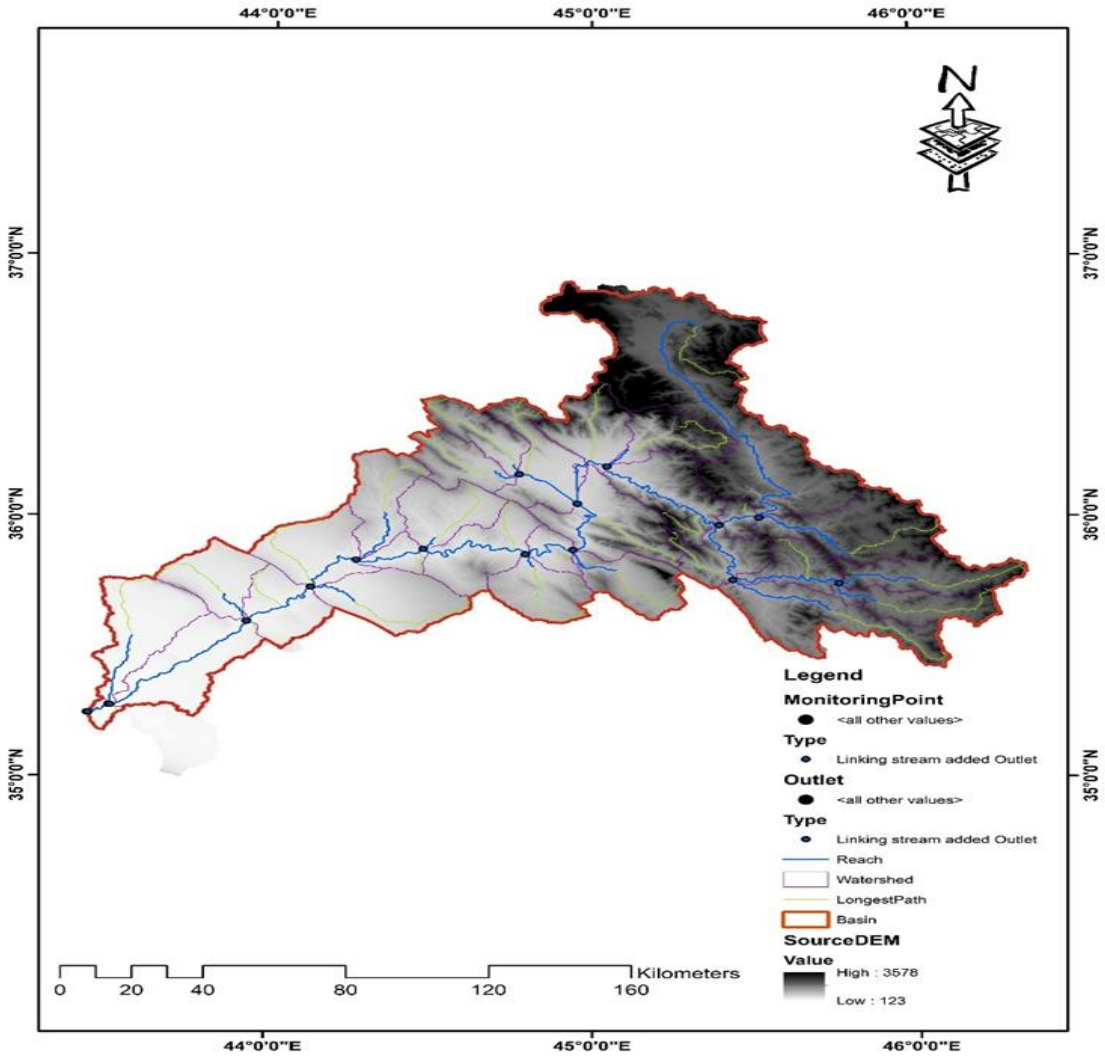


Fig (4.6) Lesser Zab river basin watershed delination and stream network for dem resolution 30 m

## 4.8.2 Soil Data of the Watershed

Soil is an important input data for SWAT; the watershed subdivision (HRU) allows the model to reflect differences in evapotranspiration for different soils; runoff is predicted separately for each HRU and routed to obtain the total runoff for the watershed. Soil properties have an impact on processes such as infiltration, surface water transport, evaporation, and pollution. All models used the FAO soil dataset. Tables (4.9) show the results of FAO soil datasets identified by the SWAT model's soil definition window. According to these tables, the watershed's clay loam of the C and D hydrologic groups has the highest percentage of soil texture.

Table( 4.9) Lesser Zab river basin fao soil data classifications and percentage

| No | Class | Value | % | Texture | Hydrologic group |
|---|---|---|---|---|---|
| 1 | I-E-Xk-bc | 3108 | 5.7 | Y_Clay_Loam | D |
| 2 | I-E-bc | 3109 | 22.04 | Y_Clay_Loam | C |
| 3 | I-Rc-Xk-c | 3122 | 26.32 | Clay_Loam | D |
| 4 | Vc1-3a | 3276 | 4.39 | Loam | D |
| 5 | Vc50-3ab | 3279 | 6.4 | Sandy_Loam | D |
| 6 | Xh31-3a | 3288 | 0.57 | Loam | D |
| 7 | Xh33-3a | 3289 | 2.52 | Loam | D |
| 8 | Xk26-2/3a | 3298 | 6.94 | Loam | D |
| 9 | Xk28-b | 3300 | 15.59 | Y_Clay_Loam | D |
| 10 | Xk9-2/3a | 3312 | 0.22 | Sandy_Loam | D |
| 11 | Xy5-a | 3323 | 2.32 | Loam | D |
| 12 | Yk34-b | 3603 | 0.41 | Loam | D |
| 13 | Yy10-2ab | 3614 | 6.58 | Loam | D |

### 4.8.3 Hydrological Response Unit Analysis

The HRU threshold delineation was set on zero for slope, LULC and soil for all models, the number of HRUs for a specific LC/LU is controlled by two parameters: the LULC resolution and the number of feature classes. The LULC resolution and number of feature classes, on the other hand, are determined by the spatial resolution of the satellite image and the desired level of classification. While, for a specific DEM, one parameter, the slope.

Table (4.10) Watershed characteristics function of DEM and LU LC

| No | No of SB[1] | No of HRU[2] | Dem (m) | LU\LC (m) | Areas ($km^2$) | Elevation (m.a.s.l) | | |
|---|---|---|---|---|---|---|---|---|
| | | | | | | Min | max | mean |
| Dokan watershed | 33 | 1252 | 30 | 30 | 11545.63 | 426 | 3589 | 1392.3458 |
| Dibis watershed | 21 | 589 | 30 | 30 | 8351.34 | 195 | 2579 | 545.2880 |

1 Subbasin 2 Hydrological response units

## 4.9 Sensitivity Analysis

The goal of sensitivity analysis is to reduce the number of parameters in the calibration process by removing less sensitive parameters. A sensitivity analysis was carried out using the more reliable all-at-once (global) method.

A multiple regression approach is used to quantify sensitivity.

The number of runs needed to conduct sensitivity analysis.The evaluation score is 500 and the sensitivity of 12,8 parameters was tested in the two delineations. Scenarios were created using 500 simulation runs. The rank and type of sensitive parameters were different in the two scenarios for the same number of simulations (500) and length of historical data, as shown in tables (4.11 - 4.14) The number of iterations and length of flow and rainfall data may influence the

rank of sensitive parameters. The most sensitive flow parameters for a given watershed must be determined. Because the type of input data observations varies by region, and changes in model input parameters affect modeling results.

It is also useful to define the important hydrological processes. The four sensitive flow parameters in Dukan watershed not effective in Didis watershed As a result, the groundwater parameter in the basin is effective and contributes in the stream flow, And the snow parameter is effective in the Dukan and decreace in scenario LU/LC 2010 about LU/LC 2000 due to global warming and reduced precipitation but not effective in the Dibis watershed because of The Dukan level in the Little Zab Repository's Upstream is higher in relation to sea level than the dibis level in the same catchment's downstream

Table (4.11): Sensitivity analysis for the Dukan Watershed DEM 30 m LU/LC 2000 map

| Rank | Parameter Name | Desicription | t_Stat | P_value |
|---|---|---|---|---|
| 1 | CN2.mgt | SCS-curve number | 14.31 | 0 |
| 2 | GW_DELAY.gw | Ground water delay | -0.69 | 0.42 |
| 3 | GW_REVAP.gw | Ground water re evaporation | -3.01 | 0.31 |
| 4 | GWQMN.gw | Threshold depth of water in the shallow aquifer | -1.01 | 0.33 |
| 5 | SOL_AWC(..).sol | Soil available water capacity | 2.63 | 0.13 |
| 6 | ESCO.hru | Soil evaporation compensation factor | 1.11 | 0.22 |
| 7 | SFTMP.bsn | Snowfall temperature | 0.26 | 0.8 |

| | | | | |
|---|---|---|---|---|
| 8 | SMTMP.bsn | Snow melt temperature | 1.21 | 0.25 |
| 9 | OV_N.hru | Over flow Manining coefficient | 0.51 | 0.62 |
| 10 | SLSUBBSN.hru | Subbasin slope | -0.36 | 0.72 |
| 11 | RCHRG_DP.gw | Groundwater deep recharge | -0.37 | 0.81 |
| 12 | RAINHHMX(..).wgn | Rainfall variation of basin | 1.2 | 0.25 |

Table (4.12): Sensitivity analysis for the Dukan Watershed DEM 30 m LU/LC 2010 map

| Rank | Parameter Name | Desicription | t-Stat | P-Value |
|---|---|---|---|---|
| 1 | CN2.mgt | SCS-curve number | -22.45 | 0.89 |
| 2 | GW_DELAY.gw | Ground water delay | -0.79 | 0.53 |
| 3 | GW_REVAP.gw | Ground water re evaporation | -7.21 | 0.01 |
| 4 | GWQMN.gw | Threshold depth of water in the shallow aquifer | -2.41 | 0.16 |
| 5 | SOL_AWC(..).sol | Soil available water capacity | -1.67 | 0.21 |
| 6 | ESCO.hru | Soil evaporation compensation factor | 2.05 | 0.04 |
| 7 | SFTMP.bsn | Snowfall temperature | -0.77 | 0.88 |

| | | | | |
|---|---|---|---|---|
| 8 | SMTMP.bsn | Snow melt temperature | -1.1 | 0.28 |
| 9 | OV_N.hru | Over flow Manining coefficient | -0.84 | 0.4 |
| 10 | SLSUBBSN.hru | Subbasin slope | 0.51 | 0.61 |
| 11 | RCHRG_DP.gw | Groundwater deep recharge | -0.71 | 0.48 |
| 12 | RAINHHMX(..).wgn | Rainfall variation of basin | 0.16 | 0.89 |

Table (4.13): Sensitivity analysis for the Dibis Watershed DEM 30 m LU/LC 2002 map

| Rank | Parameter Name | Description | t-Stat | P-Value |
|---|---|---|---|---|
| 1 | CN2.mgt | SCS-curve number | -12.42 | 0 |
| 2 | GW_DELAY.gw | Ground water delay | 0.09 | 0.82 |
| 3 | GWQMN.gw | Threshold depth of water in the shallow aquifer | 0.11 | 0.83 |
| 4 | GW_REVAP.gw | Ground water re evaporation | 0.02 | 0.91 |
| 5 | ESCO.hru | Soil evaporation compensation factor | -2.01 | 0.38 |
| 6 | SOL_AWC(..).sol | Soil available water capacity | 0.63 | 0.93 |
| 7 | HRU_SLP.hru | Average slope steepness | 0.13 | 0.79 |
| 8 | PRECIPI(..){..}.pcp | precipitation | -1.26 | 0.08 |

Table (4.14): Sensitivity analysis for the Dibis DEM 30 m LU/LC 2010 map

| Rank | Parameter Name | Description | t-Stat | P-Value |
|---|---|---|---|---|
| 1 | CN2.mgt | SCS-curve number | -11.63 | 0 |
| 2 | GW_DELAY.gw | Ground water delay | 0.13 | 0.76 |
| 3 | GWQMN.gw | Threshold depth of water in the shallow aquifer | 0.26 | 0.92 |
| 4 | GW_REVAP.gw | Ground water re evaporation | 1.7 | 0.81 |
| 5 | ESCO.hru | Soilevaporation compensation factor | 1.2 | 0.78 |
| 6 | SOL_AWC(..).sol | Soil available water capacity | 0.45 | 0.64 |
| 7 | HRU_SLP.hru | Average slope steepness | 1.02 | 0.51 |
| 8 | PRECIPI. (..){..}.pcp | precipitation | -0.57 | 0.15 |

## 4. 10 Calibration and Validation

### 4.10.1 Runoff Modeling Evaluation

By comparing simulated runoff to observations, the model's response to various topographic and LC/LU data was tested. As previously discussed, the model output was calibrated and validated using a set of commonly used goodness of fit indicators, with NS set as the objective function in SWAT-CUP

By optimizing an objective function, calibration reduces errors between observations and model simulations. Automatic calibration was performed in two watersheds in this study.

The obtained hydrographs of calibrated and validated models are shown in Figures 4.7 and 4.8, with the model with the highest NS during the validation period considered the best model.

For the Dukan Watershed, the model of DEM 30 m resolution (SRTM) and LC/LU 30 m resolution (from Landsat) (2000) achieved the highest NS value, with 0.81 and 0.87 of NS and $R^2$ for the calibration period (2000-2007) and 0.63 and 0.79 for validation period (2007-2010), respectively as shown in fig (4.7).

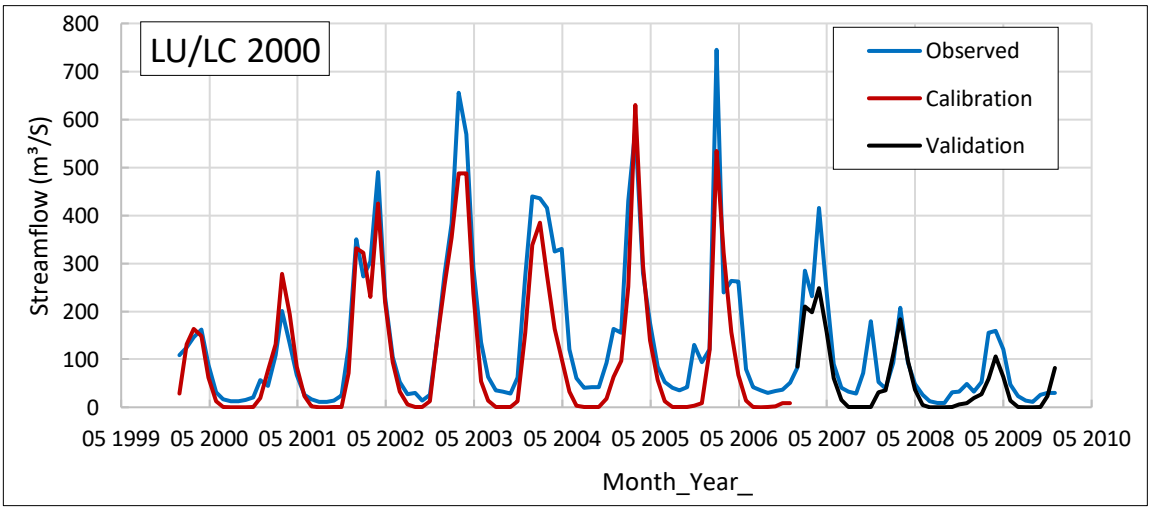


Figure (4.7): The best accurate simulated runoff for the Dukan watershed for LULC 2000.

## 4.11. 2 Water balance

Table (4.16) displays the values for the most commonly used statistical indices calculated to investigate the effect of watershed delineation on SWAT simulation accuracy. The SWAT's performance improved for the simulated flow for two LU/LC (2000-2010). Following the validation of (LULC 2000-2010), the Dukan, Dibis, the value of NSE increased by 13%, 20%, and respectively.This variation could have occurred as a result of regrouping.conversion of minor land uses to major land uses as the number of subbasins expanded

The calibration of a large scale distributed hydrologic model against river discharge may not provide enough confidence for all components of the water balance. Abbaspour et al., (2015) proposed multi criteria calibration to improve characterization of different components and to address the non uniqueness problem (narrowing prediction uncertainty).

Table (4. 15) Values of statistical indices for model calibration and validation

| | (LU/LC 2000) | | | | (LU/LC 2010) | | | |
|---|---|---|---|---|---|---|---|---|
| | Calibration | | Validation | | Calibration | | Validation | |
| | $R^2$ | NSE | $R^2$ | NSE | $R^2$ | NSE | $R^2$ | NSE |
| Dukan watershed | 0.87 | 0.81 | 0.79 | 0.63 | 0.74 | 0.71 | 0.76 | 0.76 |
| Dibis watershed | 0.82 | 0.76 | 0.8 | 0.63 | 0.9 | 0.89 | 0.85 | 0.83 |

The results show that higher NS models do not always produce the best water balance for the validation period when compared to observed. The water balance for the calibration and validation periods is shown in appendix B .

For two cases during the validation period, the models of (LU/LC 2000-LU/LC 2010) output simulated flow was closer to the observed flow than the other models, for Dukan watershed

For the Dukan Watershed, the model of DEM 30 m resolution (SRTM) and LuLc 30 m resolution (from Landsat) (2010) achieved the highest NS value, with 0.71 and 0.74 of NS and $R^2$ for the calibration period (2010-2017) and 0.76 and 0.76 for validation period (2017-2022), respectively.as shown in fig(4.8)

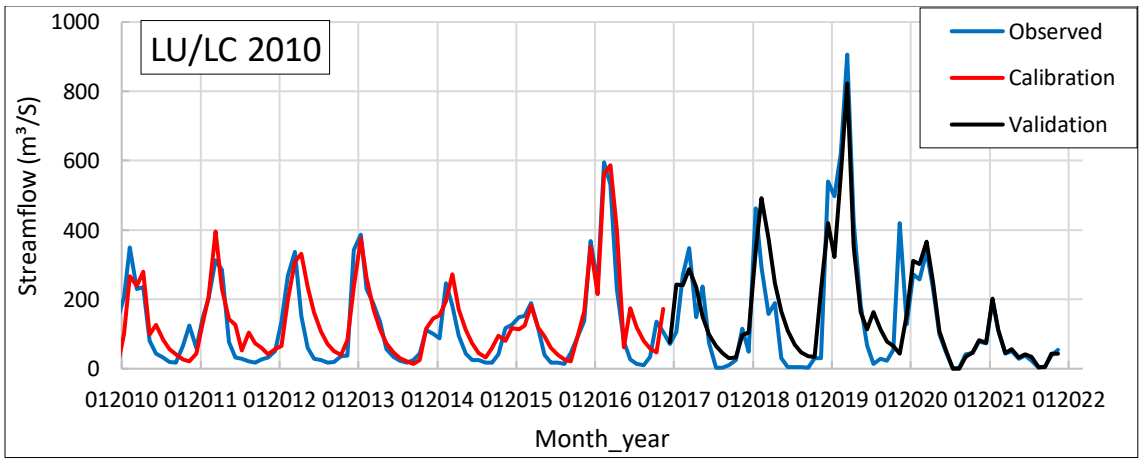


Figure (4.8): The best accurate simulated runoff for the Dukan watershed for LU/LC 2010.

For the Dibis Watershed, the model of DEM 30 m resolution (SRTM) and LC/LU 30 m resolution (from Landsat) (2002) achieved the highest NS value, with 0.76 and 0.82 of NS and R2 for the calibration period and 0.63 and 0.80 for validation period, respectively as shown in Fig ( 4.9)

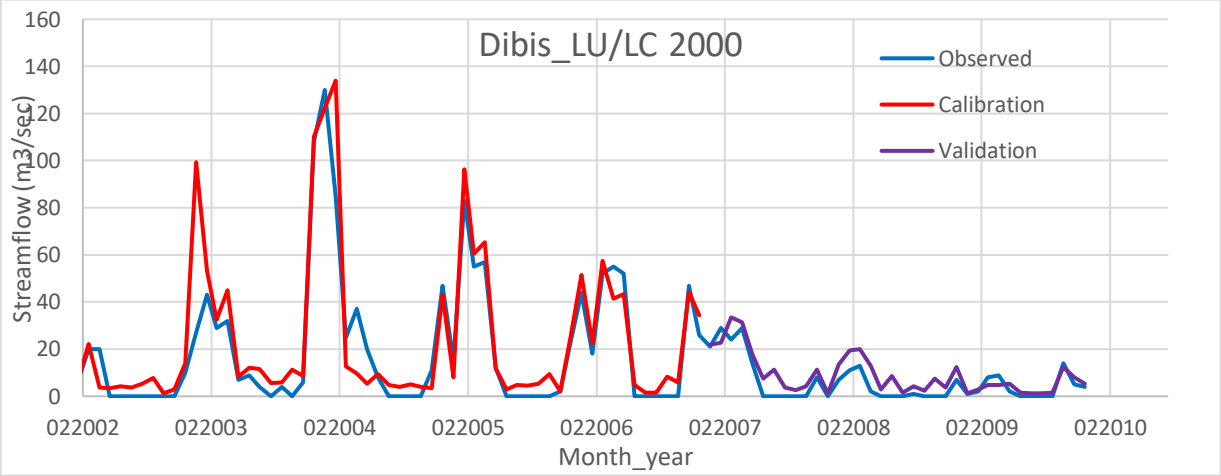


Figure (4.9): The best accurate simulated runoff for the Dibis watershed for LU/LC 2002.

For the Dibis Watershed, the model of DEM 30 m resolution (SRTM) and LC/LU 30 m resolution (from Landsat) (2010) achieved the highest NS value, with 0.89 and 0.90 of NS and R2 for the calibration period and 0.83 and 0.85 for validation period, respectively, as shown in Fig (4.10)

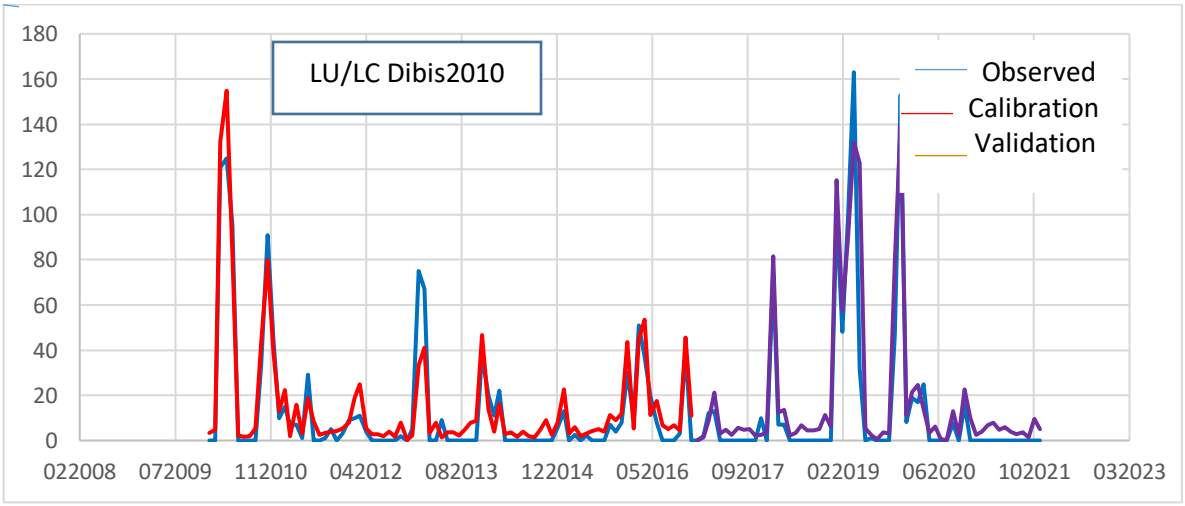


Figure (4.10): The best accurate simulated runoff for the Dibis watershed for LU/LC 2010.

# Chapter Five

# Conclusions and Recommendations

## 5.1 Conclusions

The current study applied remote sensing data and GIS technology to delineate land use and land cover (LU/LC) images and assess and identify alterations in the Lesser Zab Basin (LZB) during 1989, 1999, 2010, and 2021.

### 5.1.1 Land Use and Land Cover Alteration

- According to the supervised image classification process, seven general classes have been identified; water bodies, forest lands, agricultural lands, bare lands, and urban lands.
- Agricultural lands can be considered as the prevailing class;
- Agricultural lands decreased from 51.06 in 1989 to 39.96% in 2021.
- Shrinkage in water bodies has been one of the causes of reducing the agricultural areas.
- There had been a speedy alteration in agricultural lands to urban lands. In 1989, urban lands covered 0.46%, but in 2021, it increased to 5.59% compared to 1989.
- Natural ecology and biodiversity would be lost due to expanding urban areas.

### 5.1.2 Normalized Difference Vegetation Index

Based on Normalized difference vegetation index (NDVI) analysis, vegetation land cover during 1989, 1999, 2009, 2019, and 2021 was also recognized.

- The vegetation cover showed a decreasing trend from 2009 to 2021, with a ratio of 27.2% for low-density plants area. However, the vegetation-free area displayed a rising trend of about 28.6%.
- NDVI areal distribution is caused, generally, by alterations of the weather variables, such as precipitation and temperature.
- There were substantial variations in the vegetation cover from 2009 to 2021 due to the climate change impact linked to anthropogenic activities.

### 5.1.3 Land Use/Land Cover Prediction

The CA–Markov model has been applied to predict prospect LU/LC alterations, contributing to an enhanced consideration of potential LU/LC alterations and their dynamic influences. The results reveal that:

- Between 1999 and 2021, basin-wide urban areas increased considerably, whereas agricultural lands, forest cover and bare lands decreased.
- It is expected that by 2041, the built-up area will be about 5200 km2 (26%), while the coverage area of agricultural lands, forest, bare lands, and water bodies are expected to decrease.
- Urban areas would continue to expand mainly at the cost of agricultural, bare and forest areas.
- Agricultural lands have revealed a notable drop from 1999 to 2021, and future predictions established that this tendency would remain (i.e. from 2021 to 2041).
- LU/LC changing aspects are human-driven, which in turn distresses individuals and changes the availability of natural resources such as plants, water bodies, soil, and livestock.

- The map of 2041 would be used as a standard for decision-making, preparation, ecological management of the atmosphere, and biodiversity protection.

### 5.1.4 Hydrological Modeling

Arc SWAT software was examined and used for the period from 2000 to 2021 to simulate the Lesser Zab river flow The following conclusions can be drawn from the findings:

- The streamflow characteristics changed due to the LU/LC variations.
- The SWAT model evaluation revealed that the annual surface runoff in the Dukan watershed increased due to the flood wave that occurred in 2019.
- Asnow melt sensitive parameters effective in Dukan watershed as years progress, the thickness of the snow decreases and its contribution to the stream flow and not effective in Dibis watershed

## 5.2 Recommendations

Several recommendations would be suggested for further research associated with to hydrological impact of LU/LC change on LZRB.

- Frequently performing LU/LC changes detection.
- Explore different LU/LC classes by satellites, such as the Google Earth Engine platform and Sentinel.
- Identification of LU/LC and climate change impacts on the hydrological characteristics of a basin in arid to semi-arid regions.
- Estimating seasonal land surface temperature (LST) variations over different LU/LC classes using CA-Markov simulation and simulating future LU/LC and seasonal LST variations for 2041

## References


Abbaspour, K.C. (2015) SWAT-Calibration and Uncertainty Programs (CUP) A User Manual. Swiss Federal Institute of Aquatic Science and Technology, Eawag, Duebendorf, 1-100.

Abbaspour K.C., Yang J., Maximov I., Siber R., Bogner K., Mieleitner J., Zobrist J. and Srinivasan R. (2007). Modelling hydrology and water quality in the pre-alpi/alpine Thur watershed using SWAT. J. Hydrol. 333, 413–430.

Abdulrahman, A. I.,and Ameen, A. A. (2020). Predicting Land use and land cover spatiotemporal changes utilizing CA-Markov model in Duhok district between 1999and 2033. Academic Journal of Nawroz University (AJNU), Vol.9, No.4, 2020, Copyright ©2017. e-ISSN: 2520-789X

Abraham, A. Collins, D. and Martindale, R. (2006). The coaching schematic: validation through expert coach consensus. Journal of sports sciences, 24 (6). 549 - 564. ISSN 0264- 0414 DOI: https: //doi.org /10.1080 /02640410500189173

Alam A, Bhat, M, and Maheen M. (2020). Using Landsat satellite data for assessing the land use and land cover change in Kashmir valley. GeoJournal (2020) 85:1529–1543 https://doi.org /10.1007 /s10708-019-10037-x

Alkaradaghi, K., Ali, S. S., Al-Ansari, N., and Laue, J. (2018). Evaluation of land use& land cover change using multi-temporal Landsat imagery: a case study Sulaimaniyah Governorate, Iraq. Journal of Geographic Information System, 10(3), 247-260. https://doi.org/10.4236/jgis.2018.103013

Al-Saady, Y., Merkel, B., Al-Tawash, B., and Al-Suhail, Q. (2015). Land use and land cover (LULC) mapping and change detection in the Little Zab River Basin (LZRB), Kurdistan Region, NE Iraq and NW Iran. FOG-Freiberg Online Geoscience 43.

Al-Saady, Y. I., Al-Tawash, B. S., and Al-Suhail, Q. A. (2016). Effects of land use and land cover on concentrations of heavy metals in surface soils of Lesser Zab River Basin, NE Iraq. *Iraqi Journal of Science, 57*(2C), 1484–1503.

Arnold, J.G., Morias, D.N., Gassman, P.W., Abbaspour, K.C., White, J.M., Srinivasan, R., Santhi,C., Harmel, R.D., Van Griensven, A., Van Liew, M.W., Kannan,N., and Jha, M.K. (2012). SWAT: Model use, calibration and validation. ransactions of the ASABE 2012 American Society of Agricultural and Biological Engineers ISSN 2151-0032

Arnold, J. G., Srinivasan, R., Muttiah, and Williams, J.R. (1998). Large area hydrologic modelling and assessment; part I. model development. J. of Amer. Water Res. Assoc.34(1):73-89

Antonio, D. G., Louisa, J. M., and Jansen. (2000). Land Cover Classification System (LCCS): Classification Concepts and User Manual. Environment and Natural Resources Service (SDRN). GCP/RAF/287/ITA Africover – East Africa Project

Atulley j, Kwaku A A., Owusu-Ansah., Ampofo S., Jacob A., and Nii. O. S. (2022). Modeling the impact of past and future land cover changes on a reservoir catchment hydrology in Semi-arid, Africa. https://doi.org/10.21203/rs.3.rs-1505575/v1

Azizi, Malakmohamad, and Jafari. (2016). Land use and land cover spatiotemporal dynamic patternand predicting changes using integrated CA-Markov model. Global J. Environ. Sci. Manage., 2(3): 223-234, Summer 2016 DOI: 10.7508/gjesm. 2016.03.002

Barron, O. V, Pollock, D. W. and Dawes, W. R. (2009) 'Evaluation of catchment connectivity and storm runoff in flat terrain subject to urbanisation.', *Hydrology & Earth System Sciences Discussions*, 6(5).

Belihu, M., Tekleab, S., Abate, B., and Bewket, W. (2020). Hydrologic response to land use land cover change in the Upper Gidabo Watershed, Rift Valley Lakes Basin, Ethiopia. HydroRese Volume 3, 2020, Pages 85-94

Beven, K. J. (2001). "Rainfall-Runoff Modelling". The Primer. BOO, New York,Lancaster University, UK.

Breiman, L. (2001). Random forests. Machine learning, 45(1), 5-32.

Buyuksalih,G. (2016). Landsat Images Classification and Change Analysis of Land Cover /Use in Istanbul. International Journal of Environment and Geoinformatics /Arşiv/Cilt: 3 - Sayı: 2/56 -65 Watershed, Rift Valley Lakes Basin, Ethiopia. HydroResearch

Congalton, B. R., Green, G. K., (2019). Assessing the Accuracy of Remotely Sensed Data

Principles and Practices, Third Edition, https://doi.org /10.1201 /9780429052729

Chaudhary, B.S., Saroha, G.P., and Yadav, M. (2008). Human Induced Land Use Land Cover Changes in Northern Part of Gurgaon District, Haryana, India: Natural Resources Census Concept. Journal of Human Ecology, 23(3), pp. 243-252.

Cui, L., Zhao, Y., Liu, J., Wang, H., Han, L., Li, J., and Sun, Z. (2021). Vegetation Coverage Prediction for the Qinling Mountains Using the CA–Markov Model. ISPRS International Journal of Geo-Information, 10(10), 679

Daba, M. H., and You, and S., (2022). Quantitatively assessing the future land-use/land-cover changes and their driving factors in the upper stream of the Awash River based on the CA–markov model and their implications for water resources management. Sustainability, 14(3), 1538

Degife, A., Worku, H., Gizaw, S., and Legesse, A. (2019). Land use land cover dynamics, its drivers and environmental implications in Lake Hawassa Watershed of Ethiopia. Remote Sensing Applications: Society and Environment, 14, 178-190. https://doi.org/10.1016/j.rsase.2019.03.005

Dibaba, W. T., Demissie, T. A., and Miegel, K. (2020). Drivers and implications of land use/land cover dynamics in Finchaa catchment, northwestern Ethiopia. Land, 9(4), 113. https://doi.org/10.3390/land9040113

Engida, T.G., Nigussie, T.A., Aneseyee, A.B., and Barnaba, J. (2021). Land Use/Land Cover Change Impact on Hydrological Process in the Upper Baro Basin, Ethiopia. Applied and Environmental Soil Science Volume 2021, Article ID 6617541, 15 pages https://doi.org/10.1155/2021/6617541

ESRI. (2011). ArcGIS Desktop: Release 10. Environmental Systems Research Institute, Redlands

FAO, (1998). World Reference Base for Soil classification. http://www.fao.org/soils-portal/soil-survey/soil-classification/world-reference-base/en/

Food and Agriculture Organization (FAO). (1995). The Digital Soil Map of the World and Derived Soil Properties. http://www.fao.org/soils portal/ soilsurvey/soil-maps-and-databases /faounesco-soil-map-of-the-world /en/

FAO, The Food and Agricultural Organization. (2022). [Online] Available from https:// www. fao. org/ in- action/ action- again stdesertific ation/ overv iew/ deser tific ation- and- land- degra dation/ en/ [Accessed: 10th January 2022

Farhan, A. M. (2016). Estimation of Surface Runoff in Arid Regions by using Soil and Water Assessment Tool (SWAT) (Case study: A part of the Iraqi Western Desert). M.SC. Thesis, University of Baghdad, Baghdad, Iraq.

Fitzgerald. R. W., and Less, B. G. (1994). Assessing the classification accuracy of multisource remote sensing data.Remote Sensing of Environment ,Volume 47, Issue 3, March 1994, Pages 362-368

Frenken, K. (2009). Irrigation in the Middle East Region in Figures AQUASTAT Survey-2008. FAO Water Reports, 34, 355-375. http://www.fao.org/3/a-i0936e.pdf

Fouad, H. S. (2016). Assessing the Accuracy of Runoff Modelling with Different Spectral and Spatial Resolution Data Using SWAT Model. M.SC. Thesis, Technology University of, Baghdad, Iraq

Fuka, D. R., Walter, M. D., MacAlister. C., and Degaetano, A, T. (2014). Using the Climate Forecast System Reanalysis as weather input data for watershed models. Hydrological processes, https://doi.org/10.1002/hyp.

10073 Volume28, Issue22 30 October 2014

Gassman, P. W., Reyes, M. R., Green, C. H., & Arnold, J. G. (2007). The Soil and Water Assessment Tool: Historical Development, Applications, and Future Research Directions. Transactions of the ASABE, 50, 1211-1250.

https://doi.org/10.13031/2013.23637

Ghalehteimouri, K. J., Shamsoddini, A., Mousavi, M. N., Ros, F. B., and CKhedmatzadeh , A. (2022). Environmental Challenges. Predicting spatial and decadal of land use and land cover change using integrated cellular automata Markov chain model based scenarios (2019–2049) Zarriné-Rūd River Basin in Iran. Environmental Challenges 6 (2022) 100399

Gidado, K. A., Kamarudin, M. K. A., Hammad, M., Ghurah, S. A., Wahab, N. A., Saad, M. H. M., and Potikengrith, T. (2019). Application of Ca-Markov Model for the Analysis of Urban Growth in Kenyir Catchment. International Journal of Academic Research in Business and Social Sciences, 9(2), 449-458

Gupta, H. V., and Sorooshian , S (1999). Status of automatic calibration for hydrologic models:comparison with multilevel expert calibration J. Hydrol. Eng.25,135–143. https://doi.org/10.1002/fut.20174

Hadi, S. J., Shafri, H. Z. M., and Mahir, M. D. (2014). Modelling LULC for the period 2010-2030 using GIS and Remote sensing: a case study of Tikrit, Iraq. IOP Conference Series: Earth and Environmental Science IOP Conf. Series: Earth and Environmental Science 20 (2014) 012053 https://doi:10.1088/1755-1315/20/1/012053

Hagos, M. K., Egilson , D., Bjornsson , B. B., Thorarinsdottir ,T., and Gudmundsson , J. (2014). Analysing the effect of Land Use Land Cover change on catchment discharge. Land Restoration Training Programme Keldnaholt, 112 Reykjavik, Iceland.

Hamad, R., Balzter, H., and Kolo, K. (2018). Predicting Land Use/Land Cover Changes Using a CA-Markov Model under Two Different Scenarios. Sustainability, Sustainability 2018, 10, 3421; https://doi:10.3390/su10103421

Hishe, S., Bewket, W., Nyssen, J., and Lyimo, J. (2020). Analysing past land use land cover change and CA-Markov-based future modelling in the Middle Suluh Valley, Northern Ethiopia. Geocarto International, 35(3), 225-255

Hussain, S., Mubeen, M., Ahmad, A., Masood, N., Hammad, H.M., Amjad, M., Imran, M., Usman, M., Farid, U. M., Fahad,S., Nasim, W., Javeed, H. M. R., Ali, M., Qaisrani, S. A., Farooq, A., Khaild, M. S., and Waleed, M. (2021). Satellitebased evaluation of change in cultivated land in Southern Punjab (Multan region) through dynamics of vegetation and land surface temperature. *Open Geosciences, 13*(1), 1561–1577. https:// doi. org/ 10. 1515/ geo- 2020- 0298

Hussain, S., Mubeen, M., Akram, W., Ahmad, A., Habib-ur-Rahman, M., Ghaffar, A., Amin, A., Awais, M., Farid, H. U., Farooq, A., and Nasim, W. (2020b). Study of land cover/land use changes using RS and GIS: A case study of Multan district. *Pakistan. Environmental Monitoring and Assessment, 192*(1), 1–15

Hussain, S., Mubeen, M., and Karuppannan, S. (2022b). Land use and land cover (LULC) change analysis using TM, ETM+ and OLI Landsat images in district of Okara, Punjab, Pakistan. *Physics and Chemistry of the Earth, Parts a/b/c*. https://doi. org/ 10. 1016/j. pce. 2022. 103117

Hussain, S., Lu, L., Mubeen, M., Nasim, W., Karuppannan, S., Fahad, S., Tariq, A., Mousa, B. G., Mumtaz, F., and Aslam, M. (2022a). Spatiotemporal variation in land use land cover in the response to local climate change using multispectral remote sensing data. *Land, 11*(5), 595. https:// doi. org/ 10.3390/ land1 10505 95

http://globalweather.tamu.edu /

http://earthexplorer.usgs.gov/

Hyandye, C., and Martz, L.W. (2017). A Markovian and cellular automata landuse change predictive model of the Usangu Catchment. Int J Remote Sens 38:64–81

Jassim, S.Z., and Goff, J.C., (2006) Geology of Iraq. 1st Edition, Published by Dolin, Prague and Moravian Museum, Brno, Printed in the Czech Republic.

Jensen, J. R. (2005) Introductory Digital Image Processing: A Remote Sensing Perspective. 3rd Edition, Prentice Hall, Upper Saddle River, 505-512.

Jensen, J. R. (1996). Introductory digital image processing: a remote sensing perspective (No. Ed. 2). Prentice-Hall IncKan-In, K., Khunrattanasiri, W. (2020). Comparative Study on CA-Markov Model and CLUE-S Model for Land Use Changed Prediction in National Reserved Forest, Nan Province (Doctoral dissertation, Kasetsart University).

Juliev, M., Pulatov, A., Fuchs, S., and Hübl, J. (2019). Analysis of Land Use Land Cover Change Detection of Bostanlik District,Uzbekistan. Polish Journal of Environmental Studies, 28(5). https://doi.org/10.15244/pjoes/94216

Kafle, S.CH., (2019). Correlation and Regression Analysis Using SPSS. OCEM Journal of Management, Technology & Social Sciences

Karimi, H., Jafarnezhad, J., Khaledi, J., and Ahmadi, P. (2018). Monitoring and prediction of land use/land cover changes using CA-Markov model: a case study of Ravansar County in Iran. Arabian Journal of Geosciences, 11(19), 1-9.

Khan, Z., Saeed, A., and Bazai, M. H. (2020). Land use/land cover change detection and prediction using the CA-Markov model: A case study of Quetta city, Pakistan. Journal of Geography and Social Sciences, 2(2), 164-182

Khwarahm, N. R., Qader, S., Ararat, K., and Al-Quraishi, A. M. F. (2021). Predicting and mapping land cover/land use changes in Erbil/Iraq using CA-Markov synergy model. Earth Science Informatics, 14(1), 393-406.

https://doi.org /10.1007 /s12145-020-00541-x

Khwarahm, N. R., Najmaddin, P. M., Ararat, K., and Qader, S. (2021). Past and future prediction of land cover land use change based on earth observation data by the CA–Markov model: a case study from Duhok governorate, Iraq. Arabian Journal of Geosciences, 14(15), 1-14

Li, K., Feng, M., Biswas, A., Su, H., Nu, Y., and Cao , J. (2020). Driving Factors and Future Prediction of Land Use and Cover Change Based on Satellite Remote Sensing Data by the LCM Model: A Case Study from Gansu Province, China. Sensors, 2020, 20, 2757; https://doi.org/10.3390/s20102757

Lin, X., Xu, M., Cao, C., Singh, P. R., Chen, W., and Ju, H. (2018). Land-use/land-cover changes and their influence on the ecosystem in Chengdu City, China during the period of 1992–2018. Sustainability, 10(10), 3580. https://doi.org/10.3390/su10103580

Li, X., Wang, M., Liu, X., Chen, Z., Wei, X., Che, W. (2018). Mcr-modified ca–markov model for the simulation of urban expansion. Sustainability, 10(9), 3116

Lillesand, T. M. and Kiefer, R, W. (1999). “Remote Sensing and Image Interpretation,” John Willey and Sons, New York

Leta, M. K., Demissie, T.A., and Tränckner, J. (2021). Hydrological Responses of watershed to Historical and Future Land Use Land Cover Change Dynamics of Nashe Watershed, Ethiopia. Water, 13, 2372. https:// doi.org / 10.3390/ w13172372

Mahmoud, S. H., and Alazba, A. A. (2015). Hydrological Response to Land Cover Changes and Human Activities in Arid Regions Using a Geographic Information System and Remote Sensing. PLoS ONE 10(4): e0125805. https://doi:10.1371/journal.pone.0125805

Matlhod, B., Kenabatho, P.K., Parida, P. B., and Maphanyane, J. G. (2021) . Analysis of the Future Land Use Land Cover Changes in the Gaborone Dam Catchment Using CA-Markov Model:Implications on Water Resources. Remote Sensing, Remote Sens. 2021, 13, 2427. https:// doi.org/ 10.3390/rs13132427

Maury, C., and Sharma, V. N. (2020). Land use/Land cover Change Detection in Auranga River Basin, Jharkhand

Mengist, k. t. (2009). Watershed Hydrological Responses to Changes in Land Use and Land Cover, and Management Practices at Hare Watershed, Ethiopia .M.SC.Thesis, Universität Siegen. Siegen,Germany

Messele, T. A., and Moti, D. M. (2019). Modeling change of Land use on Hydrological Response of River by Remedial Measures using Arc SWAT: Case of Weib Catchment, Ethiopi. International Journal of Innovative Technology and Exploring Engineering (IJITEE), ISSN: 2278-3075, Volume-8 Issue-11, September 2019.

Mengistu, A. G., Rensburg, L. D. V., and Woyess, Y. E . (2019). Techniques for calibration and validation of SWAT model in data scarce arid and semi-arid catchments in South Africa. Journal of Hydrology: Regional Studie

Mohammed, J. (2013). Land use and cover change assessment using Remote Sensing and GIS: Dohuk City, Kurdistan, Iraq (1998-2011). International journal of Geomatics and Geosciences, 3(3), 552

Mohammed, R., and Scholz, M. (2016). Impact of Evapotranspiration Formulations at various ElevationsOn the Reconnaissance Drought Index. Water Resoure Manage

DOI 10.1007/s11269-017-1590-0

Mohammed, R., and Scholz, M. (2016). Impact of climate variability and streamflow alteration on groundwater contribution to the base flow of the Lower Zab River (Iran and Iraq). Environmental Earth Sciences, 75(21 https://link.springer.com /article/10.1007/s12665-016-6205-1

Mohammed, R., Scholz, M., and Kermani., M. Z. (2017). Temporal Hydrologic Alterations Coupled with Climate Variability and Drought for Transboundary River Basins. D ɜsour Manage DOI 10.1007/s11269-017-1590-0

Mohammed, R., Scholz, M. (2018). Climate change and anthropogenic intervention impact on the hydrologic anomalies in a semi-arid area: Lower Zab River Basin, Iraq.

Environmental Earth Sciences, 77(10), 1-19. https://link.springer.com/article_/10.1007%2Fs12665-018-7537-9

Molina, N. E., Hallack, A. M., Martínez, P. S., Ramírez, H. J., Mungaray, M. A., and Sastre, M. (2016). A Hydrological modeling and climate change impacts in an agricultural semiarid region. Case study: Guadalupe River basin, Mexico. Agric Water Manag 175:29–42. https://doi.org /10.1016/j. agwat. 2015.10.029

Mondal, M. S., Sharma, N., Kappas, M., and Garg, P. K. (2019). Ca Markov modeling of land use land cover dynamics and sensitivity analysis to identify sensitive parameter (S). The International Archives of Photogrammetry, Remote Sensing and Spatial Information Sciences, 42, 723-729.

Mondal, M. S., Sharma, N., Kappas, M., and Garg, P. K. (2020). Cellular automata (CA) contiguity filters impacts on ca Markov modeling of land use land cover change predictions results. The International Archives of Photogrammetry, Remote Sensing and Spatial Information Sciences, 43, 1585-1591.

Moreira , L. L., Schwamback, D. D. and Rigo . (2018). "Sensitivity analysis of the Soil and Water Assessment Tools (SWAT) model in streamflow modeling in a rural river basin," Ambient. Água - An Interdiscip. J. Appl. Sci., vol. 13, p.1 https://doi.org/10.4136/Ambi-Agua.2221

Moriasi, D.N., Arnold, J. G., Liew, M. W., Van, Bingner, R. L., Harmel, R. D., and Veith. T. L . (2007). Model evaluation guidelines for systematic quantification of accuracy in watershed simulation D.Colomb. Med. https://doi.org /10.1234 /590

Munthali, M. G., Mustak, S., Adeola, A., Botai, J., Singh, S. K., and Davis, N. (2020). Modelling land use and land cover dynamics of Dedza district of Malawi using hybrid Cellular Automata and Markov model. Remote Sensing Applications: Society and Environment, 17, 100276.

Musgrave, G.W. (1955). How Much of the Rain Enters the Soil? In The United States Department of Agriculture, Ed. Water: Year book of Agriculture, The United States Department of Agriculture, Washington DC, 151-159.

Nash, J. E., and Sutcliffe, J. V. (1970). River flow forecasting throligh conceptual models part 1 -A discussion of principles.J. Hydrol. Eng.10,282–290.

https://doi.org / 10.1080/00750770109555783

Neitch, S. L., Arnold, J. G., Kiniry J. R., and WilliamsJ. R. (2005). 'Soil and Water Assessment Tool – Theoretical Documentation-Version. Grassland, Soil and Water Research Laboratory, Agricultural Research Service, Texas,2005. pages 9 to 11.

Nii, O. S. (2022). Modeling the impact of past and future land cover changes on a reservoir catchment hydrology in Semi-arid, Africa DOI: https://doi.org /10.21203 /rs.3.rs-1505575/v1 License : This work is licensed under a Creative Commons Attribution 4.0 International License

Oliver, T. H., and Morecroft, M. D. (2014). Interactions between climate change and land use change on biodiversity: attribution problems, risks, and opportunities. Wiley Interdisciplinary Reviews: Climate Change, 5(3), 317-335. https://doi.org/10.1002/wcc.271

Omar, N. Q., Ahamad, M. S. S., Wan Hussin, W. M. A., Samat, N., and Binti Ahmad, S. Z. (2014). Markov CA, multi regression, and multiple decision making for modeling historical changes in Kirkuk City, Iraq. Journal of the Indian Society of Remote Sensing, 42(1), 165-178

Omani, N., Tajrishy, M., and Abrishamchi, A. (2007). Modeling of a River Basin Using SWAT Model and GIS, June 6-8, 2007, Riverside Kuching, Sarawak, Malaysia

Padmaja, G., and Giridhar, M. V. S. S. (2022). Utility of Geomatics in Land Use Land Cover Change Detection and Accuracy Analysis. In Advanced Modelling and Innovations in Water Resources Engineering (pp. 517-527). Springer, Singapore

Regmi, R, R, Saha, S, K., and Subedi, D, S. (2017). Geospatial Analysis of Land Use Land Cover Change Modeling in Phewa Lake Watershed of Nepal by Using GEOMOD Model. Himal. Phys. 6, 65–72.

Refsgaard, J. C., (1996). Terminology, modelling protocol and classification of hydrological model codes. In Abbott MB, Refsgaard JC (Eds), Distributed Hydrological Modelling. Kluwer Academic Publishers, 17-39

Richards, J. A., (2013). Supervised classification techniques. In Remote Sensing Digital Image Analysis (pp. 247-318). Springer, Berlin, Heidelberg

Rwanga, S. S., and Ndambuki, J. M. (2017). Accuracy Assessment of Land Use/Land Cover Classification Using Remote Sensing and GIS. International Journal of Geosciences, 2017, 8, 611- https://doi.org/ 10.4236/ijg.2017.84033

Sahu,M., Lahari, S., Gosain, A.K., and Ohri, A. (2016). Hydrological Modeling of Mahi Basin Using SWAT. Journal of Water Resource and Hydraulic Engineering, Sept. 2016, Vol. 5 Iss. 3, PP. 68-79

Sakthivel, M., Priyadharshini, J., and Vijayakumar, S. (2021). Accuracy Assessment of Land Use Land Cover Classification using GIS and Remote Sensing Approach: A Case

Study of Tiruchirappalli District, Tamil Nadu, India. The International journal of analytical and experimental modal analysis, XIII(VIII), 861-875.

Saleh, A. M., and Ahmed, F. W. (2021). Analyzing Land Use/Land Cover Change Using Remote Sensing and GIS in Mosul District, Iraq. Annals of the Romanian Society for Cell Biology, 4342–4359. https://www.annalsofrscb.ro /index.

Php /journal /article /view /1928

Setegn, S. G., Srinivasan, R., and Dargahi, G. (2008). Hydrological Modelling in the Lake Tana Basin, Ethiopia Using SWAT Model. The Open Hydrology Journal, 2008, 2, 49-62

Shen,Q., Zhang, A., and Zhang, H. (2021). Analysis of Land Use Change in Nanjing Based on Landsat Remote Sensing Images. Earth and Environmental Science, IOP Conf. Ser.: Earth Environ. Sci. 783 012129

Singh, V. P., and Woolhiser, D.A. (2002). Mathematical Modelling of Watershed Hydrology. Journal of Hydrological Engineering, ASCE, 7, 270-292

Singh, V. P. (1995). Computer models of watershed hydrology, V. P. Singh, ed., Water

Resources Publications, Littleton, Colo., 1–22.

Soil Conservation Service Engineering Division, 1972

Tadele, H., Mekuriaw, A., Selassie, Y. G., and Tsegaye, L. (2017). Land use/land cover factor values and accuracy assessment using a gis and remote sensing in the case of the Quashay watershed in Northwestern Ethiopia. JNRD-Journal of Natural Resources and Development, 7, 38-44. https://doi.org /10.5027 /JNRD.V7I0.05

Tades, S., Soromess, T., and Bekele, T. (2021). Analysis of the Current and Future Prediction of Land Use/Land Cover Change Using Remote Sensing and the CA-Markov Model in Majang Forest Biosphere Reserves of Gambella,Southwestern Ethiopia. Hindawi. The Scientific World Journa, Volume 2021 |Article ID 6685045, https://doi.org /10.1155 /2021 /6685045

Tembo, N., and Volk, J. (2022). Effects of Land-Use Land-Cover Change on River flow in Chalimbana River Catchment,Chongwe District, Zambia. International Journal of Innovative Science and Research Technology, ISSN No: 2456-2165

Thompson, C. (2022). Remote Sensing Methods for Assessing Abrupt Land Cover Change A Case Study of the Central Luangwa Valley in Zambia. M.SC.Thesis, Harvard University, Division of Continuing Education.

UN. (2017). Department of economic and social affairs, population division. World population prospects: The 2017 revision, Volume II: Demographic Profiles. ST/ESA/SER.A/400

UN. (2013). World Environment Day 2013: How environmental damage causes food insecurity in Iraq. https://reliefweb.int/sites/reliefweb. int/files/resources/Factsheet-WorldEnvironment-English.pdf. Accessed 31 Mar 2020

United States' National Resources Conservation Service (NRCS, 2007)

USDA-SCS. (1986). Urban Hydrology for Small Watersheds. Technical Release No. 55 (TR-55). USDASCS, Washington DC.

Viera, A. J., and Garrett, J. M. (2005). Understanding inter observer agreement: the kappa statistic. Fam med 37(5), 360-363. PMID: 15883903.

Viessman, W. (2003) Introduction to Hydrology fifth edition.

Wang, S., and Zheng, X. (2022). Dominant transition probability: combining CA-Markov model to simulate land use change. Environment, Development and Sustainability, 1-19

Wang, L., Yu, D., Liu, Z., Yang, Y., Zhang, J., Han, J., and Mao, Z. (2018). Study on NDVI changes in Weihe Watershed based on CA–Markov model. Geological Journal, 53, 435-441

Welde, K., and Gebremariam, B. (2017). Effect of land use land cover dynamics on hydrological response of watershed: Case study of Tekeze Dam watershed, northern Ethiopia, International Soil and Water Conservation Research

Wincell, M. F., Peranginangin, N., Srinivasan. R, and Chen W. (2017). Soil and Water Assessment Tool model predictions of annual maximum pesticide concentrations in high vulnerability watersheds. Integrated Enviromental Assessment and Management https://doi.org /10.1002 /ieam.2014

Winnaar, G. De., Jewit, G. P.W., and Horan, H. (2007). A GIS-based approach for identifying potential runoff harvesting sites in the Thukela River basin, South Africa. ScienceDirect. Physics and Chemistry of the Earth, Parts A/B/C Volume 32, Issues 15–18, 2007, Pages 1058-1067

Wu, H., and Chen, B. (2015). Evaluating uncertainty estimates in distributed hydrological modeling for the Wenjing River watershed in China by GLUE, SUFI-2, and ParaSol methods. Ecol Eng 76:110–121.

https://doi.org/10.1016/j. ecoleng.2014.05.014

Yeneneh, N., Eliasa, E., and Feyisa, G.L. (2022). Detection of land use/land cover and land surface temperature change in the Suha Watershed, North-Western highlands of Ethiopia. Environmental Challenges 7 (2022) 100523

Yesuph, A. Y., and Dagnew, A. B. (2019). Land use/cover spatiotemporal dynamics, driving forces and implications at the Beshillo catchment of the Blue Nile Basin, North Eastern Highlands of Ethiopia. Environmental Systems Research, 8(21), 1-30

Yi, S., Zhou, Y., and Li, Q. (2022). A New Perspective for Urban Development Boundary Delineation Based on the MCR Model and CA-Markov Model. Land, 11(3), 401

Zhang, L., Nan, Z., Xu, Y., and Li , S. (2016). Hydrological Impacts of Land Use Change and Climate Variability in the Headwater Region of the Heihe River Basin, Northwest China. PLoS ONE 11(6): e0158394. https://doi:10.1371/journal . pone. 0158394.

# Appendix A

Table (A.1) Details of the mathematical calculations for kappa coefficient and Accuracy evaluation for 1989

$$OA^{*}\% = \frac{47}{53} \times 100 = 88.67$$

$$KI^{**}\% = \frac{(47*53)-((10*12)+(9*9)+(10*7)+(7*10)+(10*9)+(7*6))}{2809-((10*12)+(9*9)+(10*7)+(7*10)+(10*9)+(7*6))} \times 100$$

$$= 86.559\%$$

| Class | User accuracy calculation% | Procedure accuracy calculation% |
|---|---|---|
| $WB^{1}$ | $\frac{10}{10} \times 100 = 100$ | $\frac{10}{12} \times 100 = 83.3$ |
| $FO^{2}$ | $\frac{9}{9} \times 100 = 100$ | $\frac{9}{9} \times 100 = 100$ |
| $AL^{3}$ | $\frac{7}{10} \times 100 = 70$ | $\frac{7}{7} \times 100 = 100$ |
| $BL_D^{4}$ | $\frac{6}{7} \times 100 = 85.7$ | $\frac{6}{10} \times 100 = 60$ |
| $BL_L^{5}$ | $\frac{9}{10} \times 100 = 90$ | $\frac{9}{9} \times 100 = 100$ |
| $UL^{6}$ | $\frac{6}{7} \times 100 = 85.7$ | $\frac{6}{6} \times 100 = 100$ |

Table (A.2) Details of the mathematical calculations for kappa coefficient and Accuracy evaluation for 1999

$$OA^{*}\% = \frac{56}{61} \times 100 = 91.8$$

$$KI^{**} = \frac{(56*61)-((10*10)+(10*9)+(10*12)+(10*10)+(12*16)+(7*6)}{3721-((10*10)+(10*9)+(10*12)+(10*10)+(12*16)+(7*6)\ )} \times 100$$

$$= 90.08\%$$

| Class | User accuracy calculation% | Procedure accuracy calculation% |
|---|---|---|
| $WB^{1}$ | $\frac{10}{10} \times 100 = 100$ | $\frac{10}{10} \times 100 = 100$ |
| $FO^{2}$ | $\frac{10}{10} \times 100 = 100$ | $\frac{9}{9} \times 100 = 100$ |
| $AL^{3}$ | $\frac{10}{12} \times 100 = 83.3$ | $\frac{10}{10} \times 100 = 100$ |
| $BL_D^{4}$ | $\frac{9}{10} \times 100 = 90$ | $\frac{9}{10} \times 100 = 90$ |
| $BL_L^{5}$ | $\frac{12}{12} \times 100 = 100$ | $\frac{12}{16} \times 100 = 75$ |

| | | |
|---|---|---|
| $UL^6$ | $\frac{6}{7}\times100=85.7$ | $\frac{6}{6}\times100=100$ |

Table (A.3) Details of the mathematical calculations for kappa coefficient and Accuracy evaluation for 2010

$$OA^{*}\ \% = \frac{\mathbf{71}}{\mathbf{74}}\times100 = 95.9$$

$$(KI)^{**}\ \% = \frac{(71*74)-((12*12)+(12*12)+(12*10)+(12*13)+(13*13)+(12*13)}{5476-((12*12)+(12*12)+(12*10)+(12*13)+(13*13)+(12*13))} \times$$

$$\mathbf{100} = \frac{4365}{4587}*100 = 95.16$$

| Class | User accuracy calculation% | Procedure accuracy calculation% |
|---|---|---|
| $WB^1$ | $\frac{12}{12}\times100=100$ | $\frac{12}{12}\times100=100$ |
| $FO^2$ | $\frac{12}{12}\times100=100$ | $\frac{12}{12}\times100=100$ |
| $AL^3$ | $\frac{10}{12}\times100=83.3$ | $\frac{10}{10}\times100=100$ |
| $BL_D^4$ | $\frac{12}{13}\times100=92.3$ | $\frac{12}{12}\times100=100$ |
| $BL_L^5$ | $\frac{13}{13}\times100=100$ | $\frac{13}{13}\times100=100$ |
| $UL^6$ | $\frac{12}{12}\times100=100$ | $\frac{12}{13}\times100=92.3$ |

Table (A.4) Details of the mathematical calculations for kappa coefficient and Accuracy evaluation for 2021

$$OA^{*}\ \% = = \frac{\mathbf{55}}{\mathbf{63}}*100 = 87.3$$

$$KI^{**}\ \% = \frac{(55*63)-\left((12*12)+(8*9)+(11*4)+(12*10)+(10*16)+(11*11)\right)}{3969-\left((12*12)+(8*9)+(11*4)+(12*10)+(10*16)+(11*11)\right))} \times \mathbf{100}$$

$$= \frac{2804}{3308}*100 = 84.76$$

| Class | User accuracy calculation% | Procedure accuracycalculation% |
|---|---|---|
| $WB^1$ | $\frac{12}{12}\times100=100$ | $\frac{12}{12}\times100=100$ |
| $FO^2$ | $\frac{8}{9}\times100=88.8$ | $\frac{8}{8}\times100=100$ |
| $AL^3$ | $\frac{4}{11}\times100=36.3$ | $\frac{4}{4}\times100=100$ |
| $BL_D^4$ | $\frac{10}{10}\times100=100$ | $\frac{10}{12}\times100=83.3$ |

| | | |
|---|---|---|
| $BL_L$[5] | $\frac{10}{10}\times100=100$ | $\frac{10}{10}\times100=100$ |
| UL[6] | $\frac{11}{11}\times100=100$ | $\frac{11}{11}\times100=100$ |

* Overall Accuracy ; ** kappa coefficient; [1]Water Bodies; [2]Forest; [3]Agricultural Lands; [4]Bare Lands Dark; [5]Bare Lands Light; [6]Urban Lands

# APPENDIX B

Table (B.1) The water balance of Dukan models for calibration period (2000 - 2007) ) and validation periods ( 2007 - 2010 )

| No | Year | Month | Observed | Simulated |
|---|---|---|---|---|
| 1 | 2000 | January | 108.1 | 29.1 |
| 2 | 2000 | February | 124.9 | 131.5 |
| 3 | 2000 | March | 146.2 | 164.0 |
| 4 | 2000 | April | 161.6 | 149.2 |
| 5 | 2000 | May | 88.4 | 62.5 |
| 6 | 2000 | June | 31.3 | 12.7 |
| 7 | 2000 | July | 16.1 | 0.0 |
| 8 | 2000 | August | 12.2 | 0.0 |
| 9 | 2000 | September | 12.7 | 0.0 |
| 10 | 2000 | October | 14.7 | 0.0 |
| 11 | 2000 | November | 20.2 | 0.2 |
| 12 | 2000 | December | 56.2 | 19.3 |
| 13 | 2001 | January | 44.7 | 77.0 |
| 14 | 2001 | February | 108.1 | 131.1 |
| 15 | 2001 | March | 201.1 | 278.2 |
| 16 | 2001 | April | 132.7 | 193.5 |
| 17 | 2001 | May | 67.9 | 84.0 |
| 18 | 2001 | June | 26.1 | 22.8 |
| 19 | 2001 | July | 16.5 | 1.5 |
| 20 | 2001 | August | 11.5 | 0.0 |
| 21 | 2001 | September | 11.2 | 0.0 |
| 22 | 2001 | October | 13.7 | 0.1 |
| 23 | 2001 | November | 25.3 | 1.2 |
| 24 | 2001 | December | 125.5 | 71.7 |
| 26 | 2002 | February | 273.0 | 321.0 |

| | | | | |
|---|---|---|---|---|
| 27 | 2002 | March | 303.0 | 230.0 |
| 28 | 2002 | April | 490.0 | 424.4 |
| 29 | 2002 | May | 230.0 | 219.9 |
| 30 | 2002 | June | 105.0 | 93.4 |
| 31 | 2002 | July | 52.0 | 32.7 |
| 32 | 2002 | August | 27.0 | 6.0 |
| 33 | 2002 | September | 30.0 | 0.5 |
| 34 | 2002 | October | 14.0 | 0.5 |
| 35 | 2002 | November | 26.0 | 13.2 |
| 36 | 2002 | December | 137.0 | 136.2 |
| 37 | 2003 | January | 278.0 | 255.8 |
| 38 | 2003 | February | 383.0 | 354.0 |
| 39 | 2003 | March | 655.0 | 487.4 |
| 40 | 2003 | April | 569.0 | 488.1 |
| 41 | 2003 | May | 290.0 | 237.3 |
| 42 | 2003 | June | 136.0 | 54.6 |
| 43 | 2003 | July | 63.0 | 13.5 |
| 44 | 2003 | August | 35.0 | 0.3 |
| 45 | 2003 | September | 33.0 | 0.1 |
| 46 | 2003 | October | 29.0 | 0.2 |
| 47 | 2003 | November | 62.0 | 12.8 |
| 48 | 2003 | December | 273.0 | 155.6 |
| 49 | 2004 | January | 440.0 | 338.3 |
| 50 | 2004 | February | 435.0 | 385.2 |
| 51 | 2004 | March | 415.0 | 275.4 |
| 52 | 2004 | April | 325.0 | 163.6 |
| 53 | 2004 | May | 330.0 | 100.7 |
| 54 | 2004 | June | 120.0 | 32.8 |
| 55 | 2004 | July | 60.0 | 3.3 |
| 56 | 2004 | August | 40.0 | 0.1 |

| | | | | |
|---|---|---|---|---|
| 57 | 2004 | September | 42.0 | 0.0 |
| 58 | 2004 | October | 42.0 | 0.1 |
| 59 | 2004 | November | 93.0 | 17.6 |
| 60 | 2004 | December | 163.0 | 63.2 |
| 61 | 2005 | January | 155.0 | 96.6 |
| 62 | 2005 | February | 430.0 | 251.1 |
| 63 | 2005 | March | 580.0 | 629.9 |
| 64 | 2005 | April | 280.0 | 295.6 |
| 65 | 2005 | May | 175.0 | 140.0 |
| 66 | 2005 | June | 85.0 | 56.0 |
| 67 | 2005 | July | 52.0 | 12.4 |
| 68 | 2005 | August | 40.0 | 0.4 |
| 69 | 2005 | September | 35.0 | 0.1 |
| 70 | 2005 | October | 42.0 | 0.2 |
| 71 | 2005 | November | 130.0 | 2.7 |
| 72 | 2005 | December | 94.0 | 8.5 |
| 73 | 2006 | January | 120.0 | 117.4 |
| 74 | 2006 | February | 745.0 | 534.0 |
| 75 | 2006 | March | 240.0 | 322.4 |
| 76 | 2006 | April | 264.0 | 156.7 |
| 77 | 2006 | May | 262.0 | 67.3 |
| 78 | 2006 | June | 79.0 | 14.0 |
| 79 | 2006 | July | 42.0 | 0.9 |
| 80 | 2006 | August | 35.0 | 0.0 |
| 81 | 2006 | September | 30.0 | 0.0 |
| 82 | 2006 | October | 34.0 | 2.5 |
| 83 | 2006 | November | 37.0 | 8.6 |
| 84 | 2006 | December | 51.0 | 9.1 |
| 85 | 2007 | January | 82.0 | 85.0 |

| | | | | |
|---|---|---|---|---|
| 86 | 2007 | February | 285.0 | 209.9 |
| 87 | 2007 | March | 232.0 | 198.6 |
| 88 | 2007 | April | 415.0 | 248.3 |
| 89 | 2007 | May | 240.0 | 156.0 |
| 90 | 2007 | June | 90.0 | 60.6 |
| 91 | 2007 | July | 41.0 | 15.4 |
| 92 | 2007 | August | 33.0 | 0.2 |
| 93 | 2007 | September | 28.0 | 0.0 |
| 94 | 2007 | October | 71.0 | 0.0 |
| 95 | 2007 | November | 180.0 | 0.3 |
| 96 | 2007 | December | 52.0 | 31.8 |
| 97 | 2008 | January | 39.0 | 35.8 |
| 98 | 2008 | February | 92.0 | 109.8 |
| 99 | 2008 | March | 207.0 | 183.9 |
| 100 | 2008 | April | 93.0 | 96.8 |
| 101 | 2008 | May | 48.0 | 36.8 |
| 102 | 2008 | June | 26.0 | 4.7 |
| 103 | 2008 | July | 13.0 | 0.0 |
| 104 | 2008 | August | 9.0 | 0.0 |
| 105 | 2008 | September | 9.0 | 0.0 |
| 106 | 2008 | October | 31.0 | 0.7 |
| 107 | 2008 | November | 33.0 | 6.3 |
| 108 | 2008 | December | 48.0 | 8.7 |
| 109 | 2009 | January | 32.0 | 19.4 |
| 110 | 2009 | February | 53.0 | 27.5 |
| 111 | 2009 | March | 155.0 | 59.4 |
| 112 | 2009 | April | 160.0 | 106.5 |
| 113 | 2009 | May | 120.0 | 63.5 |
| 114 | 2009 | June | 47.0 | 14.0 |
| 115 | 2009 | July | 23.0 | 0.2 |

| | | | | |
|---|---|---|---|---|
| 116 | 2009 | August | 14.0 | 0.0 |
| 117 | 2009 | September | 11.0 | 0.0 |
| 118 | 2009 | October | 26.0 | 0.2 |
| 119 | 2009 | November | 30.0 | 23.6 |
| 120 | 2009 | December | 30.0 | 82.2 |

Table (B.2) The water balance of Dokan models for calibration period ( 2010 - 2018 ) and validation periods( 2018 - 2021 ) For LU/LC 2010 map

| No | Year | Month | Observed | Simulated |
|---|---|---|---|---|
| 1 | 2010 | January | 138.0 | 1.85136 |
| 2 | 2010 | February | 205.0 | 101.076 |
| 3 | 2010 | March | 350.0 | 265.99 |
| 4 | 2010 | April | 230.0 | 238.873 |
| 5 | 2010 | May | 235.0 | 279.994 |
| 6 | 2010 | June | 80.0 | 99.5367 |
| 7 | 2010 | July | 43.0 | 127.008 |
| 8 | 2010 | August | 32.0 | 83.7574 |
| 9 | 2010 | September | 19.0 | 56.7597 |
| 10 | 2010 | October | 17.0 | 40.8535 |
| 11 | 2010 | November | 66.0 | 27.218 |
| 12 | 2010 | December | 125.0 | 21.7342 |
| 13 | 2011 | January | 60.0 | 42.9581 |
| 14 | 2011 | February | 146.0 | 132.145 |
| 15 | 2011 | March | 202.0 | 205.897 |
| 16 | 2011 | April | 313.0 | 395.077 |
| 17 | 2011 | May | 286.0 | 229.787 |
| 18 | 2011 | June | 77.0 | 142. 463 |
| 19 | 2011 | July | 33.0 | 126.877 |
| 20 | 2011 | August | 28.0 | 51.8677 |

| | | | | |
|---|---|---|---|---|
| 21 | 2011 | September | 22.0 | 103.777 |
| 22 | 2011 | October | 18.0 | 72.8755 |
| 23 | 2011 | November | 26.0 | 59.861 |
| 24 | 2011 | December | 33.0 | 41.0519 |
| 25 | 2012 | January | 51.0 | 55.6839 |
| 26 | 2012 | February | 135.0 | 65.4924 |
| 27 | 2012 | March | 269.0 | 199.324 |
| 28 | 2012 | April | 337.0 | 309.07 |
| 29 | 2012 | May | 152.0 | 332.165 |
| 30 | 2012 | June | 60.0 | 235.567 |
| 31 | 2012 | July | 28.0 | 161.981 |
| 32 | 2012 | August | 25.0 | 106.302 |
| 33 | 2012 | September | 18.0 | 71.876 |
| 34 | 2012 | October | 19.0 | 51.3165 |
| 35 | 2012 | November | 36.0 | 39.9933 |
| 36 | 2012 | December | 38.0 | 82.7952 |
| 37 | 2013 | January | 343.0 | 235.112 |
| 38 | 2013 | February | 387.0 | 376.229 |
| 39 | 2013 | March | 229.0 | 261.906 |
| 40 | 2013 | April | 185.0 | 171.183 |
| 41 | 2013 | May | 135.0 | 114.146 |
| 42 | 2013 | June | 57.0 | 73.6263 |
| 43 | 2013 | July | 35.0 | 47.419 |
| 44 | 2013 | August | 23.0 | 30.631 |
| 45 | 2013 | September | 17.0 | 21.108 |
| 46 | 2013 | October | 24.0 | 14.3971 |
| 47 | 2013 | November | 44.0 | 24.8693 |
| 48 | 2013 | December | 111.0 | 115.357 |
| 49 | 2014 | January | 101.0 | 145.765 |
| 50 | 2014 | February | 88.0 | 154.661 |

| | | | | |
|---|---|---|---|---|
| 51 | 2014 | March | 247.0 | 194.671 |
| 52 | 2014 | April | 181.0 | 272.943 |
| 53 | 2014 | May | 95.0 | 171.132 |
| 54 | 2014 | June | 43.0 | 110.903 |
| 55 | 2014 | July | 25.0 | 72.3713 |
| 56 | 2014 | August | 24.0 | 45.4045 |
| 57 | 2014 | September | 17.0 | 32.301 |
| 58 | 2014 | October | 18.0 | 59.1081 |
| 59 | 2014 | November | 42.0 | 94.8643 |
| 60 | 2014 | December | 117.0 | 80.8 |
| 61 | 2015 | January | 127.0 | 117.403 |
| 62 | 2015 | February | 149.0 | 113.996 |
| 63 | 2015 | March | 153.0 | 125.055 |
| 64 | 2015 | April | 190.0 | 182.64 |
| 65 | 2015 | May | 117.0 | 118.945 |
| 66 | 2015 | June | 39.0 | 92.9883 |
| 67 | 2015 | July | 18.0 | 60.181 |
| 68 | 2015 | August | 18.0 | 38.971 |
| 69 | 2015 | September | 14.0 | 26.5373 |
| 70 | 2015 | October | 46.0 | 20.74 |
| 71 | 2015 | November | 94.0 | 95.521 |
| 72 | 2015 | December | 137.0 | 164.697 |
| 73 | 2016 | January | 369.0 | 351.062 |
| 74 | 2016 | February | 242.0 | 215.797 |
| 75 | 2016 | March | 595.0 | 561.297 |
| 76 | 2016 | April | 530.0 | 586.83 |
| 77 | 2016 | May | 230.0 | 400.558 |
| 78 | 2016 | June | 79.0 | 62.63 |
| 79 | 2016 | July | 26.0 | 175.123 |
| 80 | 2016 | August | 14.0 | 118.205 |

| | | | | |
|---|---|---|---|---|
| 81 | 2016 | September | 11.0 | 80.7277 |
| 82 | 2016 | October | 35.0 | 57.4758 |
| 83 | 2016 | November | 135.0 | 47.1433 |
| 84 | 2016 | December | 104.0 | 173.255 |
| 85 | 2017 | January | 71.0 | 76.6839 |
| 86 | 2017 | February | 107.0 | 242.707 |
| 87 | 2017 | March | 268.0 | 241.646 |
| 88 | 2017 | April | 348.0 | 286.667 |
| 89 | 2017 | May | 148.0 | 235.648 |
| 90 | 2017 | June | 238.0 | 150.46 |
| 91 | 2017 | July | 74.0 | 99.0548 |
| 92 | 2017 | August | 3.0 | 65.6094 |
| 93 | 2017 | September | 2.0 | 45.2017 |
| 94 | 2017 | October | 10.0 | 30.9635 |
| 95 | 2017 | November | 24.0 | 31.4387 |
| 96 | 2017 | December | 116.0 | 97.8 |
| 97 | 2018 | January | 49.0 | 103.382 |
| 98 | 2018 | February | 462.0 | 341.193 |
| 99 | 2018 | March | 292.0 | 491.535 |
| 100 | 2018 | April | 158.0 | 375.593 |
| 101 | 2018 | May | 190.0 | 246.194 |
| 102 | 2018 | June | 30.0 | 165.723 |
| 103 | 2018 | July | 5.0 | 109.105 |
| 104 | 2018 | August | 5.0 | 96.8374 |
| 105 | 2018 | September | 5.0 | 47.899 |
| 106 | 2018 | October | 2.0 | 36.5055 |
| 107 | 2018 | November | 31.0 | 34.7323 |
| 108 | 2018 | December | 31.0 | 227.853 |
| 109 | 2019 | January | 539.0 | 419.4 |
| 110 | 2019 | February | 497.0 | 322.925 |

| | | | | |
|---|---|---|---|---|
| 111 | 2019 | March | 622.0 | 560.145 |
| 112 | 2019 | April | 906.0 | 822.59 |
| 113 | 2019 | May | 426.0 | 353.529 |
| 114 | 2019 | June | 183.0 | 163.46 |
| 115 | 2019 | July | 67.0 | 114.084 |
| 116 | 2019 | August | 14.0 | 163.935 |
| 117 | 2019 | September | 28.0 | 112.74 |
| 118 | 2019 | October | 23.0 | 78.9755 |
| 119 | 2019 | November | 54.0 | 64.9417 |
| 120 | 2019 | December | 419.0 | 44.131 |
| 121 | 2020 | January | 129.0 | 155.3 |
| 122 | 2020 | February | 273.0 | 311.2 |
| 123 | 2020 | March | 258.0 | 300.9 |
| 124 | 2020 | April | 339.0 | 365.7 |
| 125 | 2020 | May | 232.0 | 250.1 |
| 126 | 2020 | June | 98.0 | 107.7 |
| 127 | 2020 | July | 48.0 | 54.1 |
| 128 | 2020 | August | 1.0 | 0.0 |
| 129 | 2020 | September | 2.0 | 0.0 |
| 130 | 2020 | October | 41.0 | 33.2 |
| 131 | 2020 | November | 45.0 | 46.2 |
| 132 | 2020 | December | 79.0 | 81.5 |
| 133 | 2021 | January | 73.0 | 75.3 |
| 134 | 2021 | February | 197.0 | 201.3 |
| 135 | 2021 | March | 109.0 | 111.3 |
| 136 | 2021 | April | 44.0 | 45.2 |
| 137 | 2021 | May | 50.0 | 55.8 |
| 138 | 2021 | June | 29.0 | 32.5 |
| 139 | 2021 | July | 38.0 | 41.3 |
| 140 | 2021 | August | 23.0 | 34 |

| | | | | |
|---|---|---|---|---|
| 141 | 2021 | September | 3.0 | 5.3 |
| 142 | 2021 | October | 7.0 | 5 |
| 143 | 2021 | November | 37.0 | 43 |
| 144 | 2021 | December | 54.0 | 44 |

Table (B.3) The water balance of Dibis models for calibration period ( 2002- 2007) and validation periods (2007- 2010) For LU/LC 2002 map

| No | Month | Year | OUT DIBIS | OUT DUKAN | KIRKUK | C5-c6 | C4-c7 | Observed | Simulated |
|---|---|---|---|---|---|---|---|---|---|
| 1 | January | 2002 | 95 | 58 | 21 | 37 | 58 | 58 | 33.976 |
| 2 | February | 2002 | 45 | 56 | 18 | 38 | 7 | 7 | 7.321 |
| 3 | March | 2002 | 21 | 59 | 58 | 1 | 20 | 20 | 22.091 |
| 4 | April | 2002 | 14 | 69 | 75 | -6 | 20 | 20 | 3.819 |
| 5 | May | 2002 | 25 | 115 | 88 | 27 | -2 | 0 | 3.401 |
| 6 | June | 2002 | 34 | 137 | 100 | 37 | -3 | 0 | 4.339 |
| 7 | July | 2002 | 60 | 160 | 90 | 70 | -10 | 0 | 3.761 |
| 8 | August | 2002 | 85 | 165 | 80 | 85 | 0 | 0 | 5.303 |
| 9 | September | 2002 | 80 | 158 | 72 | 86 | -6 | 0 | 7.803 |
| 10 | October | 2002 | 20 | 61 | 41 | 20 | 0 | 0 | 1.301 |
| 11 | November | 2002 | 26 | 66 | 38 | 28 | -2 | 0 | 2.998 |
| 12 | December | 2002 | 45 | 65 | 30 | 35 | 10 | 10 | 14.001 |
| 13 | January | 2003 | 235 | 248 | 40 | 208 | 27 | 27 | 99.321 |
| 14 | February | 2003 | 240 | 230 | 33 | 197 | 43 | 43 | 53.207 |
| 15 | March | 2003 | 148 | 179 | 60 | 119 | 29 | 29 | 32.599 |
| 16 | April | 2003 | 98 | 141 | 75 | 66 | 32 | 32 | 45.001 |
| 17 | May | 2003 | 115 | 173 | 65 | 108 | 7 | 7 | 8.209 |
| 18 | June | 2003 | 181 | 235 | 63 | 172 | 9 | 9 | 12.213 |
| 19 | July | 2003 | 208 | 269 | 65 | 204 | 4 | 4 | 11.464 |
| 20 | August | 2003 | 216 | 286 | 65 | 221 | -5 | 0 | 5.502 |

| | | | | | | | | | |
|---|---|---|---|---|---|---|---|---|---|
| 21 | September | 2003 | 203 | 260 | 61 | 199 | 4 | 4 | 5.873 |
| 22 | October | 2003 | 72 | 143 | 65 | 78 | -6 | 0 | 11.386 |
| 23 | November | 2003 | 160 | 209 | 55 | 154 | 6 | 6 | 8.628 |
| 24 | December | 2003 | 280 | 215 | 43 | 172 | 108 | 108 | 110.239 |
| 25 | January | 2004 | 465 | 380 | 45 | 335 | 130 | 130 | 122.301 |
| 26 | February | 2004 | 405 | 370 | 50 | 320 | 85 | 85 | 133.981 |
| 27 | March | 2004 | 220 | 270 | 75 | 195 | 25 | 25 | 12.542 |
| 28 | April | 2004 | 75 | 126 | 88 | 38 | 37 | 37 | 9.739 |
| 29 | May | 2004 | 84 | 138 | 74 | 64 | 20 | 20 | 5.302 |
| 30 | June | 2004 | 140 | 215 | 83 | 132 | 8 | 8 | 9.471 |
| 31 | July | 2004 | 148 | 255 | 90 | 165 | -17 | 0 | 4.778 |
| 32 | August | 2004 | 230 | 343 | 106 | 237 | -7 | 0 | 3.906 |
| 33 | September | 2004 | 210 | 310 | 83 | 227 | -17 | 0 | 5.003 |
| 34 | October | 2004 | 203 | 275 | 65 | 210 | -7 | 0 | 4.009 |
| 35 | November | 2004 | 276 | 330 | 65 | 265 | 11 | 11 | 3.409 |
| 36 | December | 2004 | 370 | 363 | 40 | 323 | 47 | 47 | 43.091 |
| 37 | January | 2005 | 65 | 120 | 70 | 50 | 15 | 15 | 8.029 |
| 38 | February | 2005 | 155 | 115 | 43 | 72 | 83 | 83 | 96.209 |
| 39 | March | 2005 | 70 | 70 | 55 | 15 | 55 | 55 | 60.407 |
| 40 | April | 2005 | 72 | 87 | 72 | 15 | 57 | 57 | 65.302 |
| 41 | May | 2005 | 70 | 125 | 67 | 58 | 12 | 12 | 11.992 |
| 42 | June | 2005 | 210 | 290 | 71 | 219 | -9 | 0 | 3.001 |
| 43 | July | 2005 | 200 | 300 | 73 | 227 | -27 | 0 | 4.831 |
| 44 | August | 2005 | 185 | 296 | 90 | 206 | -21 | 0 | 4.573 |
| 45 | September | 2005 | 103 | 191 | 87 | 104 | -1 | 0 | 5.432 |
| 46 | October | 2005 | 125 | 206 | 80 | 126 | -1 | 0 | 9.308 |
| 47 | November | 2005 | 100 | 155 | 57 | 98 | 2 | 2 | 2.002 |
| 48 | December | 2005 | 125 | 170 | 68 | 102 | 23 | 23 | 25.299 |
| 49 | January | 2006 | 55 | 66 | 55 | 11 | 44 | 44 | 51.441 |
| 50 | February | 2006 | 64 | 110 | 64 | 46 | 18 | 18 | 22.383 |

| | | | | | | | | | |
|---|---|---|---|---|---|---|---|---|---|
| 51 | March | 2006 | 60 | 68 | 60 | 8 | 52 | 52 | 57.451 |
| 52 | April | 2006 | 53 | 51 | 53 | -2 | 55 | 55 | 41.508 |
| 53 | May | 2006 | 66 | 80 | 66 | 14 | 52 | 52 | 43.442 |
| 54 | June | 2006 | 91 | 289 | 91 | 198 | -107 | 0 | 4.891 |
| 55 | July | 2006 | 100 | 418 | 100 | 318 | -218 | 0 | 1.607 |
| 56 | August | 2006 | 107 | 345 | 107 | 238 | -131 | 0 | 1.512 |
| 57 | September | 2006 | 75 | 176 | 75 | 101 | -26 | 0 | 8.234 |
| 58 | October | 2006 | 82 | 171 | 82 | 89 | -7 | 0 | 5.903 |
| 59 | November | 2006 | 71 | 95 | 71 | 24 | 47 | 47 | 44.289 |
| 60 | December | 2006 | 48 | 70 | 48 | 22 | 26 | 26 | 34.509 |
| 61 | January | 2007 | 40 | 80 | 61 | 19 | 21 | 21 | 21.871 |
| 62 | February | 2007 | 40 | 71 | 60 | 11 | 29 | 29 | 22.671 |
| 63 | March | 2007 | 20 | 38 | 42 | -4 | 24 | 24 | 33.481 |
| 64 | April | 2007 | 18 | 25 | 36 | -11 | 29 | 29 | 31.301 |
| 65 | May | 2007 | 17 | 31 | 28 | 3 | 14 | 14 | 17.821 |
| 66 | June | 2007 | 74 | 158 | 74 | 84 | -10 | 0 | 7.431 |
| 67 | July | 2007 | 90 | 190 | 90 | 100 | -10 | 0 | 11.237 |
| 68 | August | 2007 | 150 | 232 | 81 | 151 | -1 | 0 | 3.821 |
| 69 | September | 2007 | 95 | 178 | 80 | 98 | -3 | 0 | 2.642 |
| 70 | October | 2007 | 70 | 147 | 73 | 74 | -4 | 0 | 4.321 |
| 71 | November | 2007 | 85 | 132 | 55 | 77 | 8 | 8 | 11.201 |
| 72 | December | 2007 | 110 | 198 | 83 | 115 | -5 | 0 | 1.123 |
| 73 | January | 2008 | 35 | 78 | 50 | 28 | 7 | 7 | 13.541 |
| 74 | February | 2008 | 12 | 17 | 16 | 1 | 11 | 11 | 19.541 |
| 75 | March | 2008 | 14 | 23 | 22 | 1 | 13 | 13 | 19.921 |
| 76 | April | 2008 | 15 | 40 | 27 | 13 | 2 | 2 | 13.001 |
| 77 | May | 2008 | 17 | 62 | 43 | 19 | -2 | 0 | 2.843 |

| | | | | | | | | | |
|---|---|---|---|---|---|---|---|---|---|
| 78 | June | 2008 | 31 | 102 | 71 | 31 | 0 | 0 | 8.651 |
| 79 | July | 2008 | 58 | 118 | 60 | 58 | 0 | 0 | 1.598 |
| 80 | August | 2008 | 31 | 90 | 60 | 30 | 1 | 1 | 4.39 |
| 81 | September | 2008 | 21 | 67 | 46 | 21 | 0 | 0 | 2.231 |
| 82 | October | 2008 | 100 | 178 | 70 | 108 | -8 | 0 | 7.501 |
| 83 | November | 2008 | 53 | 123 | 70 | 53 | 0 | 0 | 3.653 |
| 84 | December | 2008 | 70 | 143 | 80 | 63 | 7 | 7 | 12.531 |
| 85 | January | 2009 | 12 | 28 | 17 | 11 | 1 | 1 | 1.305 |
| 86 | February | 2009 | 7 | 27 | 22 | 5 | 2 | 2 | 2.761 |
| 87 | March | 2009 | 10 | 28 | 26 | 2 | 8 | 8 | 4.865 |
| 88 | April | 2009 | 9 | 36 | 36 | 0 | 9 | 9 | 4.671 |
| 89 | May | 2009 | 10 | 36 | 28 | 8 | 2 | 2 | 5.309 |
| 90 | June | 2009 | 14 | 57 | 37 | 20 | -6 | 0 | 1.671 |
| 91 | July | 2009 | 31 | 97 | 52 | 45 | -14 | 0 | 1.309 |
| 92 | August | 2009 | 46 | 105 | 49 | 56 | -10 | 0 | 1.301 |
| 93 | September | 2009 | 18 | 54 | 36 | 18 | 0 | 0 | 1.671 |
| 94 | October | 2009 | 24 | 47 | 37 | 10 | 14 | 14 | 12.398 |
| 95 | November | 2009 | 16 | 49 | 38 | 11 | 5 | 5 | 8.011 |
| 96 | December | 2009 | 16 | 50 | 38 | 12 | 4 | 4 | 5.229 |

Table (B.4) The water balance of Dibis models for calibration period ( 2010- 2017) and validation periods(2017- 2022) For LU/LC 2010 map

| No | Month | Year | OUT DIBIS | OUT DOKAN | KIRKUK | | | Observed | Simulated |
|---|---|---|---|---|---|---|---|---|---|
| 1 | January | 2010 | 45 | 82 | 50 | 32 | -11 | 0 | 3.211 |
| 2 | February | 2010 | 103 | 160 | 57 | 103 | -34 | 0 | 4.871 |
| 3 | March | 2010 | 70 | 89 | 62 | 27 | 121 | 121 | 132.118 |
| 4 | April | 2010 | 21 | 62 | 52 | 10 | 125 | 125 | 154.818 |
| 5 | May | 2010 | 69 | 162 | 77 | 85 | 95 | 95 | 82.102 |

| | | | | | | | | | |
|---|---|---|---|---|---|---|---|---|---|
| 6 | June | 2010 | 148 | 230 | 76 | 154 | -42 | 0 | 2.221 |
| 7 | July | 2010 | 135 | 236 | 91 | 145 | -132 | 0 | 1.541 |
| 8 | August | 2010 | 180 | 283 | 91 | 192 | -177 | 0 | 1.981 |
| 9 | September | 2010 | 112 | 202 | 81 | 121 | -87 | 0 | 5.312 |
| 10 | October | 2010 | 13 | 40 | 29 | 11 | 34 | 34 | 43.441 |
| 11 | November | 2010 | 15 | 48 | 36 | 12 | 91 | 91 | 79.71 |
| 12 | December | 2010 | 34 | 69 | 44 | 25 | 45 | 45 | 39.301 |
| 13 | January | 2011 | 10 | 30 | 30 | 0 | 10 | 10 | 12.891 |
| 14 | February | 2011 | 11 | 27 | 31 | -4 | 15 | 15 | 22.332 |
| 15 | March | 2011 | 8 | 33 | 32 | 1 | 7 | 7 | 1.854 |
| 16 | April | 2011 | 12 | 48 | 43 | 5 | 7 | 7 | 15.782 |
| 17 | May | 2011 | 16 | 72 | 57 | 15 | 1 | 1 | 2.965 |
| 18 | June | 2011 | 58 | 87 | 58 | 29 | 29 | 29 | 18.631 |
| 19 | July | 2011 | 98 | 192 | 75 | 117 | -19 | 0 | 8.369 |
| 20 | August | 2011 | 151 | 248 | 80 | 168 | -17 | 0 | 2.512 |
| 21 | September | 2011 | 27 | 85 | 59 | 26 | 1 | 1 | 3.438 |
| 22 | October | 2011 | 20 | 52 | 37 | 15 | 5 | 5 | 3.98 |
| 23 | November | 2011 | 9 | 41 | 31 | 10 | -1 | 0 | 4.329 |
| 24 | December | 2011 | 6 | 30 | 27 | 3 | 3 | 3 | 5.327 |
| 25 | January | 2012 | 19 | 62 | 52 | 10 | 9 | 9 | 7.831 |
| 26 | February | 2012 | 25 | 59 | 44 | 15 | 10 | 10 | 18.849 |
| 27 | March | 2012 | 22 | 69 | 58 | 11 | 11 | 11 | 24.891 |
| 28 | April | 2012 | 20 | 94 | 78 | 16 | 4 | 4 | 5.409 |
| 29 | May | 2012 | 21 | 82 | 61 | 21 | 0 | 0 | 2.891 |
| 30 | June | 2012 | 53 | 155 | 91 | 64 | -11 | 0 | 2.891 |
| 31 | July | 2012 | 103 | 250 | 114 | 136 | -33 | 0 | 1.839 |
| 32 | August | 2012 | 55 | 186 | 110 | 76 | -21 | 0 | 3.891 |
| 33 | September | 2012 | 23 | 83 | 59 | 24 | -1 | 0 | 1.729 |
| 34 | October | 2012 | 24 | 79 | 57 | 22 | 2 | 2 | 7.871 |
| 35 | November | 2012 | 27 | 108 | 72 | 36 | -9 | 0 | 0.331 |

| | | | | | | | | | |
|---|---|---|---|---|---|---|---|---|---|
| 36 | December | 2012 | 23 | 88 | 70 | 18 | 5 | 5 | 2.289 |
| 37 | January | 2013 | 74 | 41 | 42 | -1 | 75 | 75 | 33.451 |
| 38 | February | 2013 | 53 | 55 | 69 | -14 | 67 | 67 | 41.012 |
| 39 | March | 2013 | 13 | 74 | 61 | 13 | 0 | 0 | 3.409 |
| 40 | April | 2013 | 20 | 95 | 74 | 21 | -1 | 0 | 7.982 |
| 41 | May | 2013 | 21 | 76 | 64 | 12 | 9 | 9 | 1.304 |
| 42 | June | 2013 | 53 | 150 | 85 | 65 | -12 | 0 | 3.761 |
| 43 | July | 2013 | 150 | 259 | 99 | 160 | -10 | 0 | 3.572 |
| 44 | August | 2013 | 118 | 218 | 84 | 134 | -16 | 0 | 2.113 |
| 45 | September | 2013 | 49 | 114 | 64 | 50 | -1 | 0 | 4.892 |
| 46 | October | 2013 | 17 | 63 | 44 | 19 | -2 | 0 | 7.901 |
| 47 | November | 2013 | 17 | 81 | 64 | 17 | 0 | 0 | 8.732 |
| 48 | December | 2013 | 54 | 75 | 59 | 16 | 38 | 38 | 46.732 |
| 49 | January | 2014 | 47 | 77 | 50 | 27 | 20 | 20 | 13.901 |
| 50 | February | 2014 | 19 | 48 | 40 | 8 | 11 | 11 | 4.003 |
| 51 | March | 2014 | 12 | 30 | 40 | -10 | 22 | 22 | 16.098 |
| 52 | April | 2014 | 11 | 68 | 52 | 16 | -5 | 0 | 2.641 |
| 53 | May | 2014 | 12 | 50 | 36 | 14 | -2 | 0 | 3.658 |
| 54 | June | 2014 | 29 | 100 | 60 | 40 | -11 | 0 | 1.742 |
| 55 | July | 2014 | 108 | 178 | 70 | 108 | 0 | 0 | 4.003 |
| 56 | August | 2014 | 169 | 240 | 70 | 170 | -1 | 0 | 1.982 |
| 57 | September | 2014 | 28 | 80 | 52 | 28 | 0 | 0 | 1.401 |
| 58 | October | 2014 | 21 | 82 | 61 | 21 | 0 | 0 | 4.893 |
| 59 | November | 2014 | 41 | 106 | 65 | 41 | 0 | 0 | 8.951 |
| 60 | December | 2014 | 99 | 162 | 62 | 100 | -1 | 0 | 2.561 |
| 61 | January | 2015 | 26 | 86 | 66 | 20 | 5.516129 | 5.516129 | 7.801 |
| 62 | February | 2015 | 26 | 76 | 63 | 13 | 13 | 13 | 22.509 |
| 63 | March | 2015 | 34 | 86 | 50 | 36 | -2 | 0 | 3.081 |
| 64 | April | 2015 | 12 | 48 | 39 | 9 | 2.566667 | 2.566667 | 5.762 |
| 65 | May | 2015 | 25 | 67 | 40 | 27 | -2 | 0 | 1.813 |

| | | | | | | | | | |
|---|---|---|---|---|---|---|---|---|---|
| 66 | June | 2015 | 29 | 67 | 40 | 27 | 2.333333 | 2.333333 | 3.091 |
| 67 | July | 2015 | 92 | 134 | 37 | 97 | -5.33333 | 0 | 4.204 |
| 68 | August | 2015 | 107 | 143 | 35 | 108 | -0.58065 | 0 | 5.113 |
| 69 | September | 2015 | 55 | 92 | 35 | 57 | -2 | 0 | 3.782 |
| 70 | October | 2015 | 41 | 88 | 54 | 34 | 7 | 7 | 11.301 |
| 71 | November | 2015 | 56 | 101 | 49 | 52 | 4 | 4 | 8.998 |
| 72 | December | 2015 | 26 | 77 | 59 | 18 | 8 | 8 | 11.904 |
| 73 | January | 2016 | 74 | 81 | 37 | 44 | 30 | 30 | 43.489 |
| 74 | February | 2016 | 44 | 72 | 38 | 34 | 10 | 10 | 5.302 |
| 75 | March | 2016 | 85 | 83 | 49 | 34 | 51 | 51 | 45.077 |
| 76 | April | 2016 | 53 | 74 | 58 | 16 | 37 | 37 | 53.406 |
| 77 | May | 2016 | 48 | 74 | 46 | 28 | 19.74194 | 19.74194 | 11.293 |
| 78 | June | 2016 | 142 | 172 | 38 | 134 | 8 | 8 | 17.403 |
| 79 | July | 2016 | 152 | 197 | 43 | 154 | -2.29032 | 0 | 6.812 |
| 80 | August | 2016 | 213 | 265 | 45 | 220 | -6.96774 | 0 | 4.932 |
| 81 | September | 2016 | 148 | 201 | 49 | 152 | -4 | 0 | 6.731 |
| 82 | October | 2016 | 43 | 75 | 35 | 40 | 3 | 3 | 4.529 |
| 83 | November | 2016 | 88 | 83 | 35 | 48 | 40 | 40 | 45.509 |
| 84 | December | 2016 | 37 | 72 | 35 | 37 | -0.32258 | 0 | 11.009 |
| 85 | January | 2017 | 49 | 87 | 34 | 53 | -4 | 0 | 0.012 |
| 86 | February | 2017 | 41 | 93 | 54 | 39 | 2 | 2 | 1.403 |
| 87 | March | 2017 | 50 | 101 | 63 | 38 | 12 | 12 | 8.711 |
| 88 | April | 2017 | 53 | 73 | 33 | 40 | 13 | 13 | 21.132 |
| 89 | May | 2017 | 51 | 76 | 17 | 59 | -8 | 0 | 3.112 |
| 90 | June | 2017 | 43 | 112 | 67 | 45 | -2 | 0 | 4.871 |
| 91 | July | 2017 | 46 | 98 | 39 | 59 | -13 | 0 | 2.508 |
| 92 | August | 2017 | 52 | 123 | 61 | 62 | -10 | 0 | 5.503 |
| 93 | September | 2017 | 46 | 101 | 53 | 48 | -2 | 0 | 4.672 |
| 94 | October | 2017 | 49 | 89 | 39 | 50 | -1 | 0 | 5.129 |
| 95 | November | 2017 | 50 | 148 | 89 | 59 | -9 | 0 | 2.101 |

| | | | | | | | | | |
|---|---|---|---|---|---|---|---|---|---|
| 96 | December | 2017 | 50 | 123 | 83 | 40 | 10 | 10 | 2.604 |
| 97 | January | 2018 | 95 | 140 | 40 | 100 | -5 | 0 | 3.741 |
| 98 | February | 2018 | 135 | 103 | 42 | 61 | 74 | 74 | 81.409 |
| 99 | March | 2018 | 70 | 106 | 43 | 63 | 7 | 7 | 12.401 |
| 100 | April | 2018 | 50 | 88 | 45 | 43 | 7 | 7 | 13.501 |
| 101 | May | 2018 | 40 | 80 | 39 | 41 | -1 | 0 | 2.315 |
| 102 | June | 2018 | 99 | 146 | 40 | 106 | -6.66667 | 0 | 3.392 |
| 103 | July | 2018 | 141 | 194 | 42 | 152 | -11 | 0 | 6.751 |
| 104 | August | 2018 | 134 | 187 | 44 | 143 | -9 | 0 | 4.402 |
| 105 | September | 2018 | 118 | 165 | 40 | 125 | -7.06897 | 0 | 4.501 |
| 106 | October | 2018 | 47 | 105 | 42 | 63 | -16 | 0 | 5.001 |
| 107 | November | 2018 | 66 | 114 | 46 | 68 | -2 | 0 | 11.224 |
| 108 | December | 2018 | 79 | 137 | 50 | 87 | -8 | 0 | 6.208 |
| 109 | January | 2019 | 145 | 82 | 38 | 44 | 101 | 101 | 115.32 |
| 110 | February | 2019 | 131 | 123 | 40 | 83 | 48 | 48 | 57.548 |
| 111 | March | 2019 | 260 | 200 | 40 | 160 | 100 | 100 | 90.441 |
| 112 | April | 2019 | 915 | 802 | 50 | 752 | 163 | 163 | 131.981 |
| 113 | May | 2019 | 452 | 496 | 76 | 420 | 32 | 32 | 122.908 |
| 114 | June | 2019 | 195 | 262 | 61 | 201 | -6 | 0 | 5.396 |
| 115 | July | 2019 | 215 | 283 | 69 | 214 | 1 | 1 | 2.432 |
| 116 | August | 2019 | 202 | 282 | 70 | 212 | -10 | 0 | 0.432 |
| 117 | September | 2019 | 197 | 268 | 70 | 198 | -1.16667 | 0 | 3.671 |
| 118 | October | 2019 | 78 | 120 | 40 | 80 | -2.25806 | 0 | 2.983 |
| 119 | November | 2019 | 90 | 83 | 40 | 43 | 47 | 47 | 79.671 |
| 120 | December | 2019 | 177 | 64 | 40 | 24 | 153 | 153 | 140.023 |
| 121 | January | 2020 | 141 | 181 | 48 | 133 | 8.258065 | 8.258065 | 11.323 |
| 122 | February | 2020 | 102 | 133 | 50 | 83 | 18.89655 | 18.89655 | 21.402 |
| 123 | March | 2020 | 71 | 104 | 50 | 54 | 17 | 17 | 24.674 |
| 124 | April | 2020 | 67 | 105 | 63 | 42 | 24.92857 | 24.92857 | 13.821 |
| 125 | May | 2020 | 59 | 124 | 62 | 62 | -3 | 0 | 3.398 |

| | | | | | | | | | |
|---|---|---|---|---|---|---|---|---|---|
| 126 | June | 2020 | 91 | 164 | 67 | 97 | -5.66667 | 0 | 6.312 |
| 127 | July | 2020 | 158 | 232 | 70 | 162 | -4.41935 | 0 | 0.431 |
| 128 | August | 2020 | 160 | 235 | 70 | 165 | -4.51613 | 0 | 0.321 |
| 129 | September | 2020 | 95 | 155 | 68 | 87 | 7.5 | 7.5 | 13.001 |
| 130 | October | 2020 | 162 | 280 | 66 | 214 | -52 | 0 | 2.431 |
| 131 | November | 2020 | 193 | 233 | 56 | 177 | 15.93103 | 15.93103 | 22.651 |
| 132 | December | 2020 | 150 | 202 | 51 | 151 | -1.16129 | 0 | 9.901 |
| 133 | January | 2021 | 20 | 82 | 60 | 22 | -2 | 0 | 2.391 |
| 134 | February | 2021 | 12 | 56 | 44 | 12 | 0 | 0 | 3.891 |
| 135 | March | 2021 | 9 | 74 | 58 | 16 | -7.32258 | 0 | 6.613 |
| 136 | April | 2021 | 10 | 78 | 64 | 14 | -4 | 0 | 7.836 |
| 137 | May | 2021 | 10 | 70 | 55 | 15 | -4.54839 | 0 | 4.761 |
| 138 | June | 2021 | 16 | 78 | 56 | 22 | -5.63333 | 0 | 5.861 |
| 139 | July | 2021 | 31 | 94 | 55 | 39 | -8 | 0 | 3.877 |
| 140 | August | 2021 | 71 | 129 | 55 | 74 | -2.64516 | 0 | 2.671 |
| 141 | September | 2021 | 30 | 92 | 55 | 37 | -7.06667 | 0 | 3.631 |
| 142 | October | 2021 | 18 | 90 | 64 | 26 | -8.09677 | 0 | 1.301 |
| 143 | November | 2021 | 29 | 93 | 57 | 36 | -7.03448 | 0 | 9.672 |
| 144 | December | 2021 | 22 | 85 | 60 | 25 | -3.06452 | 0 | 4.981 |

## الخلاصة

يعد استخدام الأراضي والغطاء الأرضي أحد أكبر المكونات النشطة للبيئة، والتي كانت تختلف بشكل غير منتظم عن الوقت الذي أعقب ثورة التصنيع في عمليات متنوعة.

تهدف الدراسه الحاليه الى التحقق في نمط استخدام الأراضي وغطاء الأراضي وقياس تغيير الارتباط في المناخات الجافه وشبه الجافه من خلال اخذ حوض نهر الزاب الصغير في شمال شرق العراق. تم اخذ صور لاندسات للسنوات 1989و 1999 و 2010 و2021 بشكل عام تم تصنيف الى سته أنواع رئيسيه وقد أظهرت النتائج في عام 1989 شكلت الأراضي الحضريه 0,46% مع ذلك في عام 2021 زادت الأراضي الحضريه الى 5,59 من اجمالي مساحة الأرض حيث شهد الحوض انخفاضا في الأراضي الزراعيه والقاحله بينما اتسعت الأراضي الحضريه وكان هناك تذبذبا في المنطقه التي شغلتها المسطحات كذلك تهدف الدراسه الى التنبؤ المستقبلي بالتغيرات المحتملة لاستخدام الأراضي وغطاء الأراضي من خلال تطبيق نموذج ماركوف الخلوي,تم استخدام الخرائط المصنفة للسنوات الثلاث (1999-2010)( 2010-2021) لتصميم خرائط استخدام الأراضي وغطاء الأراضي المتنبئة للسنوات 2021 و2041. تم انشاء خريطة التنبؤ لعام 2021 للتاكد من صحة اخراج النموذج و كانت دقة الاتفاقيات بين الصور المصنفة والمتنبئة

Klocation = 0.8541 و Kstandard = 0.7851 و Kno= 0.8635

بهذا الترتيب. يتم التحقق من صحة احتمالات التوقع بين عامي 2021 و 2041، سترتفع المنطقة الحضرية بنسبة 364.4٪ (من 1118 إلى 5192 كم $^2$) ، والمسطحات المائية 33٪ (من 90 إلى 120 كم $^2$). ومع ذلك، فإن الأراضي العارية / باللون الفاتح ، والأراضي الزراعية، والأراضي الجرداء / الداكنة، والأراضي الغابات ستنخفض بمقدار 3.5 (من 6983 إلى 6736 كم$^2$) ، و 11.96 (من 7992 إلى 7036 كم $^2$) ، و 42.85 (من 7 إلى 4 كم $^2$) ، و 76.27 (من 3810 إلى 904 كم$^2$) ،

أيضا تهدف هذه الدراسه الى التحقق في تاثيير تغيير استخدلم الأراضي وغطاء الأراضي على العمليات الهيدرولوجيه لمنطقه الدراسه لمده 21 عام (بسبب نقص البيانات الهيدرولوجيه وتوفرها لهذه السنوات فقط) تم استخدام نموذج أداة تقييم مياه التربه سوات لمحاكاه تدفق التيار. أظهرت نتائج النموذج أن خصائص تدفق المجرى قد تغيرت بسبب تغير غطاء الأراضي واستخدام الأراضي وتغير المناخ وارتفاع وتغير وتيرة الفيضانات. اظهر تقييم نموذج سوات أن الجريان السطحي السنوي لمستجمعات المياه في .

دوكان قد زاد بسبب موجة الفيضانات التي حدثت في عام 2019 وفقًا للبيانات الهيدرولوجية التي تم الحصول عليها من وزارة الموارد المائية / المركز الوطني لإدارة الموارد المائية. نتيجة لذلك ، تم استنفاد الطاقة الاستيعابيه لسد دوكان. وتقليل الجريان السطحي في مستجمعات مياه الدبس. كان رقم المنحنى ، والقدرة المائية المتاحة لطبقة التربة ، وعامل تكوين تبخر التربة من أكثر العوامل حساسية التي تم تحديدها لتدفق مجرى النهر. وفاعلية ذوبان الثلج في مستجمعات دوكان المائية مع تقدم السنوات ، يتناقص سمك الثلج ومساهمته في تدفق مجرى المياه وغير فعال في مستجمعات مياه الدبس . من خلال استخدام برنامج سوات للمعايره والتحقق بين التدفق الحقيقي والمحاكى أظهرت النتائج معامل التحديد وقيم الكفاءة للاختبار الاحصائي للنموذج هي 0,87 و 0,81 للفتره 2000-2007افتره المعايرة و 0,79 و 0.63 لفترة2007-2010 على التوالي لفترات التحقق وقيم الكفاءة 0,74 و0,71 لفترات امعايره 2010-2017 على التوالي و 0,76 و0,76 لفترات التحقق 2017-2021 الخاصه بمنطقه دوكان ,كذلك أظهرت وقيم الكفاءة للاختبار الاحصائي للنموذج 0.82 و 0,76 للفتره 2000-2007 لفترة معامل التحديد ا المعايرة و 0,8و 0.63 للفتره 2007-2010 على التوالي لفترات التحقق وقيم الكفاءة0,9 و 0,89 لفترات امعايره 2010-2017 على التوالي و 0,85 و0,83 2017-2021 لفتره التحقق الخاصه لمستجمعات مياه الدبس ، مخرجات هذه الدراسة مفيدة للاداره الفعالة لحوض النهر

جمهورية العراق
وزارة التعليم العالي والبحث العلمي
جامعة بابل/ كلية الهندسة
قسم الهندسة المدنية

# نمذجة التأثير الهيدرولوجي لاستخدام الأراضي/ تغير الغطاء الأرضي في حوض نهر الزاب الأسفل، العراق

رسالة مقدمة إلى قسم الهندسة المدنية، كلية الهندسة، جامعةِ بابل وهي جزء مِنْ متطلبات الحصول على درجة الماجستيرعلوم في الهندسة/ الهندسة المدنية / هندسة الموارد المائية

*من قبل:*

***زهراء علي مهدي عبود***

بكالوريوس علوم في الهندسة المدنية 2010

*بأشراف:*

***أ. م. د: رقية كاظم محمد***

**كانون الثاني,1444** **January, 2023**